Characterization and performance analysis of syngas from biomass gasification

A thesis submitted in partial fulfillment of the requirement for the degree of

Master of Science in Mechanical Engineering

By

Redoy Masum Meraz

Student ID: 21MME033P

Supervisor: Prof. Dr. Mohammad Mizanur Rahman

Department of Mechanical Engineering

Chittagong University of Engineering and Technology

Chattogram-4349, Bangladesh

January, 2025

Declaration

I, the undersigned, do hereby confirm to declare that the thesis is conducted and composed of myself and the work has not been submitted anywhere for other degrees or professional qualifications. To the best of my knowledge, contained materials were not written or published by anyone, except where due references are made.

Name: Redoy Masum Meraz

Student ID: 21MME033P

Acknowledgement

All praises are for Allah, the Lord of the universe, for supporting and providing me blessings for the completion of the present work.

I'd like to express true gratefulness and profound appreciation to my supervisor Dr. Mohammad Mizanur Rahman, Professor, Department of Mechanical Engineering, Chittagong University of Engineering and Technology (CUET) for his steady supervision, incredible direction, support, and significant remarks. I would also like to acknowledge the support and experimental facilities my co-supervisor, Dr. Md. Abdus Salam provided. Also thanks to Tafsirul Hassan for his insightful suggestions.

I would like to express my gratitude to Asfia Ahmed Khan who cooperated during data curation and biomass potential in Bangladesh.

At long last, I'd like to thank my parents and my beloved wife for their support, consolation, and help all through my journey.

Abstract

Co-gasification is one of the most promising thermochemical conversion technologies for biomass derived from agricultural residue, and the co-gasification treatment of agricultural residue can effectively enhance waste management systems and green energy production. In the present study, the co-gasification of corncob, coconut coir, and coconut shell biomass in a fixed-bed gasifier is simulated using the Aspen Plus software, and the model is validated using the previously published literature. The present model investigates the effects of temperature (500-1200℃), pressure (1-20 bar), steam-to-biomass ratio (SBR) (0.2-1), and Equivalence ratio (ER) (0.1-0.6) on syngas composition, cold gas efficiency (CGE), and lower heating value (LHV) of syngas. H_2 and CO production increases with the increase in temperature and decreases with pressure and ER, whereas CO_2 shows the opposite trend. A higher steam-to-biomass ratio enhances the production of H_2 and CO_2. However, the amount of CO reduced sharply with higher SBR. The LHV of syngas decreases with the increase in temperature, SBR, and ER. However, an increase in pressure increases the LHV. In this study, Two Machine learning models were developed to optimize the operating conditions of the co-gasification process. The random forest (RF) and the gradient boosting regression (GBR) model are considered. The result shows that the GBR model has better accuracy($R^2 \geq 0.99$ and RMSE ≤ 2.66) for the optimization of the operating conditions. The model showed that maximum H_2 (54.13%), CO (29.52%), CGE (90.30%), and LHV (9.57 MJ/m^3), and minimum CO_2 (14.97%) produced at the operating conditions of 850℃, 1 bar pressure, SBR of 0.2, and blend ratio of corncob, coconut coir, and coconut shell of (1:1:2). This research investigated the potential of biomass in Bangladesh and the energy content in biomass, which encourages the commercial use of co-gasification technology and helps rural communities manage their waste sustainably and efficiently.

সারসংক্ষেপ

কো-গ্যাসিফিকেশন হল কৃষি অবশিষ্টাংশ থেকে প্রাপ্ত জৈববস্তুপুঞ্জের জন্য সবচেয়ে আশাব্যঞ্জক থার্মোকেমিক্যাল রূপান্তর প্রযুক্তিগুলির মধ্যে একটি এবং কৃষি অবশিষ্টাংশের কো-গ্যাসিফিকেশন ট্রিটমেন্ট কার্যকরভাবে বর্জ্য ব্যবস্থাপনা ব্যবস্থা এবং সবুজ শক্তি উৎপাদনকে বাড়িয়ে তুলতে পারে। বর্তমান গবেষণায়, অ্যাস্পেন প্লাস সফ্টওয়্যার ব্যবহার করে একটি ফিক্সড-বেড গ্যাসিফায়ারে কর্নকোব, নারকেল নারকেল এবং নারকেল শেল বায়োমাসের কো-গ্যাসিফিকেশন সিমুলেট করা হয়েছে এবং মডেলটি পূর্বে প্রকাশিত সাহিত্য ব্যবহার করে বৈধ করা হয়েছে। বর্তমান মডেল তাপমাত্রা (500-1200°C) চাপ (1-20 বার) বাষ্প-থেকে-বায়োমাস অনুপাত (SBR) (0.2-1) এবং সমতুল্য অনুপাত (ER) (0.1-0.6) সিনগ্যাস গঠন, ঠান্ডা গ্যাস দক্ষতা (CGE) এবং কম গরম মান (LHV) এর প্রভাব তদন্ত করে। তাপমাত্রা বৃদ্ধির সাথে সাথে H_2 এবং CO উৎপাদন বৃদ্ধি পায় এবং চাপ ও ER এর সাথে হ্রাস পায়, যেখানে CO_2 বিপরীত প্রবণতা দেখায়। একটি উচ্চতর বাষ্প-থেকে-জৈববস্তুপুঞ্জের অনুপাত H_2 এবং CO_2 এর উৎপাদন বাড়ায়। তবে, উচ্চ SBR এর সঙ্গে CO এর পরিমাণ দ্রুত হ্রাস পেয়েছে। তাপমাত্রা, SBR এবং ER বৃদ্ধির সাথে সিনগাসের LHV হ্রাস পায়। যাইহোক, চাপ বৃদ্ধি LHV বাড়ায়। এই গবেষণায়, কো-গ্যাসিফিকেশন প্রক্রিয়ার অপারেটিং অবস্থার অনুকূলকরণের জন্য দুটি মেশিন লার্নিং মডেল তৈরি করা হয়েছিল।র্যান্ডম ফরেস্ট (আরএফ) এবং গ্রেডিয়েন্ট বুস্টিং রিগ্রেশন (জিবিআর) মডেল বিবেচনা করা হয়। ফলাফল দেখায় যে GBR মডেলের অপারেটিং অবস্থার অপ্টিমাইজেশনের জন্য আরও ভাল নির্ভুলতা ($R^2 \geq 0.99$ এবং RMSE ≤ 2.66) রয়েছে। মডেলটি দেখায় যে সর্বাধিক H_2 (54.13%), CO (29.52%), CGE (90.30%), এবং LHV (9.57 MJ/m^3) এবং সর্বনিম্ন CO_2 (14.97%) 850°C এর অপারেটিং অবস্থায় উত্পাদিত, 1 বার চাপ, এসবিআর 0.2, এবং কর্নকোব, নারকেল কোয়ার এবং নারকেল শেলের মিশ্রণ অনুপাত (1:1:2). এই গবেষণাটি বাংলাদেশে জৈববস্তুপুঞ্জের সম্ভাবনা এবং জৈববস্তুপুঞ্জের শক্তির পরিমাণ অনুসন্ধান করে, যা সহ-গ্যাসীকরণ প্রযুক্তির বাণিজ্যিক ব্যবহারকে উৎসাহিত করে এবং গ্রামীণ সম্প্রদায়কে তাদের বর্জ্যকে টেকসই ও দক্ষতার সাথে পরিচালনা করতে সহায়তা করে।

List of Publications

The published articles from the thesis are as follow.

1. *Redoy Masum Meraz, Md. Mizanur Rahman, Tafsirul Hassan, Md. Shamaoun Ali, Md. Abdus Salam.* Characterization and performance analysis of syngas from corn cob gasification using aspen plus simulation. Mechanical Engineering Research Journal (MERJ), Vol.13, 2024 (Accepted)
2. *Redoy Masum Meraz, Md Mizanur Rahman, Tafsirul Hassan, Abdullah Al Rifat, Abidur Rahman Adib.* A review on algae biodiesel as an automotive fuel. Bioresource Technology Reports, 2023
3. *MD Farhan Imtiaz Chowdhury, MD Fahim Sadat Bari, Muhaiminul Islam, Wasif Sadman Tanim, Redoy Masum Meraz.* Unlocking the potential of green hydrogen for a sustainable energy future: a review of production methods and challenges. Future Energy, 2024

Table of Contents

List of Figures

List of Tables

Nomenclature

MC	Moisture content	HHV	Higher heating value
VM	Volatile matter	LHV	Lower Heating Value
FC	Fixed carbon	CGE	Cold Gas Efficiency
ASH	Ash content	P_g	Gasification Pressure
SBR	Steam to biomass ratio	LDPE	Low-Density Polyethylene
ER	Equivalence ratio	CGR	Co-gasification ratio
SR	Steam flow rate	OFMSW	Organic Fraction of Municipal Solid Waste
AFR	Air fuel ratio	MSW	Municipal Solid Waste
SFR	Syngas flow rate	RDF	Refused Derived Fuel
S/F	Steam-to-feed ratio	ML	Machine Learning
PE	Polyethylene	RF	Random Forest
		GBR	Gradient boosting regression

Chapter 1

Introduction

1.1 Background

Energy, which powers growth, sustainability, and societal advancement, is essential to human existence and civilization. The need for energy is continuously rising with regard to of production as well as usage due to growing population density and an increasing rate of industrialization [1]. Rapid rise in population, urbanization, high living standard, and industrialization led to increased demand for energy. Depletion of fossil fuel is increasing to meet the demand. Global petroleum oil consumption has increased from 24577 terawatt-hours in 1969 to 53620 terawatt-hours in 2019. Petroleum oil consumption has increased by about 118% in last 50 years [2]. Fig. 1.1 demonstrates major energy consumption by source. If the consumption rate of fossil fuel continues, energy reserves will be depleted in near future. Hence, increased focus on renewable energy sources has become mandatory to avoid such energy crisis.

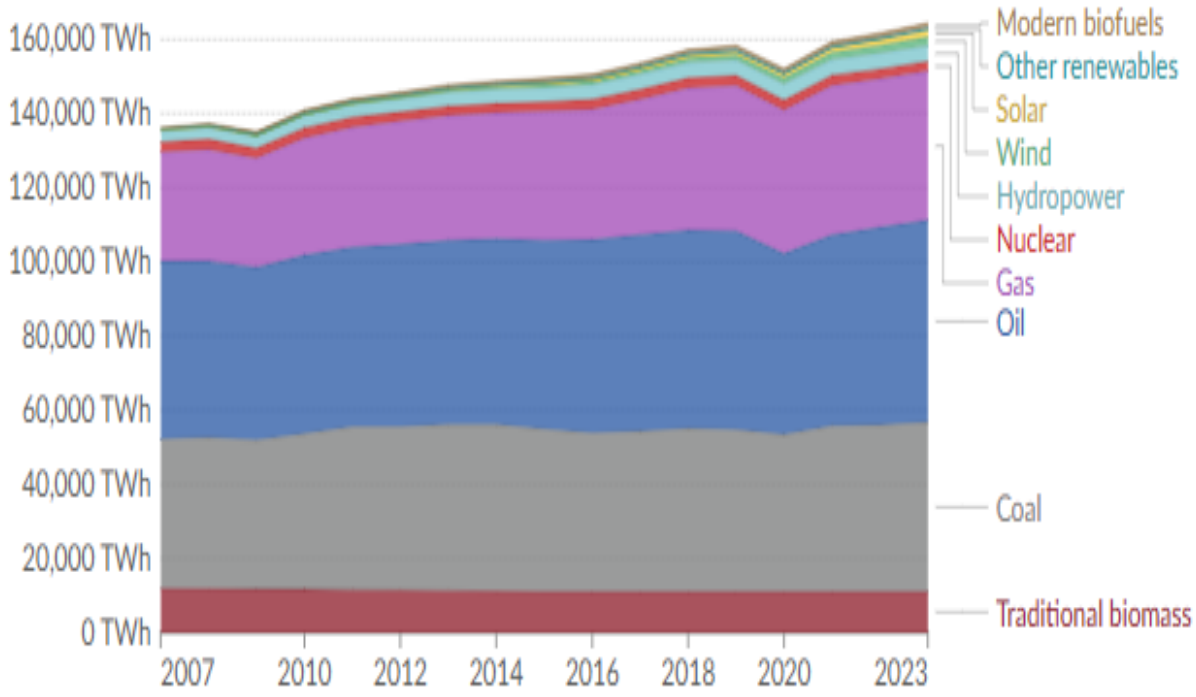

Fig. 1.1: Major energy consumption by source [3].

Traditional energy sources, such as those derived from coal, oil, and natural gas, have shown to be quite successful in advancing economic development [4]. All the listed sources are nonrenewable energy sources and referred to as fossil fuel. In 2023, the total quantity of fossil fuels burned worldwide was 140,231 terawatt-hours. It is the highest value over the time under investigation (1965-2023) and has increased rapidly [5]. Fossil fuel consumption is rising fast because of their excellent energy conversion efficiency and little need for post-extraction treatment. Rising Demand for fossil fuels has been leading to a notable depletion of reserves and an increased risk of their extension because they are non-renewable and have a limited supply. Because of this, people all around the world are becoming increasingly concerned that an energy crisis may arise soon if fossil fuel supplies continue to run low [6]. Moreover, fossil fuel combustion releases emissions into the atmosphere that lead to climate change, temperature rise, and air pollution, all of which have a negative impact on public health and standard of living [7]. Petroleum diesel is vastly utilized in automobiles, marines, locomotives, and industrial applications. Diesel engines are readily known for high thermal efficiency and limited carbon dioxide (CO_2) emission. However, they are liable for high emission of nitrogen oxides (NOx), carbon monoxide (CO), unburned hydrocarbon (HC), and particulate matter (PM) [8]. The harmful emissions produced by petrodiesel negatively affect ecosystem and human health.

The disadvantages of fossil fuels have spurred scientists to explore the possibility of obtaining energy from renewable sources and thus it is important to transit to alternative greener fuel sources. With the waste-to-energy industry expanding and developing quickly, biofuels from biomass have surprisingly grown to be a significant source of the world's energy supply among the numerous renewable energy sources [9]. At present, biofuel is getting attention for being renewable, biodegradable, and environmentally friendly [10]. In addition, PM, HC, and CO emissions are significantly reduced except NO_X for the application of biofuel [11]. Being oxygenated fuel, the usage of biofuel in CI engines helps enhance complete combustion and thus reduce exhaust emissions. Biofuel has some distinct advantages over fossil fuels. For example, biofuel possesses higher cetane number (CN) and lubricity, contains less sulfur and aromatics, and emits less green-house gases [12]. However, some problems and concerns associated with biofuel are limiting its wide application in automotive sectors. For example, biofuel has higher viscosity, higher density, and lower calorific value that lead to poor engine performance [13–20]. Application of biofuel in colder environment is also restricted by the poor cold flow properties of biofuel [21].

Everything that is organic and comes from plants is referred to as biomass (including algae, plants and grains). All vegetation, both on land and in water, as well as all organic wastes, are considered biomass because it is created when green plants perform photosynthesis to transform daylight into plant material [22]. Energy from biomass can be obtained using thermochemical and biochemical processes [23]. Biochemical conversion involves process like fermentation that transforms biomass into biofuels through the digestive process of living organisms [9]. Biological transformation of low-value lignocellulosic biomass continues to confront difficulties because of its low effectiveness and economy [24]. Gasification, pyrolysis, and combustion are typical thermochemical techniques [25]. The net efficiency of burning biomass to generate power is often relatively low, ranging from twenty to forty percent [26]. The broad adoption of biomass pyrolysis technology has been hampered by the limited applications and challenges associated with downstream bio-oil handling [27]. The most well-known thermochemical method for converting waste and biomass to energy is gasification, which is attracting increasing amounts of research and economic attention [28]. A thermochemical method where solid biomass is subjected to a small amount of gasifying medium is known as gasification, which produces useful gases like methane (CH_4), carbon dioxide (CO_2), carbon monoxide (CO), hydrogen (H_2) as well as char as byproduct [29]. In its entirety, gasification is the process of converting a solid or liquid feedstock into a usable gaseous fuel or chemical feedstock that may be burned to release useful energy [30]. One of the most effective methods of releasing the energy contained in biomass is gasification, which turns biomass into a mixture of gases by partial oxidation [31]. This mixture of gases resulted from gasification is identified as syngas. The impact of feedstock variety and blend on syngas production by co-gasification is currently grabbing the attention of scientists [32]. The process of combining two or more fuels for gasification is called co-gasification. Biomass and coal of different grades, woody biomass and nonwoody biomass, or any combination of two or more fuels can be used [33]. Co-gasification has a benefit over traditional gasification in that it allows for the modification of the feedstocks and blend ratio to get the intended syngas composition. It can used for a variety of feedstocks, including metropolitan solid garbage, glycerol, black liquor, and drainage sludge. Such feedstocks are challenging to gasify using traditional methods, which emphasizes the necessity of co-gasification [32].

Application of catalysts in gasification technology is proved to provide better output. When catalysts are added during biomass gasification, a number of processes are accelerated, including tar cracking, steam reforming, thermal cracking, and dry reforming [34]. Tar

breakdown produces gaseous species such as H_2, CO, CH_4, and CO_2 from tar, the undesirable gasification byproduct. When employed in biomass gasification, catalysts promote heat and mass transmission between particles, resulting in better gasification reactions such as partial combustion, steam methane reforming and water gas reactions [35]. When biomass is gasified, several catalysts are employed to remove tar from the resulting syngas and raise the level of H_2 in the syngas. Because of their unique qualities and capacity to minimize tar and modify the dispersion of gases, dolomite, olivine, alkali catalysts and nickel-based catalysts are the most widely used and favored catalysts in biomass gasification [35, 36]. Syngas is considered as a source of fuel specially hydrogen fuel. The gasification syngas can be applied in power generation, automotive fuel, fuel cell etc.

Optimization of the operating conditions of the co-gasification process to maximize H_2 production, CGE, LHV, and syngas yield is another crucial point in this study. Machine learning (ML), a new data-driven approach, has recently caught the attention of academic scholars [37]. ML techniques have been extensively used to model and interpret the techniques for converting biomass and offering guidance to maximize the circumstances of operation [38].

1.2 Biomass Potential in Bangladesh

Through photosynthesis, biomass converts solar energy into chemical energy that may be stored. As a result of absorbing sunlight, plants produce glucose (a sugar) and oxygen (O_2) from carbon dioxide (CO_2) in the air and water (H_2O) in the soil. The molecular connections between the glucose molecules store energy. To create more complex molecules like cellulose and lignin, which comprise plant structures like stems, leaves, and roots, plants utilize glucose and other sugars created during photosynthesis. Chemical connections between carbon and hydrogen (C-H) and carbon and carbon (C-C) allow these molecules to store energy. The chemical energy stored in biomass is released as fuel, heat, or electricity when it is burned, digested, or chemically treated.

There are numerous benefits to using biomass energy resources, including increased capacity, reduced cost, reduced sulfur content, reduced ash content, and renewability. However, it also has certain drawbacks, including a larger water content, a lower unit thermal output, a big volume, a decentralized resource, and an inability to be collected, stored, or transported.

However, a number of factors, including local conditions, appropriate potentiality measurements, the application of existing science and technology, the choice of a sensible technical program, the adoption of cutting-edge techniques, the creation of new energy conversion methods, attention to the economy of biological systems and energy utilization efficiency, and the development of advanced techniques, can make biomass resources more effective and efficient for the nation to meet its future energy needs [39]. Bangladesh's extensive agricultural operations, large animal population, and production of organic waste make it a country with enormous potential for using biomass energy. Biomass already plays a vital part in the nation's energy mix because a sizable portion of the rural population depends on conventional fuels like firewood and crop wastes.

Table 1.1: Land Distribution of Bangladesh [40]

Land Type	Area (mha)	Percentage (%)
Cultivated Land	10.43	70.678
Forest	2.57	17.41
Urban	1.16	7.86
Others	0.597	4.052
Total	14.757	100

The total area of Bangladesh is 56,977 square miles, or 1,47,570 square kilometers. In Bangladesh, forest areas make up around 17% of the country's total area, while agricultural land makes up 70%. Agricultural land, forestland, and urban area are the primary land use types in Bangladesh. Currently, 10.43 million hectares (mha) of agricultural land, 2.57 mha of forest, and 1.16 mha of urban area are available in the country. Tea, rubber gardens, water, and other land use account for the remaining 0.597 million hectares. Table 1.1 indicates that approximately 70% of the land area is allocated for agricultural purposes. Such a high percentage of cultivated land is found in only a few countries worldwide.

Numerous meteorological factors, such as temperature, precipitation, solar radiation, and atmospheric carbon dioxide, affect a nation's capacity to produce agricultural goods. Additionally, the rain-fed environment produces a huge amount of biomass resources. Bangladesh frequently experiences monsoon weather that is subtropical. The most prevalent seasons are winter, summer, and monsoon, yet there are six different seasons in a year. June to October is when the monsoon season occurs. During this period, 80% of the total rainfall takes

place. The average annual rainfall is between 1429 and 4338 millimeters. The coastal areas of Chattogram and the northern Sylhet district receive the greatest rainfall, while the western and northern parts of the country receive the least. The nation thus boasts a climate that is ideal for the year-round development of biomass plants. In some places (large floodplains), sediments deposited by yearly floods naturally nourish the soil, resulting in fertile soil. River water that is rich in minerals and nutrients is carried by floods and deposits as sediment on the ground. The soil is restored by this procedure, becoming extremely productive and fit for farming [40, 41].

The primary renewable energy source utilized for cooking and heating in rural areas is biomass. Since a large portion of Bangladesh's population lives in rural areas, traditional biomass fuels constitute the primary energy source for these populations. Most rural homes have traditional cookstoves that burn biomass, called "chulas" in the local dialect. These stoves burn firewood, manure, or crop waste to cook food every day. In certain locations, biogas is becoming a more well-liked and sustainable alternative due to small-scale biogas operations. In certain locations, biogas is becoming a more well-liked and sustainable alternative due to small-scale biogas operations. Nonetheless, there is a significant risk to indoor air quality and health due to these stoves' frequent inefficiency, particularly for women and children who spend more time in the kitchen. Households also must gather a lot of fuel due to this inefficiency, which in some areas leads to deforestation. Programs for improved cookstoves are intended to reduce smoke emissions and boost biomass burning efficiency. Because they use less fuel and produce less smoke, these stoves help to promote health and reduce deforestation.

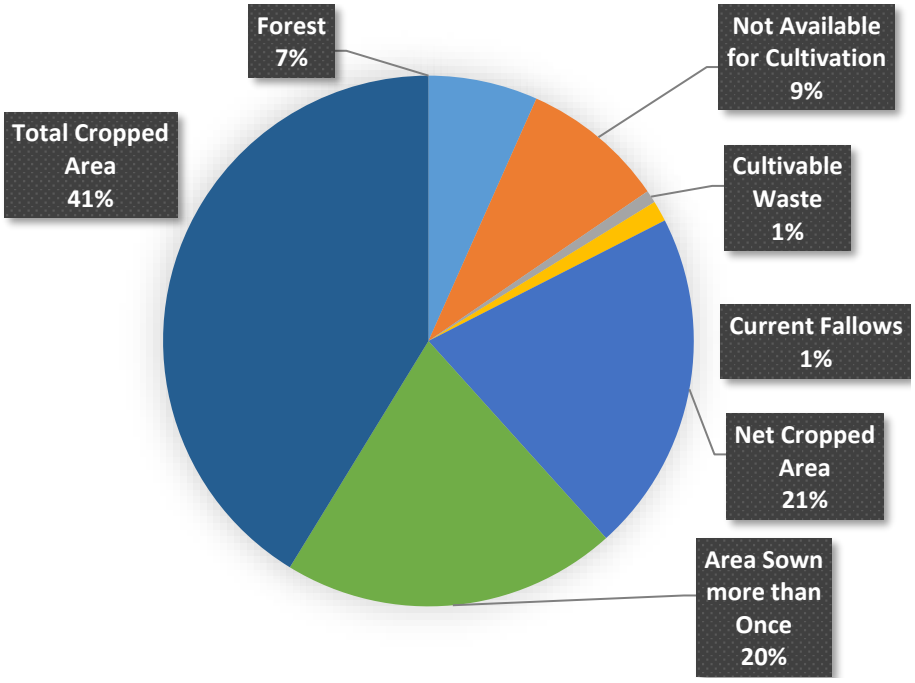

Fig.1.2: Land utilization of Bangladesh.

This study analyzed the availability of biomass residues across various land types in the country. The area encompasses forests totaling 6,363 thousand acres and a Net Cropped Area of 20,081 thousand acres. Collectively, these regions account for 72% of the nation's total area. Due to insufficient data on biomass production, it was not possible to evaluate the supply of biomass residues from Cultivable Waste (671 thousand acres), Current Fallow (1066 thousand acres), and Not Available for Cultivation (8284 thousand acres) lands, as illustrated in Fig. 1.2. The total area is comprised of 28% from these categories. Some of these lands are utilized for livestock grazing, fodder production, and tree cultivation. From the perspective of biomass supply, these areas can be categorized as "non-cropped land" designated for fodder production and "non-forest land" intended for tree cultivation. The total area classified as Not Available for Cultivation includes various water bodies that are unsuitable for biomass production for fuel, as well as village forests and government forest land. [42]. Here, cultivable waste means the area suitable for cultivation but lying fallow for more than one year. Then, current fallow indicates the area already brought under cultivation but not cultivated during the year. Total cropped area is the total of net cropped, and area sown more than once. [40]

1.2.1 Agricultural Residue

Bangladesh is an agro-driven nation, with around 78% of its land used for agriculture (Fig. 1.2). In FY 2021–2022, the agriculture industry accounts for about 11.66% of the country's GDP. According to the preliminary report of the Quarterly Labour Force Survey 2022, around 45.33% of the labor force is employed in this industry. Rice, maize, wheat, sugarcane, vegetables, millet, cotton, groundnuts, coconut, pulses, and so on are the most often produced crops. The primary grains among them are maize, wheat, and rice. Table 1.2 displays their output over the following years.

According to [43], in 2020-21 total major cereals production in Bangladesh was 38693124 metric tons which reached 39231026 metric tons in 2021-22. In 2022-23, this number jumped into 40265372 metric tons of which, rice shares a bigger portion. These crops generate different types of waste like straw, husk, stalk, bagasse etc. As residue production depends on crops production, this estimate gives an approximate idea about the production of biomass. Among recoverable biomass, agricultural residues hold a greater fraction. Agricultural residues include two types of residues such as field residue and process residue. Field residues are left in the field after harvesting and are generally used as fertilizer [44]. Not all field residues are recoverable. The specific local climatic and soil conditions affect the percentage of field residues of a crop to be recycled onto the land. Process residues are generated during crop processing, e.g., milling. These residues are available at a central location [45]. For example - rice straw and rice husk stand out as the primary residues resulting from rice cultivation. Rice straw denotes the dried stalks of cereal plants that remain in the fields after harvesting. Conversely, rice husk constitutes the outer layer of the rice grain and rice straw, categorized as residues from the processing phase [42]. Field crop residues have an assumed recovery rate of 35%, while process crop residues are assumed to have a 100% recovery rate [46, 47]. Residue production from crops is based on the residue production rate (RPR). Numerous research has been conducted in neighboring Asian countries to calculate useful residue to yield ratio for several agricultural crops. Summarized data of residue production and residue recovery from basic types of crops are shown in Table 1.3.

Table 1.2: Crops Production in Bangladesh [40]

Crops	**2022-23**		**2021-22**		**2020-21**	
	Area '000'Acres	Production '000' Metric Tons	Area '000'Acres	Production '000' Metric Tons	Area '000'Acres	Production '000' Metric Tons
Rice	28754	39095	28891	38144	28912	37608
Wheat	783	1170	778	1086	813	1085
Maize	1227	4563	1182	4262	1186	4116
Sugarcane	172	2983	179	3087	192	3333
Jute	1804	8458	1783	8432	1686	7725
Pulse	880	440	926	432	919	425
Tea	141	93	140	98	136	90
Tobacco	93	87	100	93	100	89
Vegetables	1138	5495	1125	6010	1120	4587
Coconut	75	404	74	412	89	403
Groundnut	98	75	100	75	86	67
Soya Bean	146	107	145	99	142	91
Cotton	29	66	30	71	31	72
Jower	0.1168	0.06032	.1647	0.08001	0.134	0.063
Betelnut	97	342	97	334	115	346

Table 1.3: Crop residue characteristic factors [5, 8-11]

Crop	Residue	RPR	RRF	SAF	Total Production			Total Residue		
					2022-23	2021-22	2020-21	2022-23	2021-22	2020-21
Rice	Husk	0.267	1	0.8	39095	38144	37608	8350.692	8147.558	8033.068
	Straw	1.695	0.35	0.21				4870.5528	4752.074	4685.298
Wheat	Straw	1.75	0.35	0.2	1170	1086	1085	143.325	133.035	132.9125
Maize	Stalks	2	0.35	1	4563	4262	4116	3194.1	2,983.40	2881.2
	Cob	0.273	1					1245.699	1163.526	1123.668
Sugar cane	Leafs	0.3	0.35	1	2983	3087	3333	313.215	324.135	349.965
	Bagasse	0.29	1	0.21				181.6647	187.9983	202.9797
Jute	Stalks	3	0.35	0.5	8458	8432	7725	4440.45	4426.8	4055.625
Pulses	Residue	1.9	0.35		440	432	425	292.6	287.28	282.625
Ground nut	Straw	2.3	1	0.64	75	75	67	110.4	110.4	98.624
	Husk	0.477	1					35.775	35.775	31.959
Coconut	Shell	0.12	1		404	412	403	48.48	49.44	48.36
	Husk	0.419	1	0.57				96.48732	98.39796	96.24849
Cotton	Stalks	2.755	0.35	0.68	66	71	72	43.27554	46.55399	47.20968
Tobacco	Stalks	2	0.35		87	93	89	60.9	65.1	62.3
Barley	Straws	1.75	0.35		0.159	0.172	0.174	0.0973875	0.105607	0.106575
Betelnut					342	334	346			

RPR: Residue production ratio, RRF: Residue recovery factor (kg/kg of residue), SAF: Surplus availability factor (kg/kg of residue)

In Bangladesh, rice straw is commonly utilized as livestock, poultry, and fish feed. Notably, there has been a growing trend in the small-scale utilization of rice husk for electricity production. The rice milling sector is the primary consumer of energy derived from rice husk. In the fiscal year 2022–23, the total recoverable rice residues in Bangladesh amounted to 13221.24484 Metric tons, with an estimated overall energy potential of 0.188545341 PJ. Other energy sources from various agricultural crops, such as sugarcane, coconut husks, maize stalks,

maize husks, cotton stalks, groundnut straws, and husks, contributed to generating almost 3.88E-02 TWh electricity in the same fiscal year, as detailed in Table 1.4.

Table 1.4: Energy potential of agricultural residue [5, 8-11]

Crop	Residue	Total Residue			Moisture (%)	Dry Content (ton)	LCV (Gj/t)	Energy Content (PJ)	Electricity generation (TWh)
		2022-23	2021-22	2020-21					
Rice	Husk	8350.692	8147.5584	8033.0688	12.4	7315.206192	16.3	0.119237861	0.033121628
	Straw	4870.55284	4752.0749	4685.2987	12.7	4251.992629	16.3	0.06930748	0.019252078
Wheat	Straw	143.325	133.035	132.9125	7.5	132.575625	15.76	0.002089392	0.000580387
Maize	Stalks	3194.1	2,983.40	2881.2	12	2810.808	14.7	0.041318878	0.011477466
	Cob	1245.699	1163.526	1123.668	15	1058.84415	14	0.014823818	0.004117727
Sugarcane	Leaf	313.215	324.135	349.965	50	156.6075	15.81	0.002475965	0.000687768
	Bagasse	181.6647	187.9983	202.9797	49	92.648997	18.1	0.001676947	0.000465819
Jute	Stalks	4440.45	4426.8	4055.625	9.5	4018.60725	16.91	0.067954649	0.018876291
Pulses	Residue	292.6	287.28	282.625	20	234.08	12.8	0.002996224	0.000832284
Ground nut	Straw	110.4	110.4	98.624	12.1	97.0416	17.58	0.001705991	0.000473886
	Husk	35.775	35.775	31.959	8.2	32.84145	15.66	0.000514297	0.00014286
Coconut	Shell	48.48	49.44	48.36	8	44.6016	18.53	0.000826468	0.000229574
	Husk	96.48732	98.39796	96.24849	11	85.8737148	18.53	0.00159124	0.000442011
Cotton	Stalks	43.27554	46.55399	47.20968	12	38.0824752	16.4	0.000624553	0.000173487
Tobacco	Stalks	60.9	65.1	62.3	8.9	55.4799	17.7	0.000981994	0.000272776
Barley	Straws	0.0973875	0.1056073	0.106575	15	0.082779375	12.38	1.02481E-06	2.84669E-07

1.2.2 Animal Manure

Organic material used as fertilizer in agriculture is referred to as manure. Manure adds nutrients to the soil, including potassium, phosphorus, and nitrogen, all of which are necessary

for plant growth. Livestock such as sheep, pigs, horses, cows, and poultry are the source of animal manure. Domesticated animals raised in agricultural settings for labor and the production of goods including meat, eggs, milk, fur, leather, and wool are known as livestock.

One of the main sources of biomass energy in Bangladesh is animal manure. It is widely used for both fertilization and the production of energy-producing biogas. A common natural fertilizer in agriculture is cattle manure. By enriching the soil with essential elements like potassium, phosphorus, and nitrogen, it promotes crop development. Using manure as fertilizer is an environmentally friendly way to increase soil health and reduce the need for artificial fertilizers. Small-scale biogas facilities in rural Bangladesh are mostly powered by animal waste, particularly cow dung. These plants employ anaerobic digestion, in which microorganisms break down the organic materials in the manure to produce biogas, mostly methane, and digestate, a nutrient-rich byproduct.

Table 1.5: Number of livestock [40]

Livestock/ Poultry	**Number of Livestock**		
	2022-23	**2021-22**	**2020-21**
Cattle	248.56	247.00	245.45
Buffalo	15.16	15.08	15
Goat	38.27	267.74	266.04
Sheep	269.45	37.52	36.79
Total Ruminant	571.43	567.34	563.28
Chicken	3196.89	3118.00	3041.06
Duck	660.16	638.45	617.46
Total Poultry	3857.04	3756.45	3658.52
Total Livestock	4428.47	4323.79	4221.80

Table 1.5 shows that total head of livestock in FY 2022-23 is 4428.47 million. The dung yield for both ruminant and poultry have been gathered from neighboring Asian countries weighing 7.50 kg of wet matter per animal per day for cattle, 10 kg per animal per day for buffaloes, and 0.38 kg per animal per day for goats, sheep weigh 0.38 kg of wet matter per animal while poultry weigh 0.10 kilogram per day**.** Thus, multiplying the heads by dung yield, a total yield of 919.230089 tons/year has been estimated in Table 1.6.

Table 1.6: Residue Generation from Livestock [42]

Livestock/Poultry	Heads (millions)	Dung yield (kg/animal/day)	Residues Generation (tons/year)
Cattle	248.56	7.5	680.433
Buffalo	15.16	10	55.334
Goat	38.27	0.38	5.308049
Sheep	269.45	0.38	37.372715
Total Ruminant	571.43		778.447764
Chicken	3196.89	0.1	116.686485
Duck	660.16	0.1	24.09584
Total Poultry	3857.04		140.782325
Total Livestock	4428.47		919.230089

According to the factor, Bangladesh's expected recoverable quantities of poultry droppings and animal waste for FY 2022–2023 were 253408185 tons and 1479050752 tons, respectively. Based on the reduced calorific value and moisture content of biogas, the energy content for FY 2022–2023 was determined to be 3179.04168 PJ for livestock and 855.252624 PJ for poultry. The relative amounts of electricity generated are 883.0671324 TWh and 237.5701734 TWh, presented in Table 1.7.

Table 1.7: Energy Potential of Livestock

Livestock/ Poultry	Residues generation (ton/year)	RRF	Residues recover amount (ton)	Moisture (%)	Dry Content (ton)	LCV (Gj/ ton)	Energy content (PJ)	Electricity generation (TWh)
Cattle	680.433	0.5	340.2165	0.4	204.1299	13.86	0.00282924	0.0007859
Buffalo	55.334	0.5	27.667	0.4	16.6002	13.86	0.00023008	6.39108E-05
Goat	5.308049	0.6	3.184829	0.4	1.91089764	13.86	2.6485E-05	7.35696E-06
Sheep	37.37272	0.3	11.21181	0.4	6.7270887	13.86	9.3237E-05	2.58993E-05

Total Ruminant	778.4478	1.9	1479.051					
Chicken	116.6865	0.9	105.0178	0.5	52.50891825	13.5	0.00070887	0.000196908
Duck	24.09584	0.9	21.68626	0.5	10.843128	13.5	0.00014638	4.06617E-05
Total Poultry	140.7823	1.8	253.4082					
Total Livestock	919.2301	3.7	3401.151					

1.2.3 Municipal Solid Waste

Solid garbage produced by homes, businesses, organizations, etc. is referred to as municipal solid waste (MSW). Perishable organic trash, glass, paper, plastics, metals, and other materials make up the waste. Automobile scrap and building or demolition waste are typically excluded from MSW [48]. Economic position, food patterns, age, gender, and seasonal fluctuations within families are some of the variables that affect the amount of garbage produced per person. As a result of increased industrialization, population growth, and better living standards, solid waste rates are rising in Asian cities. In order to control the fast accumulation of trash in metropolitan areas, governments understand the need of putting Green Productivity (GP) strategies into practice, such as waste reduction, recycling, reuse, and recovery [49].

Urban and rural population shares 40.46% and 59.54% of total population of Bangladesh respectively. According to reports, Bangladesh's urban and rural areas generate 0.41 and 0.15 kilogram of waste per person per day, respectively [42].

Table 1.8: Municipal Solid Waste Generation [42]

MSW	Generation Ratio (kg/capita/day)	Population	Residue Generation (ton/year)	RRF	Waste recovery rate (million ton/year)
Urban	0.4	72,825,128	10632468.69	0.7	7.442728082
Rural	0.15	100,737,236	5515363.671	0.7	3.86075457
Total			16147832.36		11.30348265

Total residue generation is estimated by multiplying the population with the respective ratio. Thus, a total of 15856730.9 ton/year residue has been generated. The recovery factor is

estimated to be 70%. Now, residue generation is multiplied by recovery factor 0.7. Now, the waste recovered is 11.09 million ton/ year. Though rural areas generate a huge waste, waste, this waste couldn't be used as biomass because of lack of proper waste management scheme in rural areas. Also, though Bangladesh has 64 districts and 11 city corporations, waste generation data is only available for 6 major city corporations as proper management is not available. Table 1.9 shows the total energy content of Bangladesh estimated 113.305856 PJ having 45% moisture content and lower calorific value of 18.56.

Table 1.9: Energy potential of MSW in Bangladesh [42]

MSW	Waste recovery (million ton/year)	Moisture content (%)	Dry recovered waste (million ton/ year)	Lower calorific value (MJ)	Energy content (PJ)
Urban	7.4427281	0.45	4.093500445	18.56	75.97536826
Rural	3.8607546	0.45	2.123415014	18.56	39.41058265
Total	11.303483				115.3859509

1.2.4 Forest Residues

The term "forest residue" describes the organic matter that remains after forestry activities like logging or tree harvesting, as well as organic matter that naturally builds up in forests. Additionally, all types of forest leftovers and sawmill wood processing byproducts are included in the term "forest biomass." Table 1.10 displays the total potential biomass and theoretical energy content from various forest-related sources. The moisture level of wood fuel and wood processing waste is 20%. Therefore, the net quantity can be obtained by taking into account the dry content and multiplying by the total amount. Energy content is evaluated while taking into account a lower calorific value. This energy content is converted into the production of electricity. A total of 58.5033 TWh of electricity and 210.61 PJ of energy content have been produced.

Table 1.10: Energy potential of Forest residues in Bangladesh

Forest products	Amount (million tons)	Moisture content (%)	Net amount (million tons)	Lower calorific value (GJ/ton)	Energy content (PJ)
Wood fuel	15.46	20	12.368	15	185.52
Tree residue	1.82	0	1.82	12.52	22.7864
Wood residue	0.16	20	0.128	18	

1.3 Biomass Feedstock Properties

Understanding the feedstock properties is essential to determining which amount and type of fuel will be produced during the gasification process. Proximate and ultimate analysis is used to understand the characteristics of any biomass feedstock. Table 1.11 shows the ultimate and proximate analysis of different biomass, waste, coal, and plastic.

The percentages of carbon, hydrogen, nitrogen, sulfur, and oxygen contained in biomass are determined by ultimate analysis. The amount of carbon in the biomass represents the fuel content and is essential for energy generation through combustion. The higher the carbon content, the more syngas can be produced. Kartal et al.[50] showed that horse manure produces higher CO and H_2 than rice husk and wheat straw as having higher amounts of C and H content. Hydrogen contributes to the energy content when combined with oxygen during combustion and increases the proportion of hydrogen in syngas. Oxygen in the biomass reduces the calorific value, as oxygen-containing compounds lower the energy available for gas production. However, oxygen also helps the gasification reactions by lowering the external oxygen requirement. Lower oxygen content in biomass improves syngas quality, as more external oxygen can be used to maintain controlled oxidation, leading to better gas yield. The ultimate analysis helps to determine the calorific value and environmental impact of biomass during combustion, especially regarding emissions.

The proximate analysis determines the percentages of moisture, volatile matter, fixed carbon, and ash in biomass. The biomass containing high moisture content represents significantly low energy density by mass due to the mass of water. Low moisture content is ideal for efficient gasification, resulting in higher syngas yield and reduced energy losses. A high volatile matter content makes the biomass more reactive and increases the syngas

production rate. High fixed carbon content in biomass is beneficial for maintaining a steady syngas flow, though it demands more energy for complete conversion. High ash biomass can produce more ash at the end of the process, which leads to clinkering, slagging, and blockages of a gasifier. Most biomass materials have a moderate ash content of 2–15 wt%. Clinker formation can be avoided during gasification if gasification occurs at low temperatures [51]. Lower ash content is preferred for gasification, as it reduces maintenance and operational issues, leading to higher efficiency.

Selection of feedstock depends on availability and production of feedstock, cost associated with them, type of biofuel production, degree of unsaturation, regional locations, and climate conditions. Most researchers showed that biomass with high carbon, hydrogen, and volatile matter contents, and low oxygen, sulfur, nitrogen, and ash contents, is ideal for gasification, leading to high syngas yield and fewer operational and less emissions of NOx, H_2S, SOx, etc. Understanding the biomass composition through these analyses allows for better feedstock selection, reactor design, and process optimization in gasification systems.

Table 1.11: Ultimate and Proximate analysis for different feedstocks

Feedstock	Ultimate analysis (wt%)						Proximate analysis (wt%)					Ref.
	C	H	N	S	Cl	O	MC	VM	FC	ASH	HHV (MJ/kg)	
Timber & Wood waste	56.8	7.28	0.18	0.82	0.07	34.29	5.01	93.06	6.38	0.56		[52]
Almond shell	51.71	6.13	0.76	0.03	-	41.35	7.85	70.13	19.22	2.80		[50]
Cotton stalk	53.60	5.20	1.30	1	-	38.90	16.80	57.30	22.10	3.80		
Horse manure	54.33	6.81	1.54	0.16	-	37.15	11.09	59.55	20.64	8.71		
Rice husk	46.97	6.70	0.42	0.02	-	45.78	10	-	-	15.42		
Wheat straw	48.24	6.07	0.80	0.25	-	44.36	15.10	62.32	14.98	7.60		
Pine pellet	47.50	6.20	0.09	-	-	46.21	4.60	78.50	16.60	0.3		[53]
Eucalyptus type A	45.85	6.13	0.35	-	-	47.67	11.80	71	14.60	2.87		
Eucalyptus type B	49.07	6.45	0.07	-	-	44.41	11.40	68.50	19	1.19		
Pine residual forest biomass	50.8	6.5	0.25	-	-	42.45	11	71.10	16.80	1.2		

Coconut coir pith	36.20	0.92	0.36	0.81	-	61.71	11.60	70.10	14.60	3.70		[54]
Coconut coir pith char at 823 K	77.87	0.64	0.07	0.05	-	21.37	2.00	32.00	59.00	7.00		
Eucalyptus wood waste	46.31	6.33	0.03	-	-	47.33	10	73.6	14.68	2.52		[55]
Corncob	42.66	6.39	1.25	-	-	49.7	12.8	77.3	7.6	2.3		
Corncob	39.95	4.97	0.6	0.09	-	46.77	10.52	65.23	16.54	7.71	16.23	[56]
Rice husk	39.27	4.91	0.59	0.1	-	55.23	10.18	64.67	16.82	8.33	16.16	
Sesame stalks	33.67	3.81	0.98	0.16	-	44.56	10.71	55.43	16.88	16.98	14.54	
Cotton gin trash	39.3	4.7	1.21	0.2	-	49.38	10.51	68.42	15.63	5.44	18.26	
Corncob	47.60	6.10	0.52	-	-	45.78	10.1	80.06	17.82	2.12	18.56	[57]
Kitchen wastes	56 ± 6	7 ± 1	10 ± 2	0.23±0.06	-	27 ±3	16 ± 0.55	7±0.73	67±0.88	8±0.41	-	[58]
Date Seeds	47.21	6.61	0.87	0.11	-	45.20	-	83.20	14.36	2.44	19.02	[59]
Sugarcane bagasse	48.10	5.90	0.15	0	0	42.55	-	80.50	16.20	3.30	-	[60]
Bamboo	43.09	5.94	1.11	-	-	49.86	6.82	75	16.08	2.1	16.52[a]	[61]
Canola hull + mustard meal pellets	50.6	7.2	3.7	1.0	-	30.4	21.5	-	-	7.1	22.4	[62]
Oat hull + mustard meal pellets	49.8	6.9	2.6	0.7	-	35.4	19.1	-	-	4.6	21.5	
Torrefied canola hull + mustard meal pellets	53.6	7.0	4.3	1.1	-	24.7	16.6	-	-	9.3	23.0	
Torrefied oat hull + mustard meal pellets	59.1	8.0	3.4	0.8	-	18.1	16.5	-	-	10.6	25.5	
Rubber wood	48.27	6.36	0.14	0	-	45.20	18.5	81	-	0.8	20.54	[63]
Poultry litter pellets	43.98	5.16	4.63	0.75	-	31.98	7.6	63.6	15.3	13.5	-	[64]
Dried Sewage Sludge	19.1	2.3	1.1	0.1	0	5.7	8.3	8.8	19.4	71.8	20.50[a]	[65]
Manure	37.1	5.1	3.7	0.5	1	31.4	27.4	65	13.5	21.6	19.40[a]	

Date Pits Waste	49.8	6.8	4.5	0	0	37.9	5	81.8	17.2	1	34.07[a]	
Coal	52.58	5.90	1.49	1.14	-	38.90	8.18	39.79	33.81	18.22	20.19	[66]
Saw Dust	44.11	5.53	2.14	2.70	-	45.52	11.8	68.05	19.05	1.10	17.17	
Wood Pellet	44.28	6.09	1.05	0.28	-	48.62	9.19	79.00	10.16	1.65	17.46	
75% Coal + 25%Sawdust	50.46	5.80	1.65	1.53	-	40.55	12.27	47.89	36.65	3.19	18.04	
50% Coal + 50%Sawdust	48.35	5.71	1.82	1.92	-	42.21	10.92	48.23	38.41	2.44	18.75	
75% Coal + 25% wood pellet	50.50	5.86	1.38	0.92	-	41.33	9.92	80.85	6.38	2.85	19.00	
50% Coal + 50% wood pellet	48.43	5.83	1.27	0.71	-	43.76	9.32	79.13	8.83	2.72	18.28	
Rural Solid Waste	34.36	4.36	1.06	0.19	-	20.86	41.35	53.10	7.73	39.17	0.423[a]	[67]
Tree bark	41.18	5.65	0.96	0.13	-	44.75	7.33	78.83	14.30	6.87	17.66[a]	
MSW	42.04	5.95	0.65	0.14	-	51.2	4.2	74.5	8.71	12.6	22.4	[68]
Sugarcane Bagasse	43.3	6.11	0.22	0.03	-	50.3	8.4	80.9	3.6	7.9	16.4	
Rice husk	47.7	6.7	0.4	0.9	-	44.3	3.5	25.4	59.9	11.2	14.7	
Woodchips	50.28	6.14	0.17	<0.01	<0.01	43.41	13.2	83.8	15.4	0.8	19.21[a]	[69]
Woodchips (38%) + OFMSW (62%)	48.61	6.72	0.34	0.02	0.03	43.38	15	-	-	0.80	18.72[a]	
Woodchips (70%) + Sewage Sludge (30%)	39.86	4.93	0.42	0.07	0.06	34.61	15.6	-	-	20.0	15.05[a]	
Woodchips (46.5%) + Hazelnut shells (53.5%)	50.48	5.92	0.27	0.02	0.02	42.14	20.3	-	-	1.15	19.26[a]	
Rice husk	41.61	5.57	1.08	0.05	-	51.69	9.18	63.03	6.48	21.31	15.90	[70]
LDPE	83.49	14.07	0.03	0.02	-	2.39	-	99.99	-	-	47.66	
Coal	63.75	4.5	1.25	2.51	0.15	7.02	11.12	34.99	44.19	9.7	26.151[a]	[71]

Pre-treated corn straw	43.43	6.72	0.27	0.22	0	42.86	5.21	74.23	19.27	6.5	15.94[a]	
Coal	74.19	4.59	1.52	0.55	-	7.55	3.10	29.30	56	11.60	30.26[a]	[72]
Pine Bark	74.19	6.54	0.14	0.01	-	38.32	3.23	63.88	31.83	1.06	17.55[a]	
Coal + Pine Bark (1:1)	62.65	5.65	0.78	0.23	-	24.36	3.16	46.59	43.92	6.33	23.91[a]	
Coal	84.60	5.23	1.31	0.32	-	6.49	1.64	31.38	64.92	2.05	35.05	[73]
Rubber	72.97	6.38	0.09	0.5	-	5.36	0.60	48.39	36.32	14.69	33.01	
Woodchips	40.98	4.36	0.12	0.06	-	53.53	12.66	63.24	23.16	0.94	10.52	
Rice husk	44.98	4.8	1.8	0	-	48	6.74	52.5	16.4	23.52	-	[74]
Groundnut shell	46.79	8.60	0.65	0.38	-	43.28	4.23	77.6	14.46	3.25	-	
Industrial sludge	14.75	2.03	0.09	0.31	-	25.25	2.29	39.27	0.87	57.57	3.27[a]	[75]
Municipal sludge	39.79	5.44	6.46	0.95	0.13	21.83	5.54	58.71	10.35	25.40	13.54[a]	[76]
Food waste	42.25	6.47	5.25	0.45	-	37.26	3.02	69.35	19.31	8.32	16.84[a]	[77]
Feedstock	**Ultimate analysis (wt%)**						**Proximate analysis (wt%)**				**HHV (MJ/kg)**	**Ref.**
	C	**H**	**N**	**S**	**Cl**	**O**	**MC**	**VM**	**FC**	**ASH**		
Chlorella Vulgaris	45.49	6.61	10.28	0.21	-	28.69	56.64	79.98	12.30	8.72	-	[78]
Petrochemical industrial sludge	24.99	2.95	2.36	2.04	-	23.34	68.11	50.90	4.78	44.32	-	
MSW	58	9.33	0.73	0.14	-	24.96	5.65	87.21	6.04	6.84	-	[79]
Rice straw	44.28	6.84	1.28	0.29	-	40.71	5.20	78.53	14.86	6.60	-	
RDF(MSW)	41.19	5.81	0.42	0.23	-	40.27	9.16	58.57	16.5	22.92	18.45[a]	[80]
Rice straw	47.58	5.79	0.85	0.38	-	45.4	6.84	66.16	9.35	10.52	16.03[a]	
Pine bark	52.79	6.08	1.19	0.05	-	36.89	4.8	71.1	21.0	3.1	21.40	[81]
Pinewood	50.12	6.59	0.19	0.01	-	42.77	8.5	85.2	14.5	0.3	20.04	
Birch bark	56.34	7.00	0.44	0.02	-	34.83	3.7	80.1	18.5	1.4	24.18	
Birchwood	49.31	6.62	0.08	0.01	-	43.70	7.7	86.9	12.8	0.3	19.94	
Oil shale	27.49	2.75	0.06	1.47	-	16.80	0.5	47.7	0.9	51.4	9.60	
Softwood chips	47.7	5.7	1.0	0.16	-	45.5	-	76.5	22.9	0.6	22.3	[82]
Hardwood chips	46.4	5.5	0.1	0.01	-	48	-	77.3	22.1	0.6	22.4	

Sweet sorghum bagasse	43.5	5.6	0.3	0.13	-	50.5	-	69.8	23.7	6.5	23	
Pine sawdust	46.9	6.1	0	-	-	46.4	-	81.5	17.8	0.6	-	[83]
Used ground coffee	53.9	7.1	2.4	-	-	35.8	-	76.4	22.7	0.9	-	
Wheat straw	43	5.3	0.6	-	-	40.7	-	73.5	16.4	10.1	-	
Waste ethylene vinyl acetate	79.61	14.31	0	-	-	6.17	-	99.91	0.09	0	-	
HDPE	85.7	14.29	0	-	-	0.01	-	99.9	0.01	0	-	
PP	85.56	13.85	0	-	-	0.59	-	99.5	0.5	0	-	
Corncob	43.72	5.44	0.66	0.10	-	50.09	10.52	65.23	16.54	7.71	16.5	[84]
Coal	58.99	0.215	1	0.304	-	39.491	1.67	1.31	57.5	39.52	-	[85]
Briquette	56.27	2.8	0.96	0.03	-	39.94	8.85	78.63	9.41	3.11	-	
Coconut shell	53.73	6.15	0.86	0.02	-	38.45	6.98	72.93	19.48	0.61	-	
Mahua wood	47.57	6.4	0.722	0.025	-	44.96	7.88	77.41	12.63	2.08	-	
Pine sawdust	46.36	5.75	2.26	0.32	-	45.31	4.54	82.18	16.13	1.69	16.91[a]	[86]
Pomegranate woodchips	46.7	6	0.4	<0.01	-	44.7	7.71	81.77	16.03	2.2	19.54	[87]
woodchips	47.6	5.8	0.14	0.009	-	37.15	9.0	77.8	-	0.3	19.30	[88]

HHV= Higher Heating Value, [a]LHV=Lower Heating Value

1.4 Gasification

A thermochemical conversion method transforms carbon-containing materials, such as coal, biomass, or waste, into a mixture of gases known as syngas which primarily consists of carbon monoxide (CO), hydrogen (H_2), methane (CH_4), and carbon dioxide (CO_2). The process occurs in a controlled, low-oxygen environment. It is divided into four distinct zones (drying, pyrolysis, oxidation, and reduction) to streamline the intricate chemical processes involved in gasification. Table 1.12 shows the reactions that occur in the gasification process.

1.4.1 Drying Zone

The drying zone in gasification is the initial stage where the moisture content of the biomass or feedstock is removed before it undergoes further chemical reactions. Efficient drying is essential because biomass typically contains a significant amount of moisture (10-60%, depending on the type of biomass). If this moisture is not removed, it can significantly

reduce the efficiency of the gasification process by consuming energy that could otherwise be used for gas production. The temperature in the drying zone typically ranges from 100°C to 200°C, depending on the moisture content of the feedstock and the type of gasifier [89]. The drying process is mainly driven by heat transfer from the hotter zones (pyrolysis and oxidation) below the drying zone. As hot gases (steam or syngas) rise through the gasifier, they heat the feedstock from below, causing moisture to evaporate. It is a crucial part of the gasification process, where moisture is removed from the biomass, preparing it for efficient thermal decomposition and gas production in subsequent stages. Properly designed and efficient drying can significantly improve a gasifier system's overall efficiency and output.

1.4.2 Pyrolysis zone

In this stage, the feedstock is heated to a high temperature between the range of 300-900℃ in the absence of oxygen. The heat causes the material to decompose into volatile gases and solid char. The volatile gases include hydrogen, carbon monoxide, methane, tar, and other hydrocarbons. Pyrolysis involves breaking chemical bonds in the feedstock by dehydration, devolatilization, thermal cracking, polymerization, and condensation reactions, forming simpler molecules [90]. Products depend on the feedstock composition (cellulose, hemicellulose, lignin) and the process conditions (temperature, pressure, and heating rate).

1.4.3 Oxidation zone

The oxidation/combustion zone in gasification is a critical stage where partial combustion of the feedstock occurs. This stage provides the heat needed for the other stages of the gasification process, such as drying, pyrolysis, and reduction. The goal in this zone is not to completely burn the fuel (as in traditional combustion), but to allow controlled burning, or partial oxidation, to generate the necessary heat while also creating key gases like carbon monoxide (CO) and carbon dioxide (CO_2). Typical temperatures in the oxidation zone range between 900°C and 1500°C, depending on the feedstock and gasifier type. The key chemical reactions in the oxidation zone involve the conversion of carbon (C) and hydrocarbons in the biomass or fuel into CO and CO_2 through partial oxidation. The main reactions are carbon combustion, Hydrogen combustion, and partial combustion of carbon.

1.4.4 Reduction zone

The reduction/gasification zone in a gasification process is a critical part of the overall reaction system where biomass gasification occurs. In this zone, the chemical reduction of gases generated in the earlier stages (such as the oxidation and pyrolysis zone) takes place and produces syngas. This zone is essential for transforming the by-products of combustion into valuable gases for energy or chemical production in a gasifier. The main reactions are the water-gas shift reaction, Boudouard reaction, methanation, and carbon monoxide shift reaction. The temperatures in the reduction zone range between 800°C and 1000°C.

Table 1.12: Gasification reactions

NO.	Reaction	Reaction Name	Heat of Reaction (KJ/mol)
R1	$C + 0.5\ O_2 \longrightarrow CO$	Partial combustion	-111
R2	$C + O_2 \longrightarrow CO_2$	Complete combustion	-393
R3	$CO + 3\ H_2 \longrightarrow CH_4 + H_2O$	Methanation reaction	-206
R4	$CO + 0.5\ O_2 \longrightarrow CO_2$	CO partial combustion	-283
R5	$H_2 + 0.5O_2 \longrightarrow H_2O$	H_2 partial combustion	-242
R6	$C + CO_2 \longrightarrow 2\ CO$	Boudouard reaction	+172
R7	$C + H_2O \longrightarrow CO + H_2$	Water-gas reaction	+131
R8	$CO + H_2O \longrightarrow CO_2 + H_2$	Water-gas shift reaction	-41
R9	$CH_4 + H_2O \longrightarrow CO + 3H_2$	Steam-methane reforming	+206
R10	$C + 2H_2 \longrightarrow CH4$	Hydrogasification	-74.8

1.5 Gasification reactor

A gasification reactor is the core component of a gasification system where the gasification process takes place. It is a highly engineered vessel designed for converting solid or liquid carbon-based materials, such as biomass, coal, or waste, into syngas through a complex series of thermochemical reactions [91]. The reactor is designed to accept different types of carbon-based materials like coal, biomass, or waste. The size and preparation of the feedstock can vary depending on the type of reactor. Typically, it is categorized into fixed-bed, fluidized bed, entrained flow, and plasma gasifier [92].

1.5.1 Fixed bed gasifier

In fixed-bed gasifiers, solid fuel is delivered into the gasifier from the top, and the gasification processes occur over a stationary grate towards the very bottom of the gasifier [93]. It is divided into two categories. In the case of an updraft gasifier, the temperature rises up to 1400℃, the feedstock enters from the top, and the gasifying agent (air or oxygen) is introduced from the bottom. Syngas exits from the top, passing through the fuel bed, which heats up as it moves downward. It has high thermal efficiency, small pressure drops, and a slight tendency to slag formation [94]. The downdraft gasification has the advantage of higher conversion efficiencies with a low rate of tar and particulate matter generation; this type of gasifier is the most widespread reactor for small-scale biomass and carbon conversion for power generation using internal combustion engines [95, 96]. The lower tar concentration is due to gas passing through a high-temperature zone (the combustion zone), which enables the cracking of the tars formed during the gasification process [97]. Both air/oxygen and the feedstock enter from the top, and syngas exit from the bottom in the downdraft gasifier. This design reduces tar formation due to higher outlet temperature [98, 99]. The multistage fixed bed gasification system has recently proved its competence in producing high-quality syngas with minimum tar content, and its overall performance has outranked the conventional designs. Fig.1.3 shows a two-stage downdraft gasifier. Considering high-quality syngas, it represents a promising basis for hydrogen production from biomass [100].

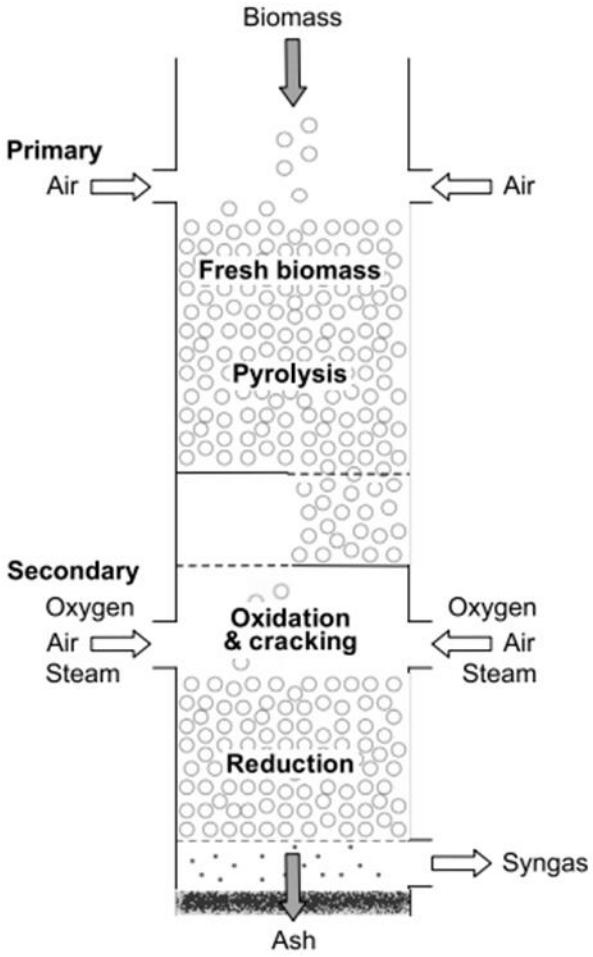

Fig.1.3: Two-stage downdraft gasifier [101].

1.5.2 Fluidized bed gasifier

In this reactor, the feedstock is suspended with a mixture of air or steam, forming a fluid-like medium. This ensures better mixing of the feedstock with the gasifying agent and provides a more uniform temperature, making it suitable for a wide range of feedstocks. Fuel and gasifying agents enter the reactor from the side and lower part of the gasifier, respectively, and syngas and slags exit from the upper and lower parts, respectively [102–104].

1.5.3 Entrained flow gasifier

Fine feedstock particles are injected into the gasifier with the gasifying agent at very high velocities. Gasification occurs at much higher temperatures (up to 1600°C), leading to

cleaner syngas with very little tar or ash content. This type is often used in coal or petroleum gasification. Fuel and gasifying agents enter the reactor from the upper part of the gasifier, and syngas and ash exit from the middle and lower parts, respectively [105].

1.5.4 Plasma gasifier

In this type of reactor, a plasma torch generates extremely high temperatures, breaking the feedstocks into syngas and a glass-like byproduct. Plasma gasifiers are particularly useful for hazardous waste and municipal solid waste.

1.6 Statement of novelty of the study

The co-gasification of agricultural residue is relatively novel and emerging technology. Gasification of various biomass has been studied by many authors. However, there is still a research gap that studies the potential of agricultural residue in Bangladesh and the co-gasification of corncob, coconut coir, and coconut shell on syngas composition. To the best of the authors' knowledge, the effects of temperature, pressure, steam-to-biomass ratio (SBR), and Equivalence ratio (ER) on syngas composition, cold gas efficiency (CGE), and lower heating value (LHV) of syngas has not been explored yet. Thus, motivated by the need, the study focuses on the co-gasification of corncob, coconut coir, and coconut shell.

1.7 Objectives of the study

The ultimate goal of the present study is to explore the effects of temperature, pressure, steam-to-biomass ratio (SBR), and Equivalence ratio (ER) on syngas composition, cold gas efficiency (CGE), and lower heating value (LHV) of syngas. The specific objectives are as follows.

1. To investigate the co-gasification of corn cob, coconut coir, and coconut shell in a downdraft fixed bed gasifier using steam and air as an oxidizing agent.
2. To characterize the proximate and ultimate analysis of the selected feedstocks such as corn cob, coconut coir, and coconut shell.
3. To analyze the effect of temperature, pressure, SBR, and ER on syngas composition, CGE, and LHV.
4. To optimize the operating conditions of co-gasification using a machine learning algorithm.
5. To study a pilot-scale industrial gasification plant.

1.8 Scopes and limitation

1.8.1 Scopes

Biomass co-gasification, the process of gasifying biomass alongside other materials like coal or different biomass types, offers a sustainable pathway for energy production, waste management, and industrial applications. It enables renewable energy generation, reduces greenhouse gas emissions, and promotes circular economies by converting agricultural residues, organic waste, and industrial byproducts into syngas for electricity, biofuels, or chemical synthesis. With its potential to reduce reliance on fossil fuels, foster rural development, and support global climate goals, co-gasification also aligns with renewable energy mandates and carbon neutrality targets. While challenges like feedstock variability, high costs, and scalability exist, advancements in technology, policy support, and carbon capture integration can enhance its viability, making it a key solution for sustainable energy transitions.

1.8.2 Limitations

Analysis of the syngas composition is one of the challenges faced in the study. The co-gasification of corncob, coconut coir, and coconut shell faces several limitations that impact efficiency and feasibility. Corncobs, while offering high volatile matter, can contribute to ash-related issues such as slagging and fouling due to their potassium and silica content. Coconut coir, with high moisture and low energy density, requires significant drying and preprocessing, adding to operational costs. Coconut shells, despite their high energy density and low ash content, present challenges in size reduction due to their hard structure, necessitating specialized grinders. Variability in biomass properties, such as energy content, moisture, and ash composition, complicates the design of gasification systems and may require precise blending ratios to achieve consistent syngas quality. Logistics and supply chain challenges, including collection, transportation, and storage of these scattered feedstocks, can increase costs, particularly for large-scale operations. Additionally, tar formation, especially from lignocellulosic materials like coconut coir, may necessitate expensive cleaning systems to protect downstream equipment. Environmental benefits, such as carbon neutrality, depend heavily on sustainable sourcing and management of feedstocks, while the lack of standardized protocols for these specific biomass types limits scalability. These constraints require technological advancements, efficient preprocessing methods, and supportive policy frameworks to enhance the viability of co-gasification using these agricultural residues.

1.9 Thesis outline

The thesis is organized in the manner described below.

Chapter 2 is dedicated to review the previous literatures that discuss the effect of temperature, pressure, SBR, and ER on syngas composition, CGE, and LHV. The effect of catalysts on syngas compositions is reviewed in this chapter. This chapter also includes the applications biomass gasification.

Chapter 3 discusses the methodology involved in this study in details. The steps involved in the gasification process are explained. The experimental setup, kinematic model description, and model validation are discussed. Finally, the chapter is concluded by summarizing the whole research outline.

Chapter 4 includes the collected data and their data reduction process from physical experiment. The physical experiment includes proximate analysis and ultimate analysis of the biomass. The elemental analysis is associated with the determination of different properties such as moisture content, volatile matter, fixed carbon, ash, C, H, N, S, and O.

Chapter 5 discusses all experimental result which is the main part of the thesis. The effect of different parameters on syngas composition, LHV, and CGE are discussed in detail. Finally, chapter 5 is closed by manifesting the comparison of the present findings with the previously reliable findings of various authors.

Chapter 6 concludes the finding of the thesis by numerical work and conveys the recommendation for future work.

Chapter 2
Literature Review

2.1 Introduction

Co-gasification of corncob, coconut coir, and coconut shell is a relatively novel and emerging technique. However, various authors studied the effect of different parameters on syngas composition, CGE, and LHV. These literatures are reviewed in this section. The literatures in this section are orderly arranged so that the effect of different parameters on the gasification process, co-gasification, catalytic effects, and application of syngas can easily be comprehended.

2.2 Effect of different parameters on syngas composition

The fuel gas mixture known as syngas, or synthesis gas, is mostly composed of hydrogen (H_2), carbon monoxide (CO), and, to a lesser degree, carbon dioxide (CO_2). It is created by gasifying a substance that contains carbon, like coal, biomass, or natural gas. The feedstock, operating conditions, and the gasification method employed can affect the precise composition of syngas. The yield of tar and char products can be determined by weighing the amount of tar collected and the difference between the weight of the sample holder before and after gasification using equations (2.1) and (2.2). The gas yield also can be calculated using Eq. (2.3).

Tar yield (wt%)= weight of collected Tar (mg) ×100 / weight of the sample (mg)……(2.1)
Char yield (wt%) = weight of collected Char (mg) ×100/ weight of the sample (mg)....(2.2)
Total Gas (wt%) = 100 − Tar (wt%) − Char (wt%)……(2.3)
Table 2.1 shows the effect of different parameters on syngas composition for different feedstocks.

2.2.1 Effects of temperature on syngas composition

Temperature affects tar and char yields, heating value, gas yield, cold gas efficiency, and carbon conversion, the most crucial operational element in the gasification process. Rising temperatures typically result in higher CO, H_2, heating value, and gas yields. A temperature rise enhances the hydrocarbon endothermic reforming process and releases more volatile matter; leading to a decrease in heavy tars and char concentrations and an increase in H_2 gas concentrations and overall gas production [93]. The Boudouard, Water-gas, and Steam-methane

reforming reactions are endothermic and require heat during the gasification. Thus, the production of hydrogen and carbon monoxide increases with an increase in gasification temperature. However, above 830℃ reverse water gas reaction activated and reduced the H_2 and CO production [86].

2.2.2 Effects of ER on syngas composition

One of the most important variables in the gasification process is the equivalency ratio, which is the ratio of the real air-fuel ratio utilized in gasification to the stoichiometric air-fuel ratio for combustion. The air equivalence ratio can be calculated using equations (2.4) and (2.5).

$$ER = \frac{\text{Rate of actual mass flow of air}}{\text{Rate of stoichiometric mass flow of air}} \quad (2.4)$$

$$\text{Rate of stoichiometric mass flow of air} = \frac{2.67C+8H-O}{0.23} \quad (2.5)$$

Where %C, %H, and %O are the weight percentages of carbon, hydrogen, and oxygen in the dry feedstock or feedstock mixture respectively. ER is one of the key parameters in the gasification process which enhances the syngas quality and calorific value.

2.2.3 Effects of SBR on syngas composition

The Steam-to-Biomass Ratio (SBR) is a critical parameter in biomass gasification, significantly affecting the efficiency, syngas composition, and overall performance of the process. Increasing the SBR enhances steam reforming reactions, leading to higher hydrogen content in the syngas. This makes the syngas suitable for hydrogen-rich applications like fuel cells or chemical synthesis. A higher SBR promotes the water-gas shift reaction, converting CO into H_2 and reducing the CO content in the syngas. Elevated steam levels suppress methane formation due to enhanced steam-methane reforming, improving syngas quality. Moderate SBR values can optimize the endothermic gasification reactions, improving thermal efficiency. However, excessively high SBR can lead to energy losses due to excessive steam requirements. Higher SBR enhances the conversion of solid carbon (char) into gaseous products, increasing the gasification efficiency and reducing unconverted residues. The ideal SBR depends on the specific biomass feedstock, gasifier type, and desired syngas application. For corncob, coconut coir, and coconut shell co-gasification, typical SBRs range between 0.4 to 1.0 to balance hydrogen production, carbon conversion, and thermal efficiency without excessive energy or water demands. The SBR plays a pivotal role in optimizing gasification performance,

influencing syngas quality, efficiency, and operational sustainability. Proper control and tuning of the SBR are essential for achieving the desired outcomes while minimizing costs and environmental impacts.

2.2.4 Effects of gasifying agent on syngas composition

Air, steam, carbon dioxide, or a mixture of these elements can be utilized as the gasification agent. In the gasification process, it affects the substance of producer gas. Air gasification is cost-friendly; however, it produces a high amount of nitrogen in the producer gas thus decreasing both the overall energy efficiency and calorific value of the gasification process. When oxygen is used as the gasification agent, the production of CO_2 and H_2O facilitates the oxidation during the process [106]. H_2 and CO production increases by using steam as a gasification agent by enhancing the water–gas shift reaction and steam methane reforming reaction but heat is needed for this reaction [107]. Using CO_2 as a gasification agent enhances the Boudouard and water–gas shift reaction and generates a high amount of CO and H_2 [108].

2.3 Lower Heating Value and Cold Gas Efficiency

The calorific value or heating value (HV) of a fuel is defined as the amount of heat released from the complete combustion of a unit of the fuel. The lower heating value (LHV) or net heating value and higher heating value (HHV) or gross heating value are the measures of the heat of combustion of a fuel [109]. Combustion characteristics and power output enormously depend on the HV of a fuel or fuel emulsion. High HV of a fuel leads to enhanced performance of a CI engine. The lower heating value of producer gas initially increased from 4.72 to 5.94 MJ/Nm^3 with increasing SBR from 0.1 to 0.35 shown in Fig. 2.1. The increment in LHV might be associated with the augmentation of hydrogen yield in producer gas. With the further increment in SBR from 0.35 to 0.4, the heating value of producer gas was decreased from 5.94 to 5.71 MJ/Nm^3. It might be due to the excess steam addition resulting in the reactor's reduced temperature and reduced combustible gas production. The CGE gradually increased from 62.1 to 85.7%, with a growing SBR from 0.1 to 0.35. It might be associated with the increment in lower heating value at higher SBR [61]. Deepak et al. [110] investigated the waste poultry litter pellets for H_2-rich syngas production in a downdraft gasifier by Aspen Plus and found the optimized values of H_2, CGE, and HHV are 0.21, 57.67%, and 5.71 MJ/Nm^3

respectively corresponding to temperature at 830.30℃, equivalence ratio of 0.2, and moisture content 16.36%.

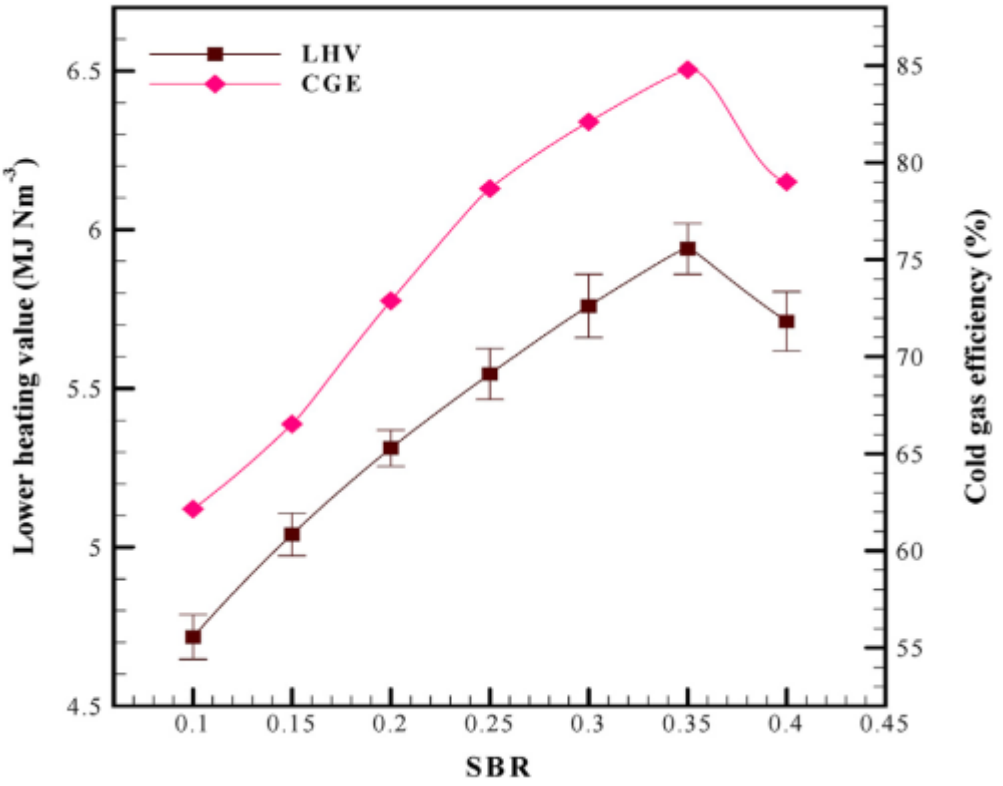

Fig. 2.1: The effect of SBR on LHV and CGE [61].

Rouanet et al. [111] investigated a two-stage downdraft gasifier by injecting steam and oxygen. They were able to enhance LHV by 65 %, gasification efficiency but it also increased tar formation. Binxuan et al. [112] examined a two-stage pulverized coal gasification, H_2 production enhanced by 48.38% over single-stage gasification. Muhammad et al. [63] examined the effect of vertical positions and angles of the rubber wood biomass feed inlet for syngas production by simulating an updraft fluidized bed gasifier. The vertical position of 200 mm yielded more CO, while 250 mm provided higher H_2 as illustrated in Fig.2.2. However, a comparison favored the 200 mm vertical position over 250 mm. The feed angle comparison demonstrated in Fig. 2.3 showed that a 45◦ angle slightly improved syngas quantities, with a small increase in CO_2.

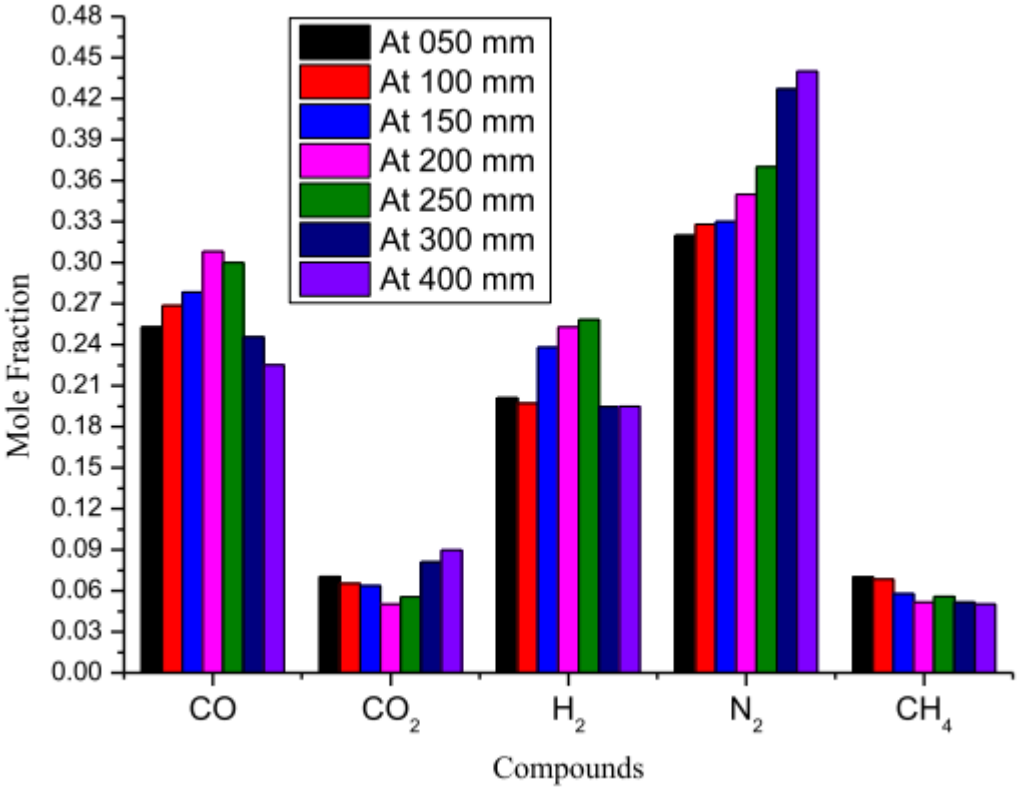

Fig. 2.2: Outlet mole compositions at different vertical positions [63].

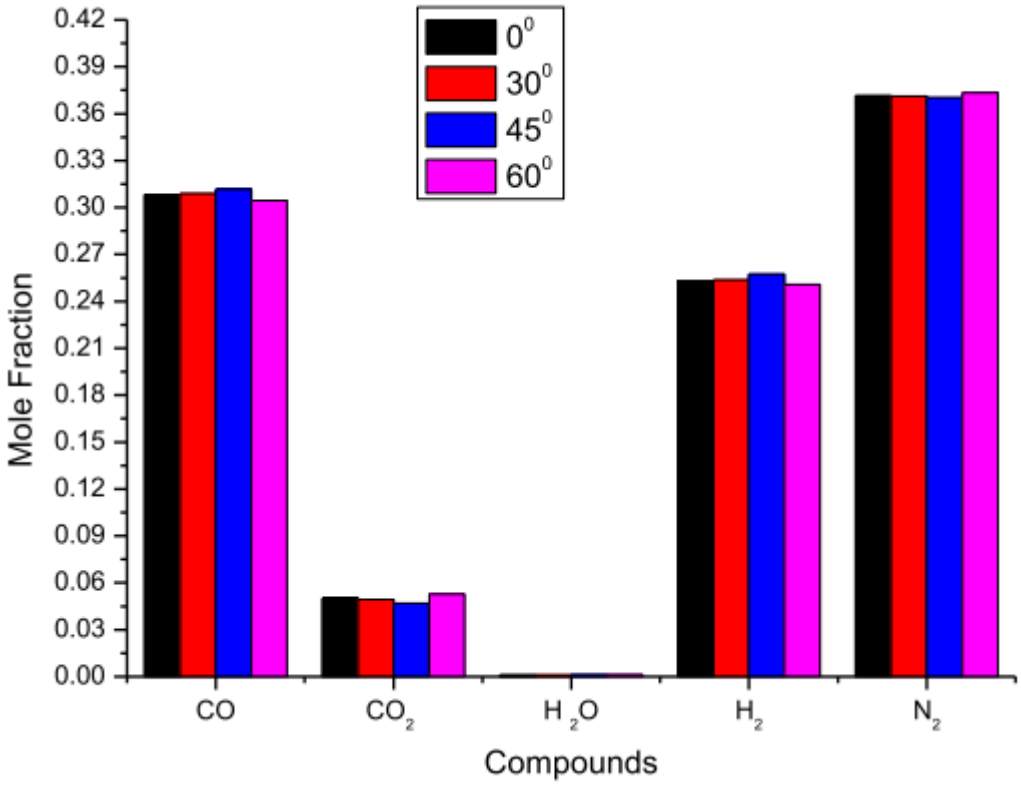

Fig. 2.3: Outlet mole compositions at different angles [63]

Table 2.1: Syngas composition in different gasifying agents for different feedstocks.

Feedstock	Gasifying agent	Operating conditions	Reactor Type & Approach	Syngas Compositions (%)					Ref.
				CO	CO_2	H_2	CH_4	N_2	
Timber & Wood waste	Air-steam	Temp.: 700℃	RGibbs ASPEN Plus	20	10	30	1.5		[52]
Cotton stalk	Steam	800℃, SBR: 0.2	bubbling bed gasifier Aspen HYSYS	43	5	47	2.8		[50]
Horse manure				43	3	46	6		
Wheat straw				38	7.5	51	2.1		
Rice husk				39	6	51	2.2		
Pine pellet	air	815℃, ER: 0.22	bubbling fluidized bed gasifier Aspen Plus	18	16	12	5.5		[53]
Eucalyptus type A				17	15.5	7.5	3.5		
Eucalyptus type B				15	14	6.5	3		
Pine residual forest biomass				17	16	11	4.5		
Coconut coir pith	Steam	1123 K, SR: 0.75	Gibbs free energy minimization equilibrium model Aspen Plus	14.86	46.62	35.24	0.69	2.6	[54]
Coconut coir pith char				34.43	19.81	28.43	15.43	1.98	
Corncob	air	SFR: 10.5, MC: 10%, AFR: 3.822	Fixed bed open-top downdraft gasifier	10.11	9.50	10.81	0.89	64.00	[55]
		SFR: 12.5, MC: 11%, AFR: 2.980		12.03	10.67	12.38	1.22	58.85	
Eucalyptus		SFR: 10.5, MC: 14%, AFR: 2.57		10.99	12.15	13.24	2.78	54.62	
		SFR: 12.5, MC: 15%, AFR: 1.72		12.58	16.8	14.1	4.89	50.40	

Corncob	air	ER: 0.279, AFR: 1.395, MC: 10.1%	downdraft	22.6	12.0	17.3	1.98	45.7	[57]
Kitchen wastes	air	800℃, EAR: 0.2	updraft fluidized bed gasifier Aspen Plus	35	2	24	0.5	-	[58]
Date seeds	steam	700 ℃ , SBR: 1.2	Updraft steam gasifier	15	14.5	70	0.5	-	[59]
Sugarcane bagasse	air	877.27 ℃, ER: 0.08, MC: 10%	Downdraft gasifier Aspen Plus	34.5	3.91	31.24	0.13	-	[60]
Feedstock	**Gasifying agent**	**Operating conditions**	**Reactor Type & Approach**	**Syngas Compositions (%)**					**Ref.**
				CO	**CO_2**	**H_2**	**CH_4**	**N_2**	
Bamboo	Air-Steam	837 k, SBR: 0.35	Downdraft gasifier	9	23.58	37.12	1	-	[61]
Pomegranate woodchips	air	685℃, ER: 0.21, MC: 7.71%, ICE power load: 7 kW	Downdraft gasifier	30.93	9.32	22.08	3.24	34.43	[87]
			Aspen Plus	30.81	7.09	25.51	3.08	33.51	
		730℃, ER: 0.25, MC: 7.71%, ICE power load: 10 kW	Downdraft gasifier	26.74	9.5	19.2	4.09	40.47	
			Aspen Plus	26.88	8.06	21.51	3.76	39.79	
Poultry litter pellets	air	800 ℃, ER: 0.2,	Downdraft gasifier Aspen Plus	26.73	9.4	19.41	-	-	[110]
Corncob	-	Carrier gas: Air at 2.5-7.5 L/min	Non-thermal arc plasma Discharge power: 25.2 W	26.4	14.5	58.5	0.6	-	[113]
Rice husk (18 kg/s)	Steam		Downdraft gasifier	36	0	53	-	-	[114]

Larch wood (15 kg/s)		1100 k, steam flow rate: 4.5 kg/s	Aspen Plus	35.5	0	54	-	-	
Wood chip (32 kg/s)				48	0	52	-	-	
Hardwood chips (MC=5.39%)	Air-steam	600-1200℃, ER: 0.1-0.8, SBR=0.75	Downdraft gasifier UniSim Design	44.94	7.82	44.45	0.45	2.33	[115]
Almond shells (MC=3.30%)				44.61	6.28	46.30	0.39	2.40	

2.4 Co-gasification

Co-gasification has received growing attention as a process where mixing different types of fuels can potentially produce a catalytic effect. Co-gasification often involves selecting feedstocks with distinct and significantly different characteristics and properties to achieve improved synergy. Researchers have been investigating the impact of biomass and coal ratio on H_2 and CH_4 production yields through catalytic co-gasification. Moreover, it has been demonstrated that mixing coal with biomass can significantly reduce the yields of SO_2, NOx, and tar while increasing gas yields. Co-gasification allows controlling the composition of produced gas by varying the feedstock ratio, consequently offsetting the disadvantages of biomass, and improving the gasification product yield and purity. Table 2.2 shows the syngas composition of co-gasification in different gasifying agents

Co-gasification of renewable biomass and coal is a promising technique to reduce greenhouse gas emissions and increase gasification performance instead of individual coal gasification. Li et al [71] studied the co-gasification of coal and corn straw blends in the Aspen Plus process software and established a co-gasification combined cycle negative-carbon emission system which improved the heat value of the syngas, decreased carbon emission, and reduced the cost of power generation by 19%. Shahabuddin et al. [72] investigated the co-gasification of pine bark and coal. They showed that increasing biomass concentration increases carbon conversion, syngas quality, and cold gas efficiency while reducing emissions. The LHV and CGE of pine bark and coal (1:1) were found 5.70 MJ/Nm^3 and 45% respectively at 1400℃ for 20% CO_2 concentration.

Gomez et al. [56] evaluated the Corncob, Sesame stalks, and Cotton gin trash blends for the three values of Rice husk (0, 15, and 30%) in a downdraft gasifier. As the Rice husk

concentration in the blend increased, the fraction of H_2, CO, and CH_4 fuel species in the syngas decreased as observed in Fig. 2.4. The ternary plots show that CO_2 production increased with higher percentages of rice husk, and was lower with high proportions of corncob or cotton gin trash shown in Fig. 2.5. It was found that syngas composition was negatively affected as the proportion of rice husks in the mixture increased, adding variability and noise to the gasification process. Tumpa et al. [62] investigated the highest H_2 (4.6 mol/kg) yield from torrefied canola hull and mustard meal pellets via supercritical water gasification at 575 ℃ in 45 minutes with a biomass-to-water ratio of 1:20. Fatin et al. [66] examined the blend of 75% coal and 25 % sawdust at the condition of 900℃ and ER at 0.30 show a maximum H_2/CO ratio in the syngas (1.58 ± 0.55) and HHV_{syngas} (5.2683 ± 1.04 MJ/Nm^3), and the blend of 55% coal and 45% wood pellet at the condition of 816℃ and ER at 0.30 show a maximum H_2/CO ratio in the syngas (1.28 ± 0.31) and HHV_{syngas} (4.8705 ± 0.65 MJ/Nm^3). The carbon conversion efficiency, CGE, and gas yield of co-gasification of RDF and Rice straw increased by 12.7 %, 26.42%, and 14.43 % respectively at the steam-to-feed ratio of 0.75 and gasification temperature of 800℃ for the separate gasification of straw and RDF which highlights the potential of this technology for sustainable waste management and renewable energy production [80]. Sinisalu et al. [81] investigated biomass and oil shale co-gasification under CO_2 conditions in a fixed-bed reactor. They found the maximum H_2, CO, and CO_2 concentrations of 2.15, 16.71, and 0.55% of total product yield for the pine bark blends with 10% oil shale.

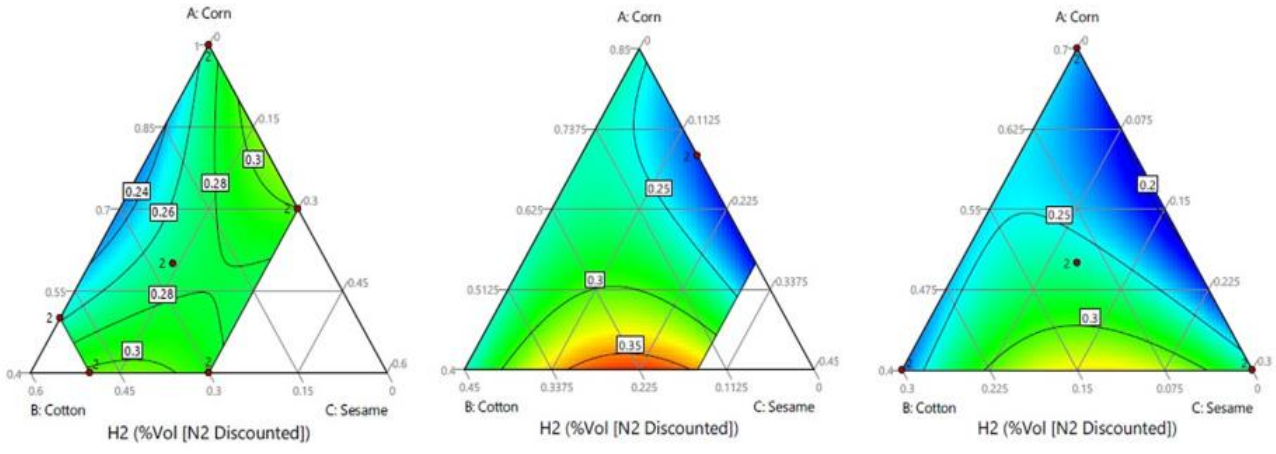

a)

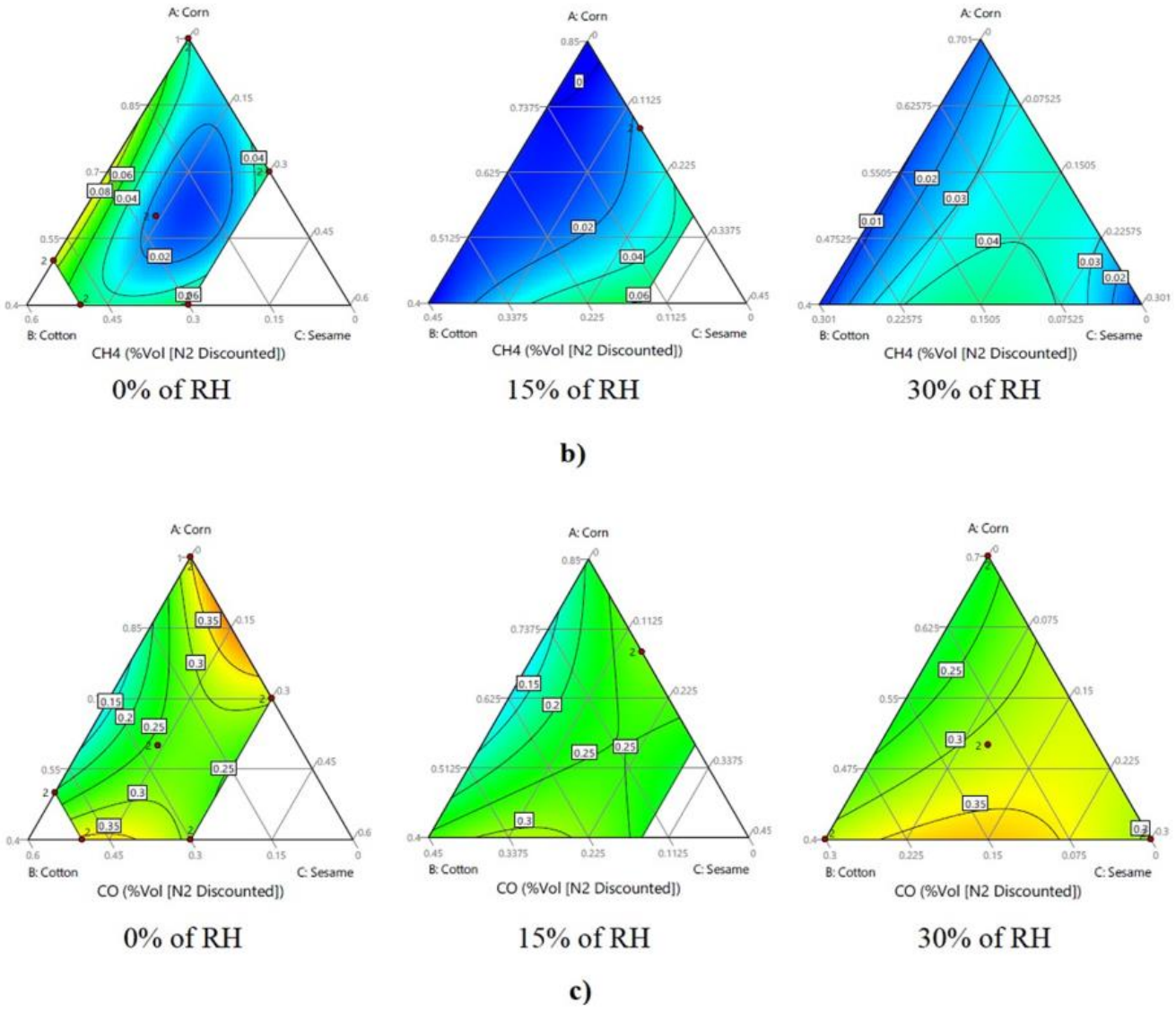

Fig. 2.4: Percentage of (a) H_2, (b) CH_4, and (c) CO in gas mixtures at different RH % [56].

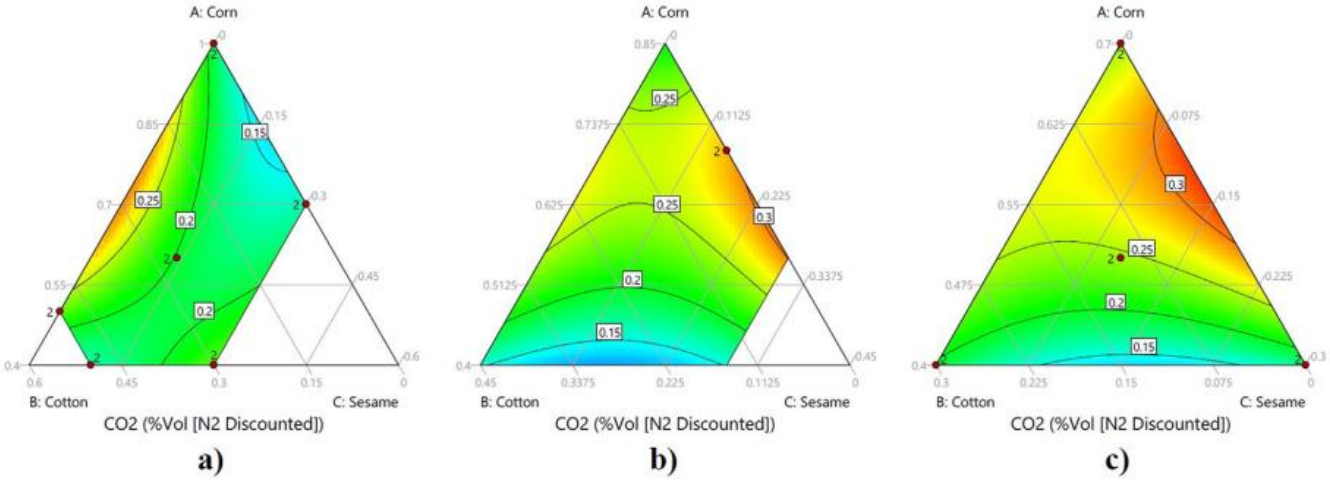

Fig. 2.5: Percentage of CO_2 in gas mixtures at (a) 0% RH, (b) 15% RH, and (c) 30% RH [56].

Co-gasification is a strategy that can be used to manage the environmental challenges of plastic and biomass disposal. The gas compositions generated for EVA co-gasified at T = 800℃ and ER = 0.15 with different biomass materials PS, UGC, and WS, as well as the char, gas, and tar yields, are compared in Fig. 2.6. Among the studied biomass materials, WS and UGC produce more hydrogen and show a higher gas yield and less tar than PS. However, the char yield from PS co-gasification is lower than its counterparts, indicating that the changes in the biomass type cause a noticeable impact on gasification products [83]. Cao et al. [116] studied an ASPEN plus model for the simulation of steam co-gasification of polyethylene and pine using various temperatures (740–830℃), steam/waste ratio (0.5–0.8) and found that H_2 content and H_2 yield gradually increased from 33.01 to 47.81% and 48.09–57.76g/kg, respectively, when PE increased from 0 to 60%.

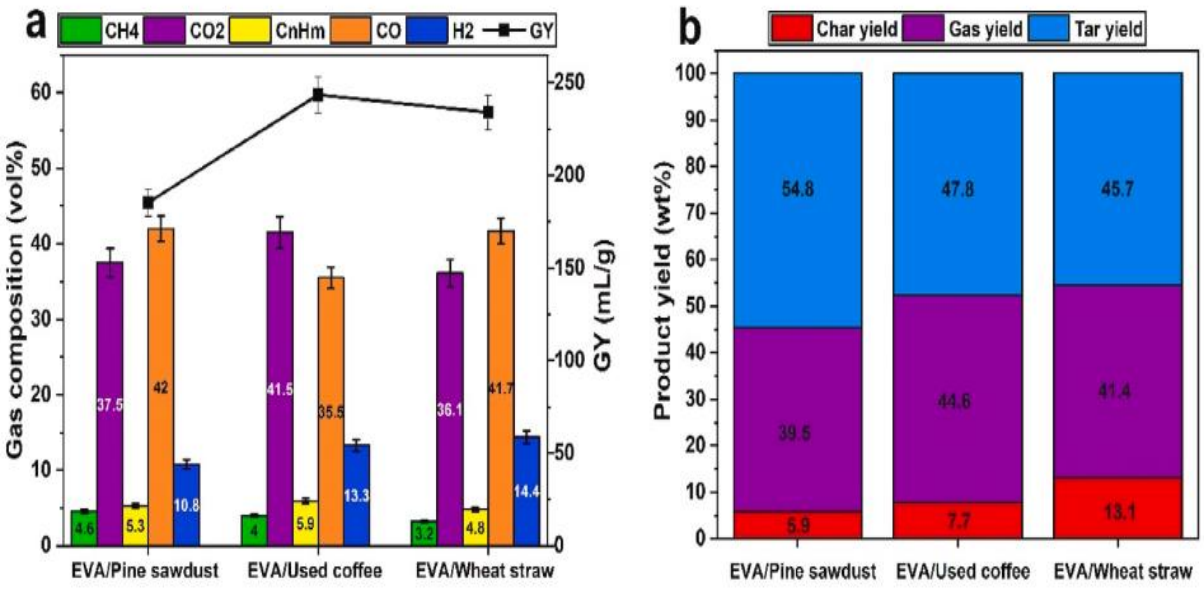

Fig. 2.6: Co-gasification of EVA plastic with different biomass types: a) gas composition; and b) product yield. Co-gasification of each sample was performed under the same conditions (T = 800 ◦C, Plastic/Biomass = 0.33, ER = 0.15) [83].

Table 2.2: Syngas composition of co-gasification in different gasifying agents.

Feedstock	Gasifying agent	Operating conditions	Reactor Type & Approach	Syngas Compositions (%)					LHV (MJ/Nm^3)	Ref.
				CO	CO_2	H_2	CH_4	N_2		
Rural solid waste and Tree bark	air	CGR=20%, ER=0.45	Fixed bed updraft in plant scale	7	16.5	6	2	-	3.0	[67]
			Fixed bed updraft in Aspen Plus simulation	8.5	10	13	1	-	2.5	
Woodchips	air	847, ER=0.335	Fixed bed downdraft	23.8	9.39	15.1	2.28	48.7	5.86	[69]
Woodchips (38%) + OFMSW (62%)		813, ER=0.328		20.9	11.1	14.4	2.80	49.7	5.83	
Woodchips (70%) + Sewage Sludge (30%)		642, ER=0.351		20.6	11.3	16.4	1.83	49.6	5.18	
Woodchips (46.5%) + Hazelnut shells (53.5%)		848, ER=0.347		20	12.3	15.5	2.46	49.1	5.44	
Pre-treated corn straw (70%) + coal (30%)	O_2	ER: 0.3-0.4	Gibbs free energy minimization equilibrium model Aspen Plus	55.39	8.90	27.48	-	7.63	-	[71]
Coal + Pine Bark (1:1)	-	1400℃	Single-stage downdraft entrained flow	45	20	4	-	-	5.70	[72]
Coal (90%) + Woodchips (10%)	steam	900℃	Fixed bed updraft	35.51	29.94	29.94	0.12	-	5.59	[73]
Coal (90%) + Rubber seals (10%)				35.51	30.43	30.53	0.14	-	5.56	
Rice husk (20%) +	air	880℃, ER:0.25	Central composite	23.53	-	13.97	3.51	-	6.17	[74]

Groundnut shell (80%)			design Numerical							
		927℃, ER:0.25	Open core gasifier Experimental	22.36	-	13.23	2.87	-	5.86	
Chlorella Vulgaris + Petrochemical industrial sludge (3:7)	steam	700℃, ER: 0.20, S/F:0	Gibbs free energy minimization equilibrium model Aspen Plus simulation	23	8	24	0.02	-	5.57	[78]
		700℃, ER: 0.20, S/F:1.0		10	18	32	0	-	4.7	
MSW + Rice husk (50:50)	steam	900℃, ER: 0.20, S/F:1	Aspen Plus simulation	23.15	13.4	62.57	0.88	-	-	[79]
Rice straw	steam	900℃	Fixed bed laboratory reactor	34.86	20.26	37.55	5.66	-	12.5	[80]
RDF	steam	900℃		35.35	19.3	38.49	5.18	-	13.2	
Rice straw + RDF (1:1)	steam	800℃, S/F:0.75		34.9	16.7	37.36	9	-	14.3	
Coal	-	600-700℃	Downdraft Fixed bed gasifier	8	11	10	1.5	72.7	2.62	[85]
Briquette				18.6	12	12	1.7	55.7	4.24	
Coal + Briquette				12.55	12.2	11	1.95	62.3	3.46	
Coconut shell				18	11.8	15	1.8	53.4	4.53	
Coal + Coconut shell				12.25	12.5	16	1.65	57.6	3.86	
Mahua wood				18.7	11.89	17.55	2.6	49.26	5.18	
Coal + Mahua wood				12.6	12.94	15	2.05	57.41	3.94	
Briquette + Mahua wood				18.65	11.5	18	1.6	50.25	4.86	
Coal + Briquette + Mahua wood				14.6	14	18.5	2.1	50.8	4.58	
Polyethylene (60%) + Pine (40%)	steam	830℃, steam/waste= 0.8	Kinetic model Aspen Plus simulation	27	8	47.81	13	-	-	[116]
Manure (16.6%), Date Pits	O_2	850℃, P_g = 1 bar, ER=	Oxygen Gasification	26.1	44.8	26.1	2.3	0.8	7.22	[117]

(41.7%), Sludge (41.7%)		1.67, H_2:CO= 1	(Direct Heat) Aspen Plus							
Industrial sludge + Food waste	steam	2500℃ , SFR: 1.1	Plasma co-gasification Aspen Plus	34.15	3.5	50.14	-	-	15	[118]
Municipal sludge + Food waste		2500℃, SFR: 0.67		37	5	45.62	-	-	14	

2.5 Catalyst

Catalytic gasification is a promising technique to reduce tar formation and enhance syngas production. The use of calcium compounds reduces thermal degradation by slowing down the pyrolysis process and this effect could be favorable to avoid the formation of tar in a process of biomass gasification [119]. Jamilu et al. [70] investigated the effect of CaO catalyst in the co-gasification of rice husk and LDPE and showed that the H_2 concentration increases from 63.94% to 69.33% and CO_2 decreases from 23.55% to 17.11% at 700℃ with an increase in the CaO-to-feed ratio from 0.25 to 1.0. Gao et al. [108] studied the gasification of pine sawdust by using a mixture of N_2 and CO_2 as a gasifying agent in the presence of the CaO catalyst; and showed that CaO absorbed CO_2 and H_2 production increased up to 10%. The addition of $CaCO_3$ with $CaCO_3$/biomass ratios up to 1% (w/w) and steam/biomass ratios near 0.11 in corncob gasification increases the cold gas efficiency from 46.8% to 59.18%, LHV from 3.9 to 4.8 MJ/Nm^3 and the H_2 yield from 238 to 310 Nml/g respectively [84]. Liao et al. [86] investigated the addition of Fe-Ce/olivine catalyst with pine sawdust in a two-stage fixed bed reactor; increasing the syngas yield from 0.46 to 0.93 Nm^3/kg biomass, H_2 yield from 5.93 to 21.37 mol/kg biomass, and carbon conversion rate from 43.47 to 55.14%, and decreasing tar yield from 18.48 to 0.15 g/Nm^3 and lower heating value from 15.92 to 11.05 MJ/m^3 at a catalytic temperature and gasification temperature of 800℃. The CO_2 gasification-reforming of biomass components (cellulose, xylan, lignin, and starch) in the presence of Ni/CeO_2 nanorod catalyst was conducted using a two-stage fixed bed reactor. The total gas yield for cellulose, xylan, lignin, and starch increased by 104.3%, 103.3%, 149.3%, and 128.3% with the addition of 2% Ni/CeO_2 by activating the C–H and C–C bonds in volatiles produced by the decomposition of biomass components [120]. Table 2.3 shows the syngas composition in different gasifying agents with catalysts for different feedstocks.

Table 2.3: Syngas composition in different gasifying agents with catalysts for different feedstocks.

Feedstock	Catalysts	Gasifying agent	Operating conditions	Reactor Type & Approach	Syngas Compositions (%)					LHV (MJ/Nm^3)	Ref.
					CO	CO_2	H_2	CH_4	N_2		
Rice husk and LDPE	CaO	steam	750℃ CaO/Feed=1, Steam/Feed=1	Aspen Plus	7.5	18	69.42	5	-	10.3	[70]
Corncob	$CaCO_3$	steam	850℃ $CaCO_3$/biomass=1, SBR=0.11	Downdraft fixed bed gasifier	42.89	22.21	31.34	3.55	-	4.8	[84]
Pine sawdust	-	steam	800℃, SBR=1.4	Two-stage fixed bed reactor	29	27	28.86	8	-	-	[86]
	Fe-Ce /olivine				19	25	51.48	5	-	-	
Pine sawdust	-	CO_2(50%)	700℃	Downdraft fixed bed gasifier	26	63	2	8	-	-	[108]
	CaO	CO_2(50%)			42	22	9	24	-	-	
	CaO	CO_2(33%)			53	9	10	24	-	-	
Cellulose	-	CO_2	600℃	Two-stage fixed bed reactor	9.9[b]	-	2.8[b]	1.9[b]	-	-	[120]
	2% Ni/CeO_2				22.5[b]		4.8[b]	2.6[b]			
Xylan	-				6.8[b]		2.2[b]	1.4[b]			
	2% Ni/CeO_2				17.2[b]		2.4[b]	1.5[b]			
Lignin	-				3.8[b]		0.8[b]	1.1[b]			
	2% Ni/CeO_2				11.7[b]		1.0[b]	1.6[b]			
Starch	-				7.1[b]		1.7[b]	1.5[b]			
	2% Ni/CeO_2				17.1[b]		3.8[b]	2.6[b]			

[b] $mmol/g_{biomass}$

2.6 Application of Syngas

Syngas is a versatile intermediate product with diverse applications across energy generation, fuel production, and chemical manufacturing. Its ability to be derived from various feedstocks (coal, biomass, waste) also makes it a critical component of future sustainable energy systems.

2.6.1 Power Generation

In recent years, there has been a significant increase in interest in biomass-based power generation and related industrial processes because of their inherent benefits, which include waste valorization potential, carbon neutrality, and renewability [121]. Syngas can be used as fuel in gas turbines and internal combustion engines to generate electricity. In an Integrated Gasification Combined Cycle (IGCC) system, syngas are used to power gas turbines, with the exhaust heat driving steam turbines for additional power generation [122]. This allows for cleaner and more efficient electricity production than conventional coal-fired plants. Figure 2.7 shows the biomass gasification combined heat power system integrated with an internal combustion engine in the ASPEN Plus. Adding diesel fuel with producer gas in a gasifier dual-fuel engine reduces diesel fuel consumption and NOx emissions. Raj et al. [85] reported that the BTE of a single-cylinder, 4-stroke, naturally aspirated compression ignition, gasifier dual fuel engine at variable load and compression ratio (12-18) condition was a maximum of 27.6% at 100% engine load and ER 0.43 for briquette and mahua wood co-gasified producer gas which was slightly lower than diesel fuel (28.37%). They observed a maximum of 63.44% diesel savings at 33.33% load and ER 0.24 for dual fuel mode coconut-based producer gas. They also showed that the minimum emissions of CO and HC were 0.01% and 127 ppm for coal + mahua wood, and CO_2 0.8% for coal + coconut shell, NOx 4 ppm for coal + briquette + mahua at 100% engine load. Yang et al. [123] introduced an innovative power generation system utilizing staged co-gasification of Shenfu bituminous coal and biomass (rice straw). The system achieved a peak power efficiency of 40.03% at a biomass blending ratio of 0.8, higher than the 34.76% efficiency of the IGCC system and the 29.57% of biomass direct-fired power plants.

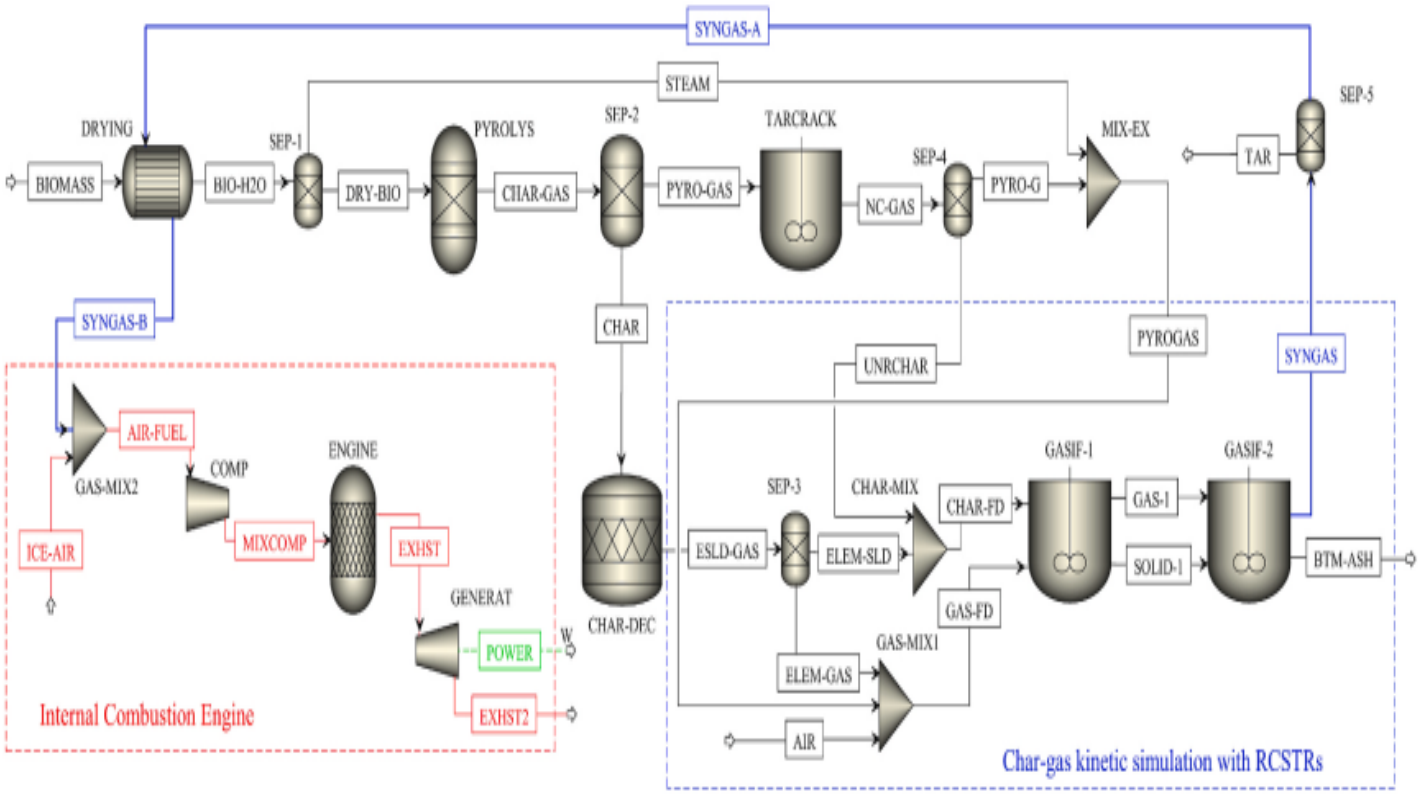

Fig. 2.7: ASPEN Plus flowsheet for the investigated biomass gasification combined heat power system integrated with an internal combustion engine [87].

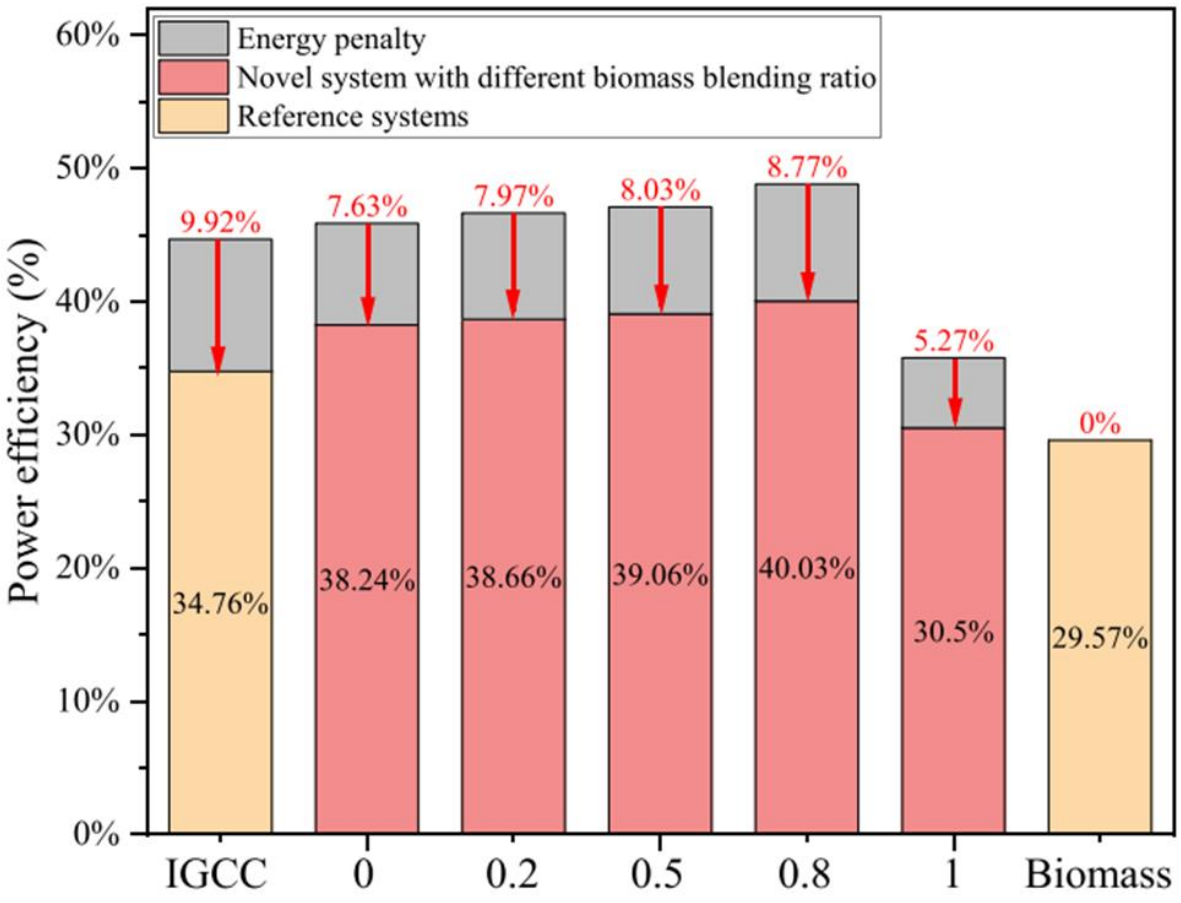

Fig.2.8: Power efficiency and energy penalty of the novel system with biomass blending ratios of 0, 0.2, 0.5, 0.8, and 1 and reference systems (IGCC system and biomass direct-fired power plant), carbon capture scenario [123].

2.6.2 Fischer-Tropsch Synthesis (FTS) for Liquid Fuels

One of the most prominent uses of syngas is in the Fischer-Tropsch process, where it is converted into liquid hydrocarbons like synthetic diesel, gasoline, and kerosene. This is a key technology for producing liquid fuels from biomass (Biomass-to-Liquids, or BTL). These fuels are cleaner than conventional fossil fuels and are sulfur-free.

2.6.3 Hydrogen Production

Syngas is a major source of hydrogen, which is used in several industrial processes. The hydrogen can be separated from the syngas and used in hydrogen fuel cells, which power electric vehicles, or as a feedstock in various chemical processes, such as ammonia production for fertilizers and oil refining. A solid oxide fuel cell converts chemical energy from a fuel (such as hydrogen, syngas, or natural gas) into electrical energy using a solid oxide electrolyte. The H_2 serves as the fuel in the anode of the SOFC, while the O_2 from the air acts as the oxidizer in the cathode [124,125]. Abouemara et al. [126] developed an integrated system that combines steam gasification of plastic waste with SOFC for power generation. They showed that the voltage and power output increased from 0.849 to 0.876 V and 0.828 to 0.867 W respectively.

2.6.4 Synthetic Natural Gas (SNG) Production

Syngas can be further processed into synthetic natural gas (SNG) through a methanation reaction, which is similar to the process that occurs naturally in fossil fuel formation. This SNG can be used as a substitute for conventional natural gas in heating, and electricity generation, and as a fuel in transportation.

2.6.5 Biofuels Production

Syngas derived from biomass (biomass gasification) can be converted into biofuels such as biodiesel or ethanol. This is considered a renewable energy pathway and helps in reducing greenhouse gas emissions. The process is part of biomass-to-liquid (BTL) technologies, which are gaining traction for producing renewable transportation fuels.

2.6.6 Poly generation

In poly generation systems, syngas is used simultaneously for producing multiple outputs like electricity, heat, and chemicals. This maximizes efficiency and reduces waste. Poly generation plants are used in industries where a combination of power, heating, and chemical production is required.

2.6.7 Gas-to-Liquids (GTL) technologies

Syngas is used in GTL processes to produce liquid hydrocarbons from natural gas. This process is similar to Fischer-Tropsch but specifically focuses on converting natural gas into high-quality diesel and jet fuels. This application is especially useful in regions rich in natural gas but lacking in oil resources.

2.6.8 Production of Chemicals and Materials

Methanol-to-Olefins (MTO): Syngas can be converted into methanol, which is further processed into ethylene and propylene—building blocks for plastics, synthetic fibers, and other materials. Fertilizers and other chemicals: Syngas can produce other important chemicals, such as formaldehyde, urea, and acetic acid, in addition to ammonia.

2.6.9 Ammonia and Methanol Production

Syngas is essential in the chemical industry for the production of ammonia (via the Haber process) and methanol. Ammonia is a precursor for fertilizers, while methanol serves as a building block for various chemicals, plastics, and is also used as a fuel or fuel additive. To achieve CO_2 capture and utilization and enable effective methanol synthesis, Liu et al. [49] developed biomass-to-methanol systems based on calcium looping coupled with dry methane reforming and reverse Boudouard reaction. They demonstrated the reduced global warming potential (GWP) and improved energy efficiency in reverse Boudouard reaction compared to dry reforming of methane. Fig. 2.9 depicts the Aspen Plus process flow diagram of biomass gasification to methanol based on calcium looping coupled with dry methane reforming and reverse Boudouard reaction.

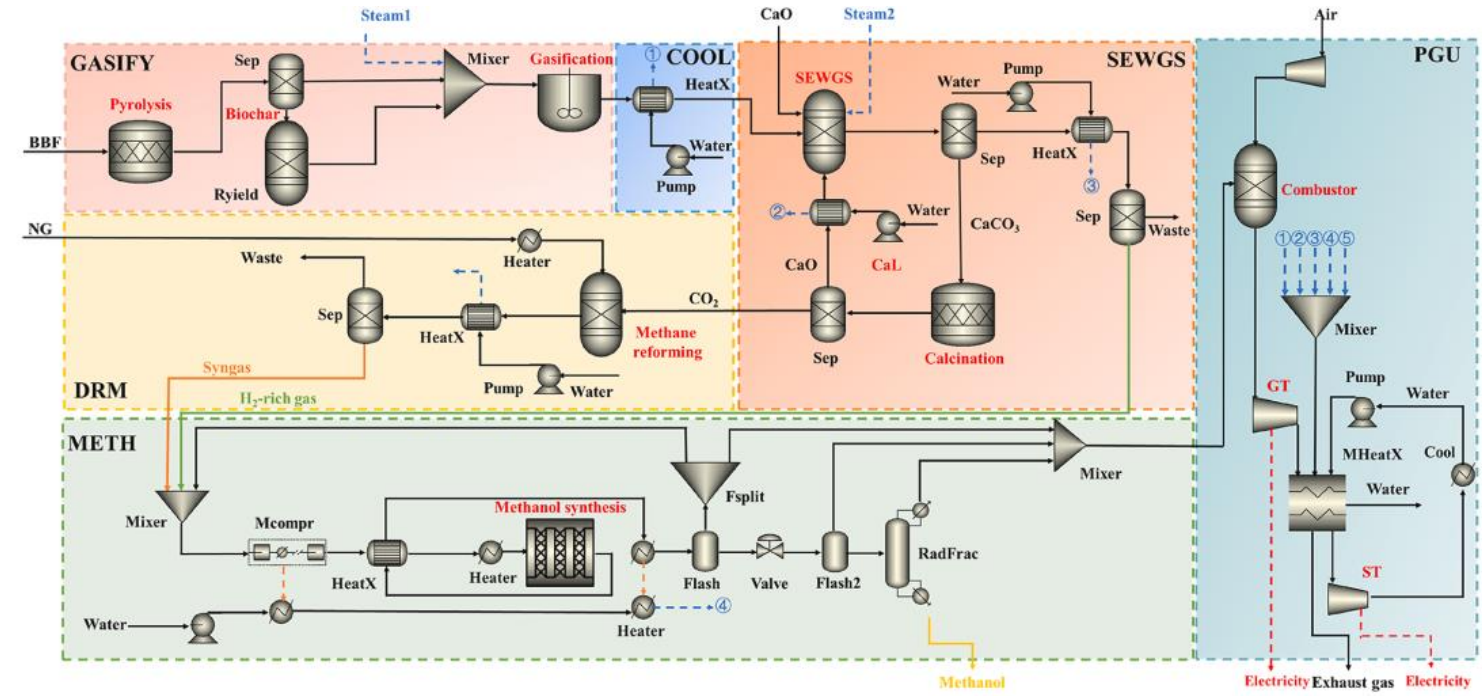

(a)

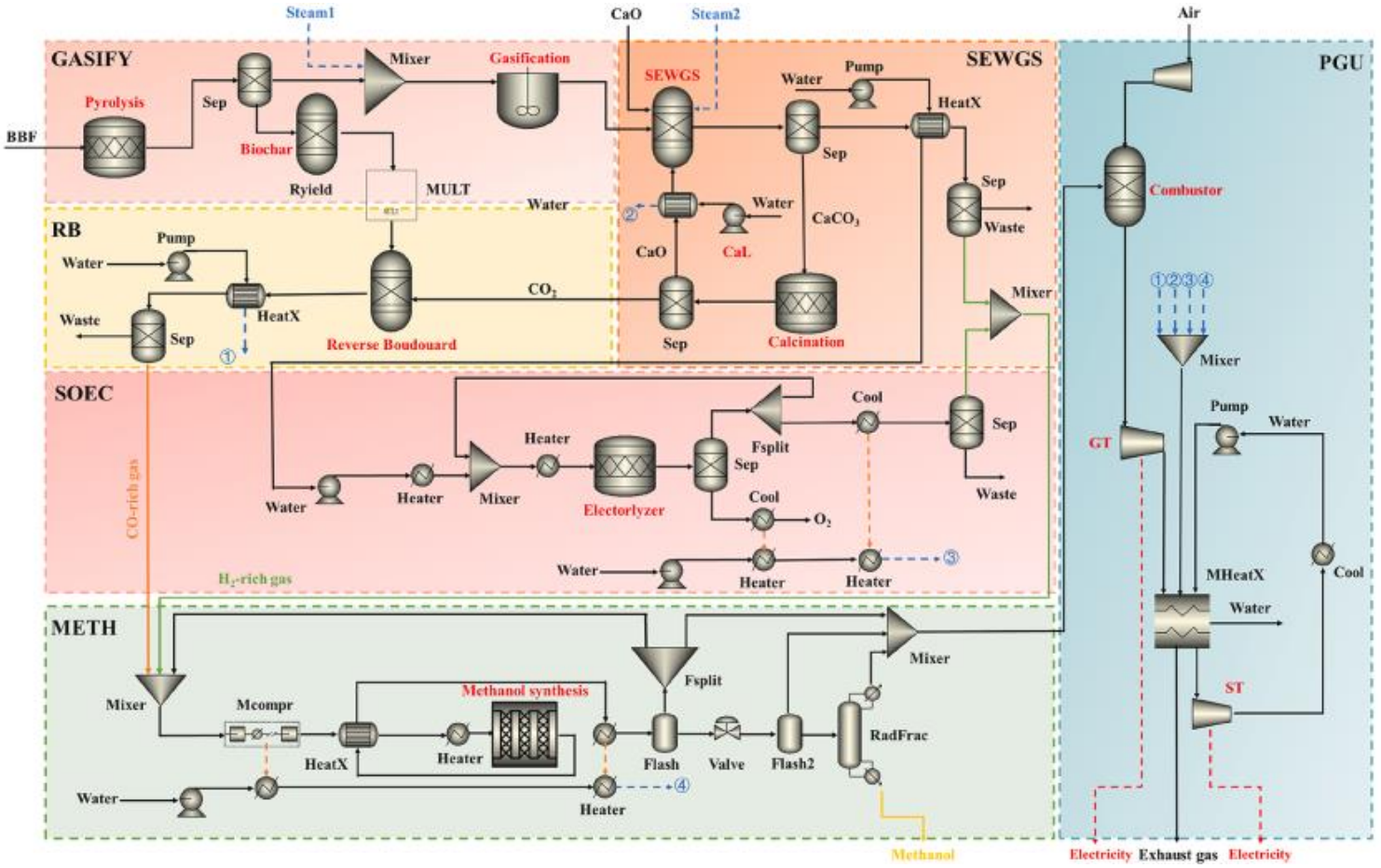

(b)

Fig. 2.9: Simulation flowcharts of biomass to methanol systems in Aspen Plus. (a) dry reforming of methane (b) Reverse Boudouard reaction [127]

2.7 Conclusion

The review of literature on biomass co-gasification highlights its potential as a sustainable and efficient method for energy production, waste management, and environmental preservation. Co-gasification, particularly with agricultural residues like corncob, coconut coir, and coconut shell, leverages the complementary properties of various feedstocks to optimize syngas production, enhance process efficiency, and reduce reliance on fossil fuels. However, challenges such as feedstock variability, ash-related issues, tar formation, and logistical constraints must be addressed to improve scalability and economic viability. Technological advancements in gasifier design, preprocessing methods, and syngas cleaning, coupled with supportive policies and incentives, are critical for maximizing its adoption. Overall, co-gasification emerges as a promising pathway to achieve renewable energy goals, reduce greenhouse gas emissions, and promote circular economies, making it a key component in the transition to sustainable energy systems.

Chapter 3
Methodology

3.1 Introduction

There are different processes that may be adopted to produce energy from biomass. Among these processes, co-gasification is one of the most efficient methods. Thus, co-gasification is used to produce syngas from agricultural residues such as corncob, coconut coir, and coconut shell in this study. The processes involved in the co-gasification using Aspen plus simulations are described here. Then the feedstock samples are prepared. This section also discusses the tools used to determine elemental analysis of samples and the co-gasification process.

3.2 Assumptions in the modeling

In the present developed model, the overall process is assumed to be steady-state due to simple construction, and lower operational cost. The biomass feedstocks are assumed to have a uniform composition and are non-conventional. The material is defined and transformed into conventional elements using the proximate and final analytical results (moisture, volatile matter, fixed carbon, ash content, and elemental composition) of the feedstocks [128]. Gasification reactions (including methane reforming, Boudouard, and water-gas shift) are assumed to reach thermodynamic equilibrium, simplifying kinetic complexities. The Gibbs-free minimization method is used to treat the gaseous products as ideal gases to achieve thermodynamic equilibrium [114]. Tar formation is neglected or modeled as a pseudo-component for simplicity [79]. It is considered that ash is inert to show non-reactive characteristics during gasification [129]. No pressure drop occurs within the gasifier. Biomass particle temperatures are uniformly distributed without gradients. All reactions proceed rapidly and attain equilibrium. Particle size distribution (PSD) has been omitted from consideration in this context. These assumptions provide a foundational framework for the established biomass gasification model, shedding light on the intricacies of the process under specified conditions.

3.3 Model Description

Using ASPEN Plus version 11, a kinetic simulation model is created for the co-gasification of biomass for the production of syngas. The Penge-Robinson equation of state with Boston Mathias alpha function (PR-BM) is used to ascertain the physical properties of the

traditional components in the gasification process [118]. The HCOALGEN and DCOALIGT models are also used to compute the density and enthalpy of biomass and ash, which are unconventional components [60].

Aspen plus simulation model block diagram for co-gasification of corncob, coconut coir, and coconut shell is displayed in Figure 3.1. Table 3.1 provides a brief overview of the blocks used in the simulation model. Corncob, coconut coir, and coconut shell streams are considered non-conventional elements, and their elemental analysis is specified by using non-conventional (NC) solid models PROXANAL, ULTANAL, and SULFANAL, respectively. Gasification agents ("Steam and Air") and feedstocks ("CORNCOB, COCOCOIR, COCOSHELL") represent the input material streams. These feedstock streams feed into the reactor at 25℃, 1 bar pressure, and feed rate 3000 kg/hr. The gasification agent steam and air feed into the reactor at 450℃ and 1 bar. RYIELD, the yield reactor is used to convert the non-conventional elements of the feedstock (Corncob, Coconut coir, and Coconut shell) into a conventional element (C, H_2, O_2, N_2, S, Cl_2, and Ash) by using ultimate analysis of the respective feedstock and the yield calculator block. RGIBBS is the Gibbs free energy reactor used for the pyrolysis of the decomposed product and produces volatile matter and char. Steam used in this segment enhances the quality of syngas by increasing H_2 content, reduces tar formation by reforming heavier hydrocarbons, and improves overall energy efficiency. The Solid split separator, SSPLIT, separates ash from the volatile product stream. The mixer, MIX, mixes the oxidizing agents air, and ash-free gas from the cyclone separator. Rplug reactor (OXI and RED), simulate oxidation and reduction reactions of the co-gasification process by known kinetic reactions. SEP is the separator that separates steam from the syngas stream. Table 3.2 shows the oxidation and reduction reactions that occur in the Rplug reactor (OXI and RED) with kinetic parameters.

To analyze the effect of operating conditions, the gasifier temperature varies from 500-1200℃ with an interval of 100℃, pressure from 1 to 20 bar, ER from 0.1 to 0.6 with an interval of 0.1, and SBR from 0.2 to 1.0 with an interval of 0.1. The effects of blend ratio on co-gasification are studied using different blends where the total feed rate is 3000 kg/hr.

3.3.1 Water gas shift reactor

After gasification, the produced syngas undergoes the water-gas (W-G) shift reaction shown in equation (3.1) which occurs in two reactors of high temperature shift

and low temperature shift. The gas from the W-G shift contains mainly H_2, CO_2, residual steam, and traces of CH_4 and CO; then to produce pure hydrogen, these gases are fed into the PSA system to obtain pure hydrogen.

$$CO + H_2O \rightarrow H_2 + CO_2 \ldots\ldots\ldots\ldots\ldots\ldots\ldots\ldots\ldots\ldots\ldots\ldots\ldots\ldots\ldots\ldots\ldots\ldots\ldots\ldots. (3.1)$$

For this part, two water-gas shift reactors were considered because W-G shift reaction is moderately exothermic, and it tends to shift to the left side at high temperature. One at higher temperature (HTWGS) and the other at lower temperature (LTWGS). In the HTWGS reactor, there is a first low conversion of CO with quick kinetics, but it is not possible to go beyond the equilibrium curve, thus the LTWGS reactor was used. In the LTWGS reactor, by reducing the operation temperature, it was possible to obtain higher conversion. HTWGS and LTWGS have been simulated at 400 and 200℃ with two Requil reactors, respectively. Requil is equilibrium reactor for which the chemical and phase equilibrium are determined by stoichiometric calculations.

3.3.2 Pressure swing adsorption (PSA)

In order to reach a high purity of hydrogen, a PSA unit is applied. Syngas passes through the PSA under high pressure, adsorbent materials (e.g., zeolites, activated carbon, or molecular sieves) adsorb other gases (CO, CO_2) and leave pure hydrogen. An input pressure of 15 bar for simulation of PSA is considered. The PSA outlet stream, denoted as H_2 contains 100% pure hydrogen.

Table 3.1: A brief description of blocks used in the simulation model.

User ID	Block ID	Description
DECOMP1	RYIELD	RYield reactor decomposes corncob into conventional components by yield distribution
DECOMP2	RYIELD	RYield reactor decomposes coconut coir into conventional components by yield distribution
DECOMP3	RYIELD	RYield reactor decomposes coconut shell into conventional components by yield distribution
RGIBBS	RGIBBS	RGibbs reactor-Equilibrium reactor with minimum Gibbs free energy for the pyrolysis of the decomposed product

SSPLIT	SEP	Separator – Separate ash from the volatile product stream
MIX	MIXER	Mixer- combine air and ash-free gas stream
OXI	RPLUG	Rplug reactor-simulate oxidation reactions of the co-gasification process by known kinetic reactions.
RED	RPLUG	Rplug reactor-simulate reduction reactions of the co-gasification process by known kinetic reactions.
SEP	SEP	Separator – Separate steam from the syngas stream

Table 3.2: Gasification reactions with kinetic parameters.

NO.	**Reaction**	**Reaction Name**	**A/k**	**E_a (MJ/Kmol)**	**Heat of reaction (MJ/Kmol)**
R1	$CH_4 + 0.5O_2 \longrightarrow CO + 2H_2$	Partial oxidation	2.4e8	126	-35.6
R2	$CO + 0.5O_2 \longrightarrow CO_2$	CO partial combustion	1.78e7	180	-283
R3	$C + CO_2 \longrightarrow 2CO$	Boudouard reaction	1.05e10	135	+172
R4	$C + H_2O \longrightarrow CO + H_2$	Water-gas reaction	200	49.9	+131
R5	$CO + H_2O \longrightarrow CO_2 + H_2$	Water-gas shift reaction	2.78	12.6	-41
R6	$CH_4 + H_2O \longrightarrow CO + 3H_2$	Steam-methane reforming	3e5	125	+206

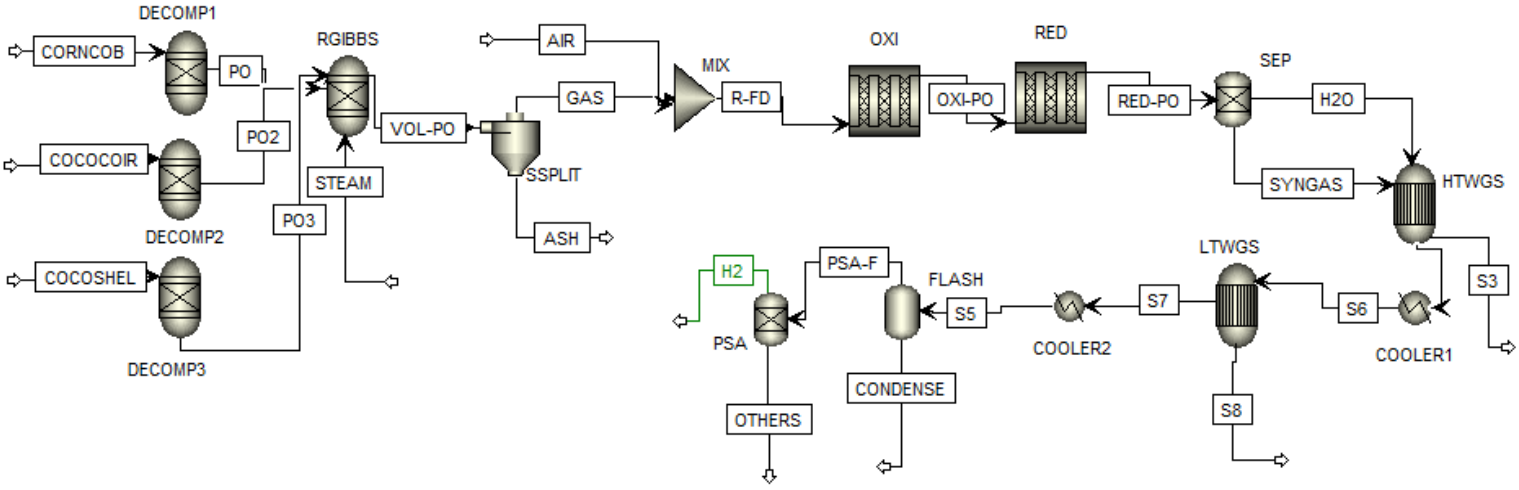

Fig. 3.1: Block diagram of the Aspen plus simulation.

3.4 Model Validation

To validate the simulation model for biomass co-gasification, the results of the present model are compared with the published data by AlNouss et al. [117] in the same conditions mentioned in Table 3.3. Figure 3.2 compares present data with the literature and shows that relative error(%) for CO, CO_2, H_2, CH_4, N_2, and LHV are 0.10, 2.67, 1.63, 1.72, 0.72, and 0% respectively. Thus, the present simulation model is valid for effective syngas production. However, the model was further modified to accommodate other features for co-gasification.

Table 3.3: Parameter used for model validation against literature [117].

Proximate analysis				Ultimate analysis					
VM	FC	MC	ASH	C	H	O	N	S	Cl
64	15.072	20	0.928	51.422	6.08	41.30	0.20	0.02	0.05
Biomass input: 1508.64 kg/hr Gasification temp.: 850℃ Gasification pressure: 1 bar				Steam-to-biomass ratio: 0.75 Gasifier steam temp.: 450℃					

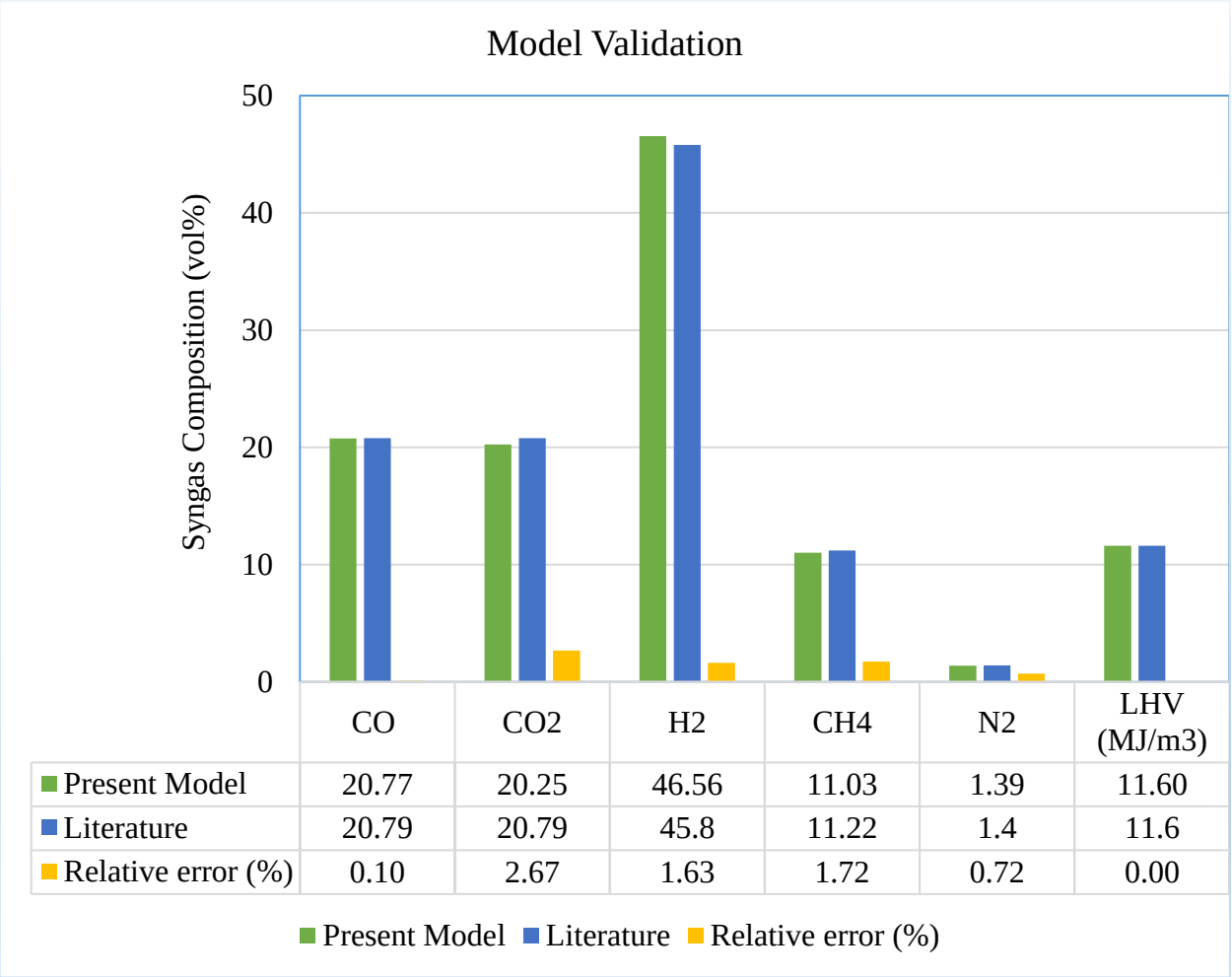

Fig. 3.2: Result comparison of the present model with the literature [117]

3.5 Feedstock Collection and Characterization

The feedstocks used in this study are corncob, coconut coir, and coconut shell collected from the southern part of Bangladesh. The proximate analysis of the feedstocks is performed according to ASTM standards E871, E872, E1358, and E1755. The higher heating value of the feedstocks is determined using a digital bomb calorimeter. Figure 3.3 shows the raw biomass used for co-gasification process.

Fig. 3.3: Feedstock used (a) Corncob, (b) Coconut coir, and (c) Coconut shell.

3.6 Machine learning model development

In this work, Two machine learning models are trained named as random forest (RF) and gradient boosting regression (GBR), to forecast the syngas composition, LHV, and CGE, and optimize the co-gasification process's operating conditions. These two models are selected based on earlier research on the use of machine learning in the gasification of biomass [130].

The Scikit-learn, pandas, and numpy libraries are used to run the machine learning algorithms in Python.

The operating conditions of the co-gasification process (gasifier temperature, pressure, SBR, ER, and blend ratio) are considered as input variables for ML development, and syngas composition (CO%, CO_2%, CH_4%, and H_2%), LHV, and CGE are considered output parameters. The dataset includes 125 data points and is arbitrarily split into two sections at an 80:20 ratio, which is a widely used tactic. To train the predictive models and adjust the hyper-parameters of machine learning algorithms, 80% of data points are designated as training sets. Leftover 20% is utilized to assess the general prediction accuracy of the ML models that have been trained.

Coefficient of determination (R^2), root mean square error (RMSE), mean absolute error (MAE) and mean square error (MSE) are among the metrics used to quantitatively assess the generic prediction performance. These metrics are determined using the actual and predicted values of the output targets and are defined by equations 3.2-3.5. A higher forecast accuracy is shown by a lower RMSE and a higher R^2 that is closer to one.

$$R^2 = 1 - \frac{\sum_{i=1}^{n}(y_i - \hat{y}_i)^2}{\sum_{i=1}^{n}(y_i - \bar{y})^2} \quad (3.2)$$

$$RMSE = \sqrt{\frac{1}{n}\sum_{i=1}^{n}(y_i - \hat{y}_i)^2} \quad (3.3)$$

$$MAE = \frac{1}{n}\sum_{i=1}^{n}|y_i - \widehat{y_i}| \quad (3.4)$$

$$MSE = \frac{1}{n}\sum_{i=1}^{n}(y_i - \hat{y}_i)^2 \quad (3.5)$$

Where n is the number of observations. y_i is the actual value, $\hat{y}_i$ is the predicted value, $\bar{y}$ is the mean of actual value.

3.7 Necessary tools

Different tools are used in this process to characterize the biomass and co-gasification process.

3.7.1 Muffle Furnace

A muffle furnace is a high-temperature laboratory device used for heating, burning, or calcining materials in a controlled environment. Its defining feature is a heating chamber isolated from the combustion products or heating elements by a refractory lining, ensuring uniform heating and protecting the samples from direct exposure to flame or gases. Figure 3.4 shows the muffle furnace.

Fig. 3.4: Muffle Furnace.

3.7.2 Digital analytical balance

An analytic balance is a form of balance that is used to quantify small masses in the milligram range. SP 404D model balance is selected for precision weighting. The specification of the magnetic stirrer is tabulated in Table A-1. Fig. 3.5 shows the digital analytic balance.

Fig. 3.5: Digital analytical balance.

3.7.3 Bomb calorimeter

A bomb calorimeter is a form of constant volume calorimeter used for the determination of the calorific value of a certain fuel. A bomb calorimeter has to withstand an intense pressure inside the calorimeter during the reaction. Electrical energy is utilized to ignite the fuel. While fuel burns in the calorimeter, it heats the air surrounding it, resulting in the expansion of the air. The expanded air exit through a tube which ejects the air from the calorimeter. The water outside the cooper tube is heated, as the air escapes through the tube. The temperature change of the water is calculated to determine the calorific value of the fuel. A VSI Microprocessor Fully Automatic Bomb Calorimeter is used to determine the calorific value of the fuel in this experiment. The specification of the bomb calorimeter is tabulated in Table A-2. The bomb calorimeter is shown in Fig. 3.6.

Fig. 3.6: Bomb calorimeter.

3.7.4 Chopper

A chopper is a machine or tool used for cutting, shredding, or chopping materials into smaller pieces or particles. In industrial and laboratory settings, choppers are commonly used for processing feedstocks, including biomass, food, and other materials. They vary in design, size, and application depending on the material being processed. Used to shred and reduce the size of biomass materials like wood, agricultural residues (e.g., corncob, coconut coir), and other organic waste before they undergo processes like gasification, combustion, or biogas production. Figure 3.7 shows the chopper machine used to cut sample into desired particle size (2-10mm).

Fig. 3.7: Chopper.

3.7.5 Bin Tipper

A bin tipper is an industrial machine designed to safely and efficiently unload bulk materials from containers, such as bins, drums, or totes, by tipping or rotating them. It is commonly used in industries like food processing, pharmaceuticals, chemicals, and agriculture for material handling. Sample placed in the bin tipper shown in figure 3.8 and it carried the sample in the gasifier reactor.

Fig. 3.8: Bin Tipper.

3.7.6 Fixed bed downdraft gasifier

A Fixed Bed Downdraft Gasifier is a type of biomass gasifier where biomass fuel is fed from the top of a fixed bed and moves downward as it undergoes various thermochemical processes to produce syngas (a mixture of gases like carbon monoxide (CO), hydrogen (H_2), and methane (CH_4)). This design is commonly used for converting solid biomass materials such as wood, agricultural residues, and other organic feedstocks into useful energy for power generation, heating, and other applications. Figure 3.9 shows the fixed bed downdraft gasifier in the laboratory.

Fig. 3.9: Fixed bed downdraft gasifier.

3.7.7 Cyclone separator

A cyclone separator is a mechanical device that uses centrifugal force to separate particles (solid or liquid) from a gas or liquid stream. It is commonly used in industrial

applications like air pollution control, material recovery, and fluid processing. Figure 3.10 shows the cyclone separator and it is used to separate char and tar from the producer gas.

Fig. 3.10: Cyclone separator.

3.7.8 Heat Exchanger

The producer gas has higher temperature and the heat exchanger shown in Figure 3.11 used to reduce the gas temperature.

Fig.3.11: Heat Exchanger.

3.7.9 Wet scrubber

A wet scrubber is a pollution control device that removes harmful particles or gases from an air stream by passing the gas through a liquid, typically water, which absorbs or

dissolves the pollutants. Wet scrubbers are commonly used in industrial processes to control emissions and improve air quality. Figure 3.12 shows the wet scrubber.

Fig. 3.12: Wet scrubber.

3.7.10 Filter bag

A filter bag in the context of gasification is a crucial component used for capturing and removing particulates, such as ash, soot, or dust, from the syngas produced during the gasification process. The syngas, which is generated from the thermal conversion of biomass or other feedstocks, typically contain fine solid particles that must be removed to ensure the gas is clean and suitable for downstream processes, including combustion, power generation, or further chemical synthesis. Filter bags are employed to trap solid particles (like ash and soot) that are suspended in the syngas produced during gasification. These particles can damage engines, turbines, and other equipment downstream if not removed. The use of filter bags ensures the syngas are free from particulate matter, improving the efficiency of combustion or conversion processes and protecting sensitive equipment. Figure 3.13 shows the filter bag.

Fig. 3.13: Filter bag.

3.8 Experimental setup

At first, the feedstock (corncob) is processed according to the required particle size (2-10mm) using the chopper machine, which then filters the particle through a net of a specific hole size. Then the processed feedstock is loaded into the bin tipper. The feedstock is transported from the bin tipper into the gasifier using a screw conveyor. This ensures a steady and controlled flow of biomass into the reactor. The total corn cob feed is 11.5 kg and gasifying agent (O_2) flow rate is 4 l/min. Then insert the oxy-acetylene torch through the ignition port and turn on the torch, direct the flame at the biomass, and hold it until the biomass material starts combusting. Gradually increases oxygen supply to maintain partial combustion. Remove the torch when the reaction is self-sustaining and then seal the ignition port tightly. In the drying zone, the biomass dried at temperatures of 100-150℃. In the pyrolysis stage, At 300-500℃, the dried biomass breaks down into gases, vapors (volatile compounds), and solid char. This process releases compounds like tar, CH_4, and H_2. Partial oxidation occurs during oxidation, producing CO and H_2 instead of CO_2 and the temperatures range from 900-1200℃. In the lower part of the gasifier, char reacts with gases like carbon dioxide (CO_2) and steam (H_2O) to produce additional CO and H_2 at the temperatures range from 700-800℃, called the reduction zone. The hot syngas leaving the gasifier contains fine particles of ash and char. It is directed through cyclone separators, which use centrifugal forces to separate and remove solid particulates from

the gas stream. After the cyclone, the syngas may still contain contaminants like tar, moisture, or acidic gases (e.g., H_2S, NH_3). It passes through the heat exchanger to reduce the temperature of the syngas. Finally, syngas passes through the wet scrubber and filter bag, to remove tars, water vapor, and other impurities, ensuring the syngas is clean and ready for use. Figure 3.14 shows the pilot scale gasification plant in the BCSIR, Chattogram used in the experiment.

Fig. 3.14: Actual experimental set up.

3.9 Flammability test

The flammability test of syngas is a critical step to verify its quality and usability as a fuel. To confirm that the syngas produced from the gasifier are flammable and suitable for combustion applications. If the syngas ignite easily, it is combustible. A blue flame typically indicates good-quality syngas with high hydrogen (H_2) and carbon monoxide (CO) content and the reddish or smoky flame might indicate impurities like tars or excessive carbon dioxide (CO_2). A stable flame indicates consistent gas quality and the sputtering or extinguishing flame may indicate low calorific value or high contamination (e.g., water vapor or inert gases). Figure 3.15 shows that the produced syngas ignited easily. Therefore, it is combustible and can be used for power production.

Fig.3.15: Flammability test of the produced syngas.

3.10 Flow diagram of the methodology

The whole methodology in brief can be illustrated as Fig. 3.16 and Fig. 3.17.

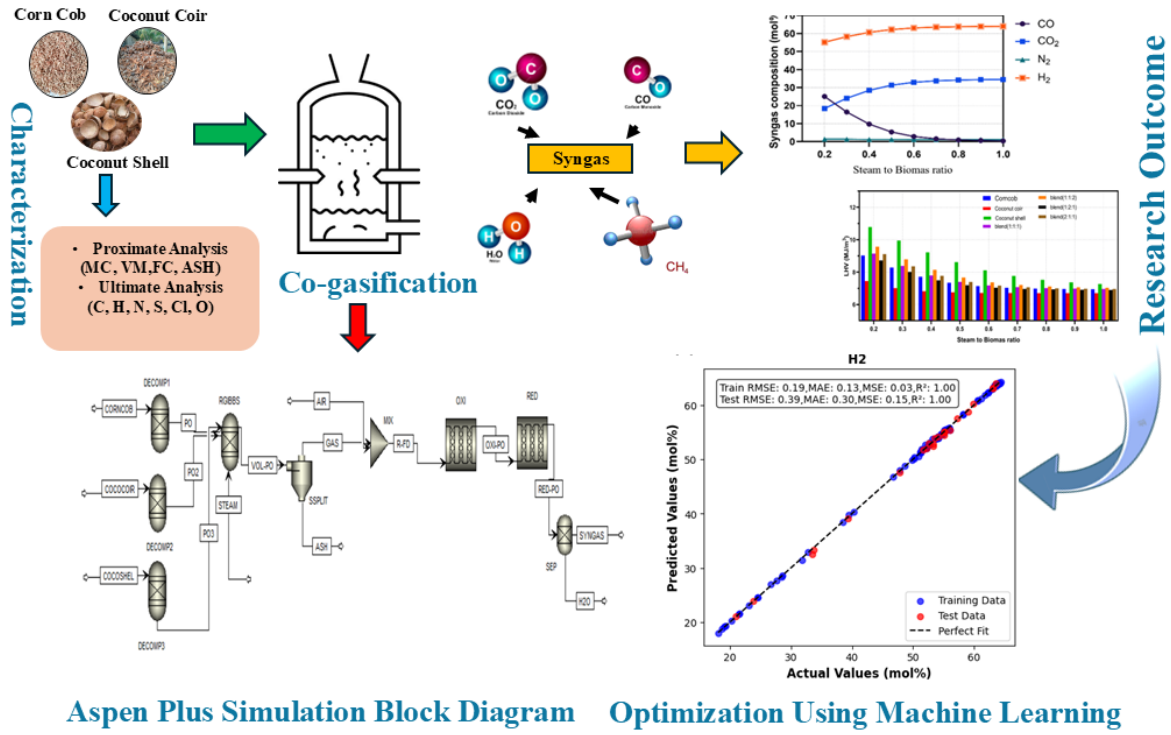

Fig. 3.16: Flow diagram of the methodology.

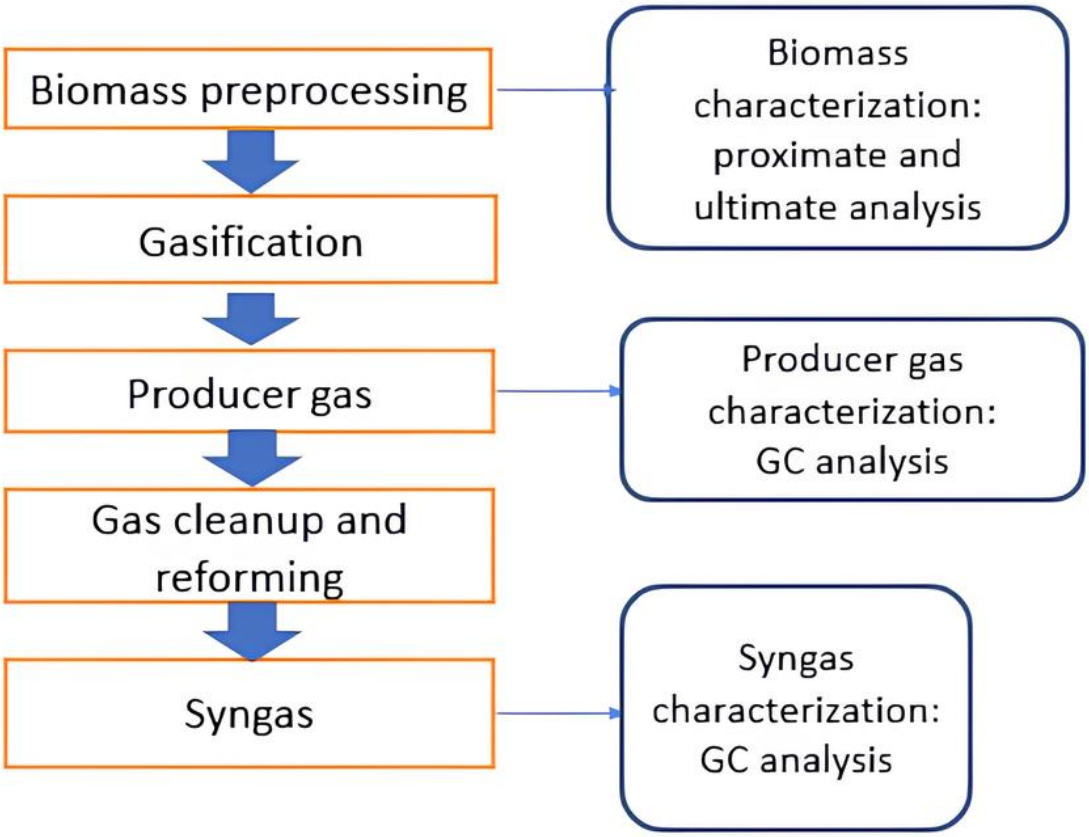

Fig. 3.17: Flow chart of the co-gasification process.

Chapter 4

Data Collection and Analysis

4.1 Introduction

Proximate and Ultimate analysis such as moisture content, volatile matter, fixed carbon, ash, C, H, N, S, and O of various biomasses such as Corncob, Coconut Coir, and Coconut Shell are determined followed by determining syngas composition, lower heating value, electrical power, and electrical efficiency.

4.2 Proximate and ultimate analysis of biomass

4.2.1 Moisture Content (MC)

To measure the water content in the sample, which affects heating value and combustion.

1. Weigh a clean, empty crucible (W1).
2. Add a known amount of the sample and weigh again (W2).
3. Place the crucible with the sample in an oven at 105°C for 1-2 hours.
4. Remove, cool in a desiccator, and weigh the sample (W3).

$$\text{Moisture } \% = (W2 - W3)/(W2 - W1) \times 100$$

4.2.2 Volatile Matter Content (VM)

To determine the volatile compounds (gases and tar) that vaporize on heating.

1. Use the moisture-free sample from the previous test.
2. Heat the sample in a muffle furnace at 950°C for 7 minutes.
3. Cool the sample in a desiccator and weigh (W4).

$$\text{Volatile Matter } \% = (W3 - W4)/(W2 - W1) \times 100$$

4.2.2 Ash Content (AC)

To determine the amount of inorganic residue left after complete combustion.

1. Take a sample in a crucible and heat it at 750°C in a muffle furnace for 2 hours.
2. Cool the crucible in a desiccator and weigh it (W5).

$$\text{Ash } \% = (W5 - W1)/(W2 - W1) \times 100$$

4.2.3 Fixed Carbon Content (FC)

This value is obtained by difference and represents the solid carbon left after the release of moisture, volatile matter, and ash.

Fixed Carbon %=100−(Moisture %+Volatile Matter %+Ash %)

4.2.4 C, H, N, O and S content

Channiwala and Parikh equation was used for predicting elemental composition, particularly for carbon, hydrogen, nitrogen, and sulfur, based on proximate analysis.

Carbon(C%)= 0.637*FC+0.455*VM
Hydrogen(H%)= 0.052*FC+0.062*VM
Nitrogen(N%)= 0.013*FC
Sulfur(S%)= 0.0016*FC
Oxygen(O%)= 100- (C+H+N+S)

4.2.5 Heating Value

Higher heating value (HHV) = $\frac{W \times 4.184 \times \Delta T}{m}$ (MJ/Kg)

Where, w = Energy equivalent of calorimeter in Cal/°C =2426 Cal/°C, m = Mass of the fuel sample in g, and ΔT = Temperature Rise in °C

Lower heating value (LHV) =HHV−(2.442×(9H+M)/100) (MJ/kg)

The ASTM standard, proximate analysis, ultimate analysis, and heating values of corncob, coconut coir, and coconut shell are tabulated in Table 4.1, Table 4.2, Table 4.3, and Table 4.4 respectively.

Table 4.1: ASTM Standard for elemental analysis of diverse agricultural residues.

Component	**ASTM Standard**	**Description**
Moisture	E871, E1358	Drying the sample in an oven at 105°C for 1-2 hours.

Volatile Matter	E872	Heating the sample in a muffle furnace at 950°C for 7 mins.
Ash	E1755	Heating the sample in a muffle furnace at 575-600°C until complete combustion
Fixed Carbon	By calculation	Fixed Carbon %=100−(Moisture %+Volatile Matter %+Ash %)

Table 4.2: Proximate analysis of selected feedstocks.

Feedstock	**Proximate analysis (wt%)**			
	MC	**VM**	**FC**	**ASH**
Corn Cob	10.87	70.56	16.12	2.45
Coconut Coir	17.49	63.47	16.31	2.73
Coconut Shell	4.52	73.78	20.44	1.26

Table 4.3: Ultimate analysis of selected feedstocks.

Feedstock	**Ultimate analysis (wt%)**					
	C	**H**	**N**	**S**	**Cl**	**O**
Corn Cob	42.37	5.21	0.21	0.026	0	49.734
Coconut Coir	39.27	4.78	0.21	0.03	0	52.98
Coconut Shell	46.59	5.64	0.26	0.04	0	46.21

Table 4.4: Calculation of Heating value for different feedstocks.

Feedstock	**Temperature rise (°C)**	**Mass (g)**	**HHV (MJ/kg)**	**LHV (MJ/kg)**
Corn Cob	0.50	0.24	21.12	19.71

Coconut Coir	0.58	0.33	17.82	16.35
Coconut Shell	1.4	0.76	18.68	17.33

4.3 Syngas Composition

During syngas composition analysis of corncob, coconut coir, and coconut shell, the effect of temperature, pressure, steam to biomass ratio, and equivalence ratio are recorded. The parameter effect was also recorded for the co-gasification of this biomass.

The syngas composition, col gas efficiency, and Lower heating value of corncob, coconut coir, coconut shell, blend (1:1:1), blend(1:1:2), blend(1:2:1), and blend(2:1:1) for the temperature range of 500-1200℃ at 1 bar pressure and SBR of 0.2 are tabulated in Table 4.5 to Table 4.11 respectively.

Table 4.5: The effect of temperature on syngas composition for corncob

Temp. (℃)	**500**	**600**	**700**	**800**	**850**	**900**	**1000**	**1100**	**1200**
CO(%)	12.22	17.80	22.08	24.26	24.26	24.27	24.28	24.31	24.34
CO_2(%)	30.07	24.94	21.03	19.04	19.04	19.03	19.03	19.01	18.99
N_2(%)	1.61	1.51	1.43	1.39	1.39	1.39	1.39	1.39	1.39
CH_4(%)	8.08	4.29	1.44	0.00	0.00	0.00	0.00	0.00	0.00
H_2(%)	48.01	51.46	54.02	55.30	55.30	55.30	55.29	55.29	55.28
LHV(MJ/m^3)	9.33	9.33	9.13	9.02	9.02	9.03	9.03	9.03	9.03

Table 4.6: The effect of temperature on syngas composition for coconut coir

Temp. (℃)	**500**	**600**	**700**	**800**	**850**	**900**	**1000**	**1100**	**1200**
CO(%)	0.55	2.83	8.32	8.69	8.76	8.84	8.99	9.17	9.36
CO_2(%)	40.36	36.83	31.38	31.07	31.03	30.97	30.88	30.76	30.64
N_2(%)	1.85	1.64	1.48	1.48	1.48	1.48	1.48	1.48	1.49
CH_4(%)	8.91	4.40	0.16	0.00	0.00	0.00	0.00	0.00	0.00
H_2(%)	48.32	54.30	58.64	58.75	58.72	58.70	58.64	58.57	58.49
LHV(MJ/m^3)	8.48	7.79	7.43	7.43	7.44	7.45	7.46	7.48	7.49

Table 4.7: The effect of temperature on syngas composition for coconut shell

Temp. (°C)	**500**	**600**	**700**	**800**	**850**	**900**	**1000**	**1100**	**1200**
CO(%)	35.12	38.00	39.53	41.00	41.38	41.39	41.39	41.39	41.39
CO_2(%)	11.82	9.53	7.64	6.22	5.85	5.85	5.85	5.85	5.85
N_2(%)	1.45	1.41	1.35	1.32	1.31	1.31	1.31	1.31	1.31
CH_4(%)	5.35	4.23	1.63	0.33	0.00	0.00	0.00	0.00	0.00
H_2(%)	46.24	46.82	49.83	51.11	51.43	51.43	51.43	51.43	51.43
LHV(MJ/m^3)	11.34	11.36	10.95	10.80	10.77	10.77	10.77	10.77	10.77

Table 4.8: The effect of temperature on syngas composition for co-gasification of blends (1:1:1)

Temp. (°C)	**500**	**600**	**700**	**800**	**850**	**900**	**1000**	**1100**	**1200**
CO(%)	13.37	18.90	22.94	25.27	25.29	25.30	25.32	25.33	25.35
CO_2(%)	29.15	24.07	20.37	18.24	18.23	18.22	18.21	18.20	18.19
N_2(%)	1.61	1.50	1.43	1.38	1.38	1.38	1.38	1.39	1.39
CH_4(%)	8.08	4.29	1.57	0.00	0.00	0.00	0.00	0.00	0.00
H_2(%)	47.77	51.22	53.68	55.09	55.09	55.09	55.08	55.07	55.06
LHV(MJ/m^3)	9.74	9.45	9.25	9.13	9.13	9.13	9.14	9.14	9.14

Table 4.9: The effect of temperature on syngas composition for co-gasification of blends (1:1:2)

Temp. (°C)	**500**	**600**	**700**	**800**	**850**	**900**	**1000**	**1100**	**1200**
CO(%)	18.44	23.50	27.22	29.52	29.52	29.52	29.53	29.54	29.55
CO_2(%)	25.25	20.53	17.10	14.97	14.97	14.97	14.97	14.96	14.96
N_2(%)	1.58	1.48	1.41	1.37	1.37	1.37	1.37	1.37	1.37
CH_4(%)	8.02	4.28	1.63	0.00	0.00	0.00	0.00	0.00	0.00
H_2(%)	46.69	50.20	52.63	54.13	54.13	54.13	54.12	54.12	54.12
LHV(MJ/m^3)	10.25	9.92	9.70	9.57	9.57	9.57	9.57	9.57	9.57
CGE(%)	83.42	86.25	88.67	90.31	90.30	90.30	90.29	90.29	90.29

Table 4.10: The effect of temperature on syngas composition for co-gasification of blends (1:2:1)

Temp. (℃)	500	600	700	800	850	900	1000	1100	1200
CO(%)	8.85	14.48	19.43	19.63	19.80	20.03	20.57	21.02	21.23
CO_2(%)	32.68	27.48	22.97	22.79	22.63	22.43	21.94	21.54	21.36
N_2(%)	1.64	1.53	1.44	1.43	1.43	1.43	1.42	1.41	1.41
CH_4(%)	8.15	4.30	1.11	0.99	0.88	0.74	0.40	0.13	0.02
H_2(%)	48.67	52.20	55.04	55.15	55.24	55.37	55.66	55.89	55.98
LHV(MJ/m^3)	9.30	9.01	8.79	8.79	8.78	8.77	8.75	8.73	8.73
CGE(%)	72.63	75.57	78.42	78.53	78.64	78.77	79.10	79.37	79.48

Table 4.11: The effect of temperature on syngas composition for co-gasification of blends (2:1:1)

Temp. (℃)	500	600	700	800	850	900	1000	1100	1200
CO(%)	13.08	18.62	22.72	25.03	25.03	25.05	25.05	25.07	25.10
CO_2(%)	29.38	24.29	20.54	18.43	18.43	18.42	18.42	18.40	18.39
N_2(%)	1.61	1.50	1.43	1.39	1.39	1.39	1.39	1.39	1.39
CH_4(%)	8.08	4.29	1.54	0.00	0.00	0.00	0.00	0.00	0.00
H_2(%)	47.83	51.28	53.76	55.14	55.14	55.14	55.13	55.13	55.12
LHV(MJ/m^3)	9.72	9.43	9.22	9.11	9.11	9.11	9.11	9.12	9.12
CGE(%)	77.33	80.32	82.80	84.31	84.30	84.33	84.30	84.31	84.31

The syngas composition, col gas efficiency, and Lower heating value of corncob, coconut coir, coconut shell, blend (1:1:1), blend(1:1:2), blend(1:2:1), and blend(2:1:1) for the pressure range of 1-20 bar at the temperature of 850℃ and SBR of 0.2 are tabulated in Table 4.12 to Table 4.18 respectively.

Table 4.12: The effect of pressure on syngas composition for corncob

Pressure (bar)	1	3	5	7	10	15	20
CO(%)	24.26	24.27	23.63	22.76	21.49	19.72	18.49
CO_2(%)	19.04	19.04	19.62	20.41	21.57	23.18	24.31
N_2(%)	1.39	1.39	1.40	1.41	1.44	1.47	1.49
CH_4(%)	0.00	0.00	0.42	1.00	1.84	3.01	3.82
H_2(%)	55.30	55.30	54.93	54.41	53.66	52.61	51.88
LHV(MJ/m^3)	9.02	9.02	9.05	9.10	9.15	9.25	9.29

Table 4.13: The effect of pressure on syngas composition for coconut coir

Pressure(bar)	**1**	**3**	**5**	**7**	**10**	**15**	**20**
CO(%)	8.76	8.76	8.77	8.67	8.23	7.54	6.97
CO_2(%)	31.03	31.02	31.02	31.11	31.52	32.16	32.68
N_2(%)	1.48	1.48	1.48	1.48	1.49	1.50	1.51
CH_4(%)	0.00	0.00	0.00	0.06	0.33	0.76	1.13
H_2(%)	58.72	58.72	58.72	58.67	58.42	58.03	57.69
LHV(MJ/m^3)	7.44	7.44	7.44	7.44	7.46	7.48	7.51

Table 4.14: The effect of pressure on syngas composition for coconut shell

Pressure(bar)	**1**	**3**	**5**	**7**	**10**	**14**	**20**
CO(%)	41.38	40.19	39.34	38.67	37.88	37.06	36.37
CO_2(%)	5.85	6.99	7.80	8.45	9.20	9.98	10.69
N_2(%)	1.31	1.34	1.36	1.37	1.39	1.41	1.43
CH_4(%)	0.00	1.02	1.74	2.31	3.00	3.69	4.44
H_2(%)	51.43	50.44	49.74	49.18	48.51	47.84	47.06
LHV(MJ/m^3)	10.77	10.88	10.95	11.00	11.09	11.13	11.25

Table 4.15: The effect of pressure on syngas composition for co-gasification of blends (1:1:1)

Pressure(bar)	**1**	**3**	**5**	**7**	**10**	**15**	**20**
CO(%)	25.29	25.29	24.55	23.64	22.32	20.50	19.50
CO_2(%)	18.23	18.22	18.90	19.74	20.94	22.60	23.52
N_2(%)	1.38	1.38	1.40	1.42	1.44	1.47	1.49
CH_4(%)	0.00	0.00	0.49	1.11	1.99	3.21	3.88
H_2(%)	55.09	55.09	54.64	54.09	53.30	52.20	51.59
LHV(MJ/m^3)	9.13	9.13	9.17	9.21	9.28	9.37	9.42

Table 4.16: The effect of pressure on syngas composition for co-gasification of blends (1:1:2)

Pressure(bar)	**1**	**3**	**5**	**7**	**10**	**15**	**20**
CO(%)	29.52	28.05	26.21	25.40	24.52	23.54	22.88

CO_2(%)	14.97	16.33	18.03	18.77	19.58	20.49	21.09
N_2(%)	1.37	1.39	1.43	1.45	1.46	1.48	1.49
CH_4(%)	0.00	1.05	2.35	2.93	3.55	4.24	4.71
H_2(%)	54.13	53.17	51.97	51.44	50.87	50.23	49.80
LHV(MJ/m^3)	9.57	9.66	9.76	9.81	9.86	9.92	9.96
CGE(%)	90.31	89.24	87.98	87.45	86.88	86.26	85.86

Table 4.17: The effect of pressure on syngas composition for co-gasification of blends (1:2:1)

Pressure(bar)	**1**	**3**	**5**	**7**	**10**	**15**	**20**
CO(%)	21.19	20.61	19.21	17.93	16.40	15.34	14.79
CO_2(%)	21.38	21.91	23.18	24.33	25.73	26.68	27.19
N_2(%)	1.40	1.41	1.44	1.46	1.49	1.51	1.52
CH_4(%)	0.00	0.37	1.26	2.08	3.06	3.74	4.10
H_2(%)	56.02	55.69	54.90	54.18	53.31	52.71	52.39
LHV(MJ/m^3)	8.72	8.75	8.81	8.86	8.93	8.97	9.00
CGE(%)	79.50	79.13	78.27	77.52	76.63	76.04	75.74

Table 4.18: The effect of pressure on syngas composition for co-gasification of blends (2:1:1)

Pressure(bar)	**1**	**3**	**5**	**7**	**10**	**15**	**20**
CO(%)	25.03	24.09	22.42	20.97	19.99	19.06	18.44
CO_2(%)	18.43	19.29	20.81	22.14	23.04	23.89	24.46
N_2(%)	1.39	1.40	1.43	1.46	1.48	1.50	1.51
CH_4(%)	0.00	0.63	1.74	2.72	3.38	4.00	4.42
H_2(%)	55.14	54.57	53.57	52.70	52.11	51.54	51.17
LHV(MJ/m^3)	9.11	9.16	9.24	9.31	9.36	9.41	9.44
CGE(%)	84.30	83.68	82.60	81.70	81.11	80.57	80.21

The syngas composition, col gas efficiency, and Lower heating value of corncob, coconut coir, coconut shell, blend (1:1:1), blend(1:1:2), blend(1:2:1), and blend(2:1:1) for the SBR range of 0.2-1 at the temperature of 850℃, air flow rate 100 kg/hr and pressure 1 bar are tabulated in Table 4.19 to Table 4.25 respectively.

Table 4.19: The effect of SBR on syngas composition for corncob

SBR	**0.2**	**0.3**	**0.4**	**0.5**	**0.6**	**0.7**	**0.8**	**0.9**	**1**
CO(%)	24.26	15.70	9.13	4.89	2.58	1.41	0.83	0.53	0.36
CO_2(%)	19.04	24.62	28.90	31.66	33.17	33.93	34.30	34.50	34.61
N_2(%)	1.39	1.29	1.22	1.17	1.14	1.13	1.13	1.12	1.12
CH_4(%)	0.00	0.00	0.00	0.00	0.00	0.00	0.00	0.00	0.00
H_2(%)	55.30	58.38	60.75	62.27	63.10	63.52	63.73	63.84	63.90
LHV(MJ/m^3)	9.03	8.28	7.71	7.34	7.14	7.03	6.98	6.96	6.94

Table 4.20: The effect of SBR on syngas composition for coconut coir

SBR	**0.2**	**0.3**	**0.4**	**0.5**	**0.6**	**0.7**	**0.8**	**0.9**	**1**
CO(%)	8.76	3.58	1.39	0.59	0.29	0.16	0.10	0.07	0.06
CO_2(%)	31.03	34.31	35.70	36.21	36.40	36.48	36.52	36.52	36.55
N_2(%)	1.48	1.41	1.38	1.37	1.36	1.36	1.36	1.36	1.36
CH_4(%)	0.00	0.00	0.00	0.00	0.00	0.00	0.00	0.00	0.00
H_2(%)	58.72	60.69	61.52	61.83	61.94	61.99	62.01	62.03	62.03
LHV(MJ/m^3)	7.45	7.01	6.82	6.75	6.72	6.71	6.70	6.70	6.70

Table 4.21: The effect of SBR on syngas composition for coconut shell

SBR	0.2	0.3	0.4	0.5	0.6	0.7	0.8	0.9	1
CO(%)	41.38	32.05	23.94	17.03	11.52	7.51	4.85	3.16	2.13
CO_2(%)	5.85	12.07	17.47	22.07	25.74	28.41	30.18	31.30	31.99
N_2(%)	1.31	1.23	1.15	1.09	1.03	1.00	0.97	0.96	0.95
CH_4(%)	0.00	0.00	0.00	0.00	0.00	0.00	0.00	0.00	0.00
H_2(%)	51.43	54.64	57.43	59.80	61.69	63.07	63.99	64.56	64.92
LHV(MJ/m^3)	10.78	9.95	9.22	8.61	8.11	7.76	7.52	7.37	7.27

Table 4.22: The effect of SBR on syngas composition for co-gasification of blends (1:1:1)

SBR	**0.2**	**0.3**	**0.4**	**0.5**	**0.6**	**0.7**	**0.8**	**0.9**	**1**
CO(%)	25.29	16.66	9.93	5.45	2.92	1.61	0.95	0.61	0.41
CO_2(%)	18.23	23.86	28.25	31.18	32.83	33.68	34.11	34.34	34.46

N_2(%)	1.38	1.29	1.21	1.17	1.14	1.12	1.12	1.11	1.11
CH_4(%)	0.00	0.00	0.00	0.00	0.00	0.00	0.00	0.00	0.00
H_2(%)	55.09	58.18	60.59	62.20	63.10	63.57	63.81	63.93	64.01
LHV(MJ/m^3)	9.14	8.38	7.79	7.40	7.18	7.07	7.01	6.98	6.96

Table 4.23: The effect of SBR on syngas composition for co-gasification of blends (1:1:2)

SBR	**0.20**	**0.30**	**0.40**	**0.50**	**0.60**	**0.70**	**0.80**	**0.90**	**1.00**
CO(%)	29.52	20.63	13.32	7.94	4.52	2.58	1.54	0.97	0.66
CO_2(%)	14.97	20.81	25.61	29.14	31.39	32.66	33.34	33.72	33.92
N_2(%)	1.37	1.27	1.19	1.14	1.10	1.08	1.07	1.06	1.06
H_2(%)	54.13	57.28	59.86	61.77	62.98	63.67	64.04	64.24	64.35
LHV(MJ/m^3)	9.57	8.79	8.14	7.67	7.37	7.20	7.11	7.06	7.03
CGE(%)	90.30	89.05	87.83	86.85	86.17	85.77	85.54	85.42	85.35

Table 4.24: The effect of SBR on syngas composition for co-gasification of blends (1:2:1)

SBR	**0.2**	**0.3**	**0.4**	**0.5**	**0.6**	**0.7**	**0.8**	**0.9**	**1**
CO(%)	21.19	12.95	7.03	3.55	1.81	0.99	0.58	0.38	0.26
CO2(%)	21.38	26.72	30.57	32.82	33.95	34.48	34.75	34.88	34.96
N2(%)	1.40	1.31	1.24	1.20	1.18	1.17	1.17	1.16	1.16
H2(%)	56.02	59.01	61.16	62.42	63.05	63.35	63.49	63.57	63.61
LHV(MJ/m3)	8.72	8.01	7.49	7.19	7.04	6.96	6.93	6.91	6.90
CGE(%)	79.50	78.29	77.30	76.66	76.33	76.16	76.08	76.04	76.02

Table 4.25: The effect of SBR on syngas composition for co-gasification of blends (2:1:1)

SBR	**0.2**	**0.3**	**0.4**	**0.5**	**0.6**	**0.7**	**0.8**	**0.9**	**1**
CO(%)	25.03	16.42	9.73	5.31	2.83	1.56	0.92	0.59	0.40
CO_2(%)	18.43	24.05	28.42	31.30	32.91	33.74	34.16	34.38	34.50
N_2(%)	1.39	1.29	1.22	1.17	1.14	1.13	1.12	1.11	1.11
H_2(%)	55.14	58.23	60.63	62.22	63.11	63.56	63.79	63.91	63.98
LHV(MJ/m^3)	9.11	8.36	7.77	7.39	7.17	7.06	7.00	6.97	6.96
CGE(%)	84.30	83.06	81.95	81.14	80.66	80.40	80.27	80.18	80.15

The syngas composition, col gas efficiency, and Lower heating value of corncob, coconut coir, coconut shell, blend (1:1:1), blend(1:1:2), blend(1:2:1), and blend(2:1:1) for the ER range of 0.1-0.6 at the temperature of 850℃, SBR of 0 and pressure 1 bar are tabulated in Table 4.26 to Table 4.32 respectively.

Table 4.26: The effect of ER on syngas composition for corncob

ER	**0.1**	**0.2**	**0.3**	**0.4**	**0.5**	**0.6**
CO(%)	31.51	19.89	14.10	13.51	13.24	12.90
CO2(%)	11.29	16.53	17.16	13.31	10.24	7.98
N2(%)	17.63	29.92	38.49	44.02	48.14	51.37
O2(%)	0.00	0.00	1.45	4.48	6.85	8.63
H2(%)	39.57	33.65	28.80	24.66	21.54	19.12
LHV(MJ/m^3)	8.24	6.14	4.89	4.37	3.99	3.69

Table 4.27: The effect of ER on syngas composition for coconut coir

ER	**0.1**	**0.2**	**0.3**	**0.4**	**0.5**	**0.6**
CO(%)	17.56	9.14	5.37	5.68	6.17	6.54
CO2(%)	22.51	25.47	24.97	20.58	16.93	14.08
N2(%)	16.50	28.43	37.34	43.09	47.36	50.72
O2(%)	0.00	0.00	1.02	3.79	6.05	7.82
H2(%)	43.42	36.95	31.30	26.85	23.47	20.83
LHV(MJ/m^3)	6.90	5.15	4.06	3.61	3.31	3.07

Table 4.28: The effect of ER on syngas composition for coconut shell

ER	**0.1**	**0.2**	**0.3**	**0.4**	**0.5**	**0.6**
CO(%)	45.50	31.07	26.85	24.54	22.67	21.04
CO_2(%)	0.00	7.26	5.14	2.80	1.22	0.20
N_2(%)	18.64	31.38	39.24	44.70	48.82	52.08
O_2(%)	0.00	0.05	3.53	6.40	8.47	9.98
H_2(%)	35.83	30.24	25.22	21.54	18.81	16.69

LHV(MJ/m^3)	9.61	7.18	6.11	5.42	4.89	4.46

Table 4.29: The effect of ER on syngas composition for co-gasification of blends (1:1:1)

ER	**0.1**	**0.2**	**0.3**	**0.4**	**0.5**	**0.6**
CO(%)	32.25	20.57	14.81	14.16	13.80	13.40
CO2(%)	10.69	15.96	16.50	12.70	9.69	7.50
N2(%)	17.66	29.97	38.49	44.01	48.12	51.35
O2(%)	0.00	0.00	1.53	4.58	6.94	8.70
H2(%)	39.39	33.49	28.65	24.54	21.43	19.04
LHV(MJ/m^3)	8.32	6.21	4.96	4.43	4.06	3.75

Table 4.30: The effect of ER on syngas composition for co-gasification of blends (1:1:2)

ER	**0.1**	**0.2**	**0.3**	**0.4**	**0.5**	**0.6**
CO(%)	35.83	27.94	24.61	22.15	20.17	18.50
CO_2(%)	7.78	8.12	5.75	4.07	2.94	2.17
N_2(%)	17.93	29.57	37.30	42.95	47.28	50.73
O_2(%)	0.00	2.59	5.60	7.76	9.33	10.52
H_2(%)	38.45	31.78	26.73	23.06	20.27	18.08
LHV(MJ/m^3)	8.68	6.96	5.99	5.29	4.74	4.29
CGE(%)	83.52	81.05	82.90	84.64	86.05	87.13

Table 4.31: The effect of ER on syngas composition for co-gasification of blends (1:2:1)

ER	**0.1**	**0.2**	**0.3**	**0.4**	**0.5**	**0.6**
CO(%)	28.89	21.37	19.07	17.48	16.15	15.01
CO_2(%)	13.38	13.97	10.78	8.37	6.65	5.41
N_2(%)	17.39	29.00	36.72	42.37	46.71	50.18
O_2(%)	0.00	1.96	4.99	7.23	8.88	10.14
H_2(%)	40.34	33.70	28.43	24.55	21.59	19.26
LHV(MJ/m^3)	8.00	6.34	5.48	4.86	4.37	3.98
CGE(%)	73.47	69.59	71.19	72.92	74.38	75.53

Table 4.32: The effect of ER on syngas composition for co-gasification of blends (2:1:1)

ER	**0.1**	**0.2**	**0.3**	**0.4**	**0.5**	**0.6**
CO(%)	32.15	24.42	21.66	19.65	18.02	16.63
CO_2(%)	10.76	11.26	8.44	6.37	4.92	3.90
N_2(%)	17.65	29.28	37.01	42.65	46.99	50.45
O_2(%)	0.00	2.24	5.27	7.48	9.09	10.32
H_2(%)	39.43	32.78	27.62	23.84	20.96	18.70
LHV(MJ/m^3)	8.32	6.62	5.72	5.06	4.54	4.12
CGE(%)	77.97	74.65	76.39	78.13	79.56	80.69

Chapter 5
Results and Discussions

5.1 Introduction

This chapter is intended to investigate the effect of the co-gasification of biomass on the syngas composition, cold gas efficiency (CGE), and LHV. Proximate analysis, ultimate analysis, and lower heating value of corn cob, coconut coir, and coconut are determined. The effect of temperature, pressure, steam-to-biomass (SBR) ratio, and equivalence ratio (ER) on syngas composition and lower heating value are determined.

5.2 Physicochemical property

5.2.1 Proximate and Ultimate analysis

The proximate analysis of the feedstocks is performed according to ASTM standards E871, E872, E1358, and E1755. The higher heating value of the feedstocks is determined using a digital bomb calorimeter. The results of these analyses are shown in Figure 5.1 to 5.3. The proximate analysis of feedstocks indicated that its MC, VM, FC, ash, and LHV are in the range of 4.52-17.49%, 63.47-73.78%, 16.12-20.44%, 1.26-2.73%, and 16.35 – 19.71 MJ/kg respectively.

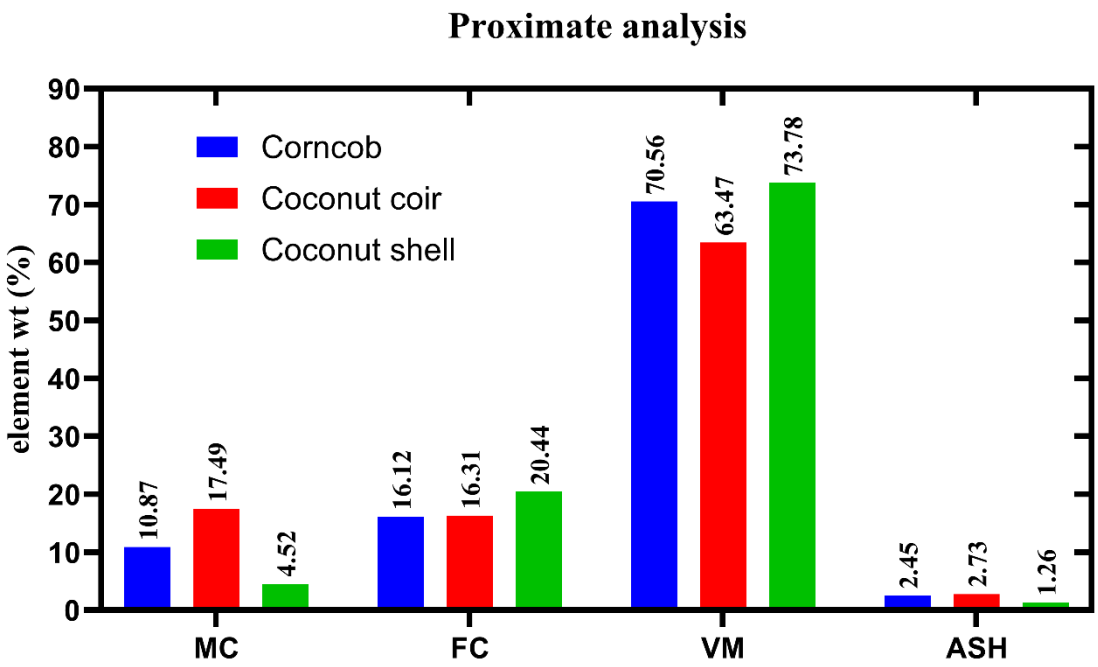

Fig. 5.1: Proximate analysis of corncob, coconut coir, and coconut shell.

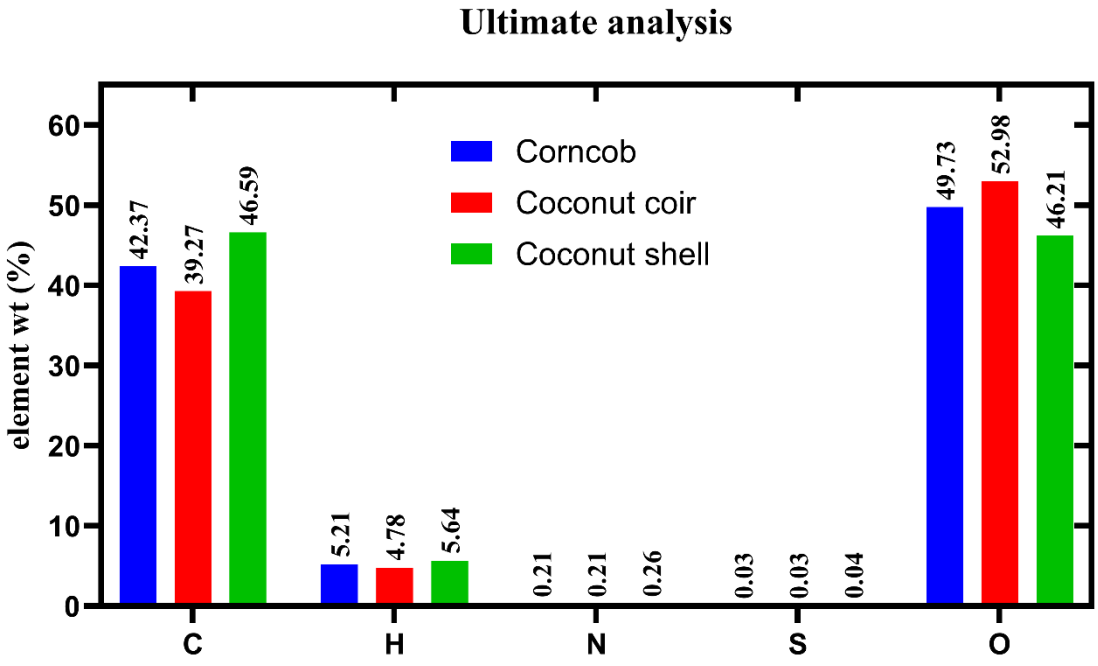

Fig. 5.2: Ultimate analysis of corncob, coconut coir, and coconut shell.

5.2.2 Heating value

Calorific value or heating value (HV) of a fuel is defined as the amount of heat released from the complete combustion of a unit of the fuel. The lower heating value (LHV) or net heating value and higher heating value (HHV) or gross heating value are the measures of the heat of combustion of a fuel [109]. Combustion characteristics and power output enormously

depend on the HV of a fuel or fuel emulsion. High HV of a fuel leads to enhanced performance of a CI engine. Figure 5.3 shows the Lower heating value of corncob, coconut coir, and coconut shell.

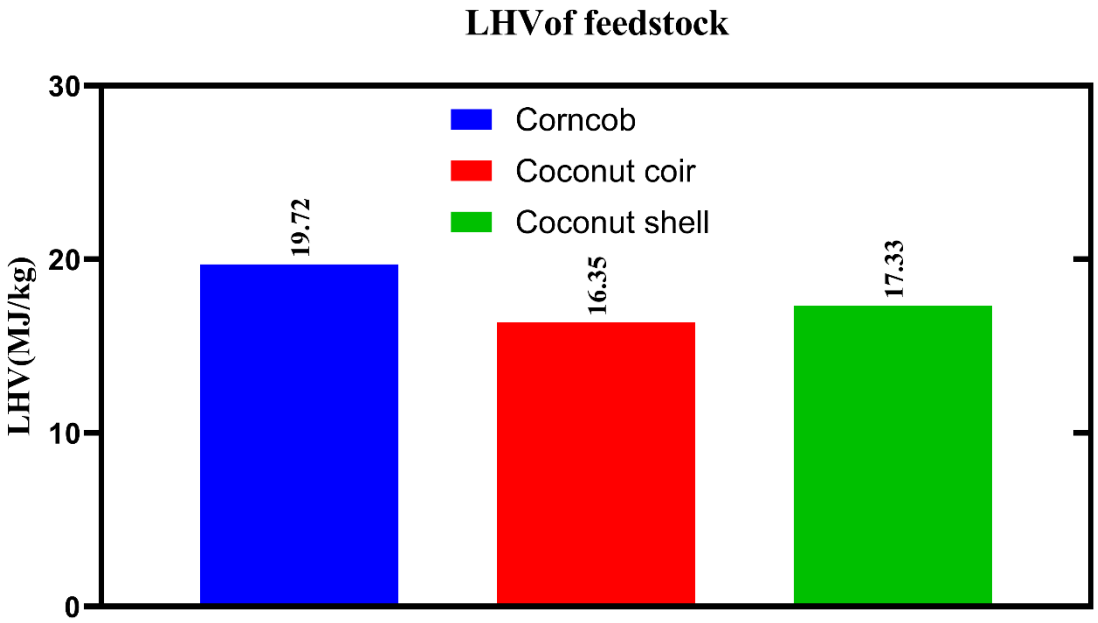

Fig. 5.3: Lower heating value of corncob, coconut coir, and coconut shell.

5.3 Syngas composition

5.3.1 Effect of temperature on syngas composition

Temperature affects tar and char yields, heating value, gas yield, cold gas efficiency, and carbon conversion, the most crucial operational element in the gasification process. Rising temperatures typically result in higher CO, H_2, heating value, and gas yields. A temperature rise enhances the hydrocarbon endothermic reforming process and releases more volatile matter; leading to a decrease in heavy tars and char concentrations and an increase in H_2 gas concentrations and overall gas production [93]. The Boudouard, Water-gas, and Steam-methane reforming reactions are endothermic and require heat during the gasification. Thus, the production of hydrogen and carbon monoxide increases with an increase in gasification temperature. However, above 830℃ reverse water gas reaction activated and reduced the H_2 and CO production [86]. The gasification temperature (T_g) effect on syngas composition is investigated in the temperature range between 500-1200℃ as shown in Figures 5.4-5.10 at the conditions of steam to biomass ratio 0.2, gasifier pressure 1 bar, air flow rate 100 kg/hr, and biomass feed rate 3000 kg/hr. An increase in temperature increases the volume fraction of H_2 and CO and decreases the amount of CO_2 and CH_4. This trend shows a good agreement with

the investigation of Cao et al. [116]. The maximum volume fractions of H_2 are 55.30%, 58.75%, 51.43%, 55.09%, 54.13%, 55.98%, and 55.12% respectively, for the corncob, coconut coir, coconut shell, blend (1:1:1), blend (1:1:2), blend (1:2:1), and blend (2:1:1) at the temp. of 850℃. The volume fractions of CO increased from 12.22 to 24.34%, 0.55 to 9.36%, 35.12 to 41.39%, 13.37 to 25.35%, 18.44 to 29.55%, 8.85 to 21.23%, and 13.08 to 25.10% respectively, for the corncob, coconut coir, coconut shell, blend (1:1:1), blend (1:1:2), blend (1:2:1), and blend (2:1:1) at the temp. of 1200℃ and reach almost peak level at 850℃. The volume fractions of CO_2 decreased from 30.07 to 18.99%, 40.36 to 30.64%, 11.82 to 5.85%, 29.15 to 18.19%, 25.25 to 14.96%, 32.68 to 21.36%, and 29.38 to 18.39% respectively, for the corncob, coconut coir, coconut shell, blend (1:1:1), blend (1:1:2), blend (1:2:1), and blend (2:1:1) at the temp. of 1200℃ and reach almost the minimum level at 850℃. CH_4 content decreased to zero with an increase in temperature up to 850℃. Thus, this analysis shows that the optimal gasifier temperature considered to be 850℃.

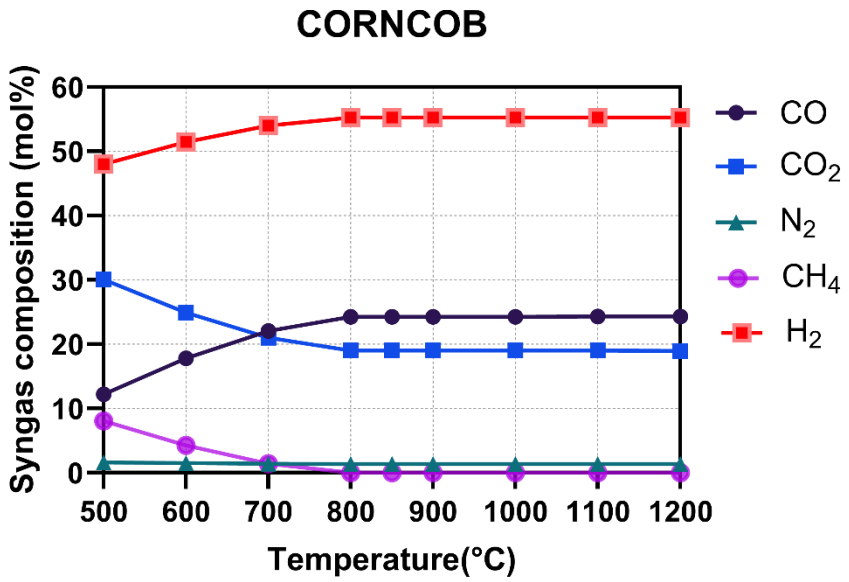

Fig. 5.4: The effect of temperature on syngas composition for corncob.

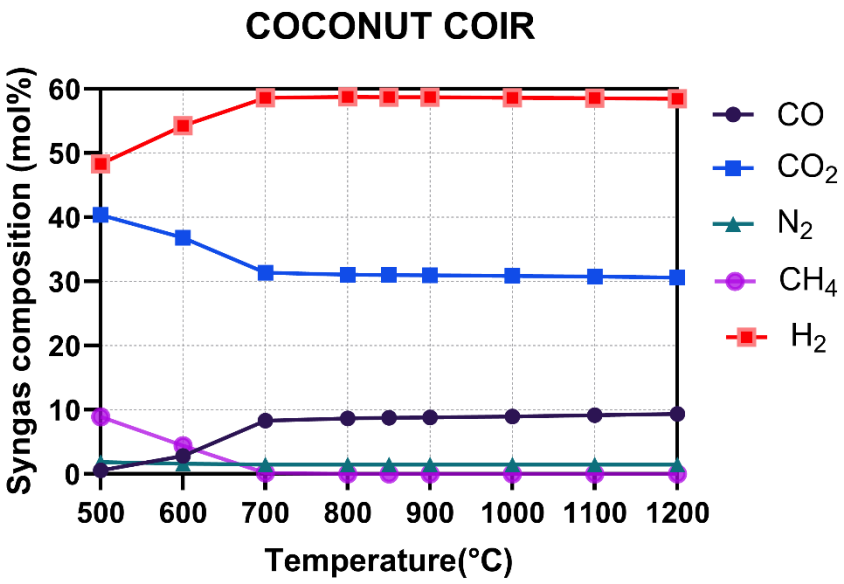

Fig. 5.5: The effect of temperature on syngas composition for coconut coir.

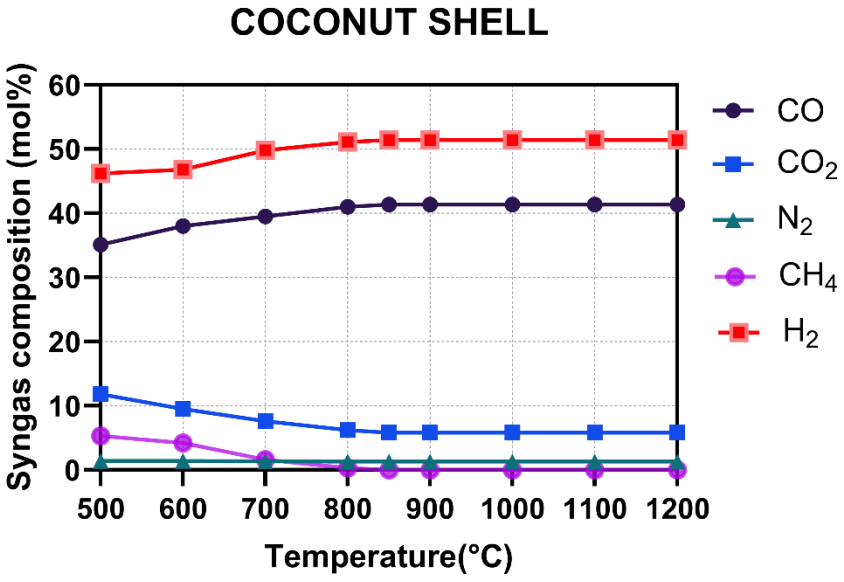

Fig. 5.6: The effect of temperature on syngas composition for coconut shell.

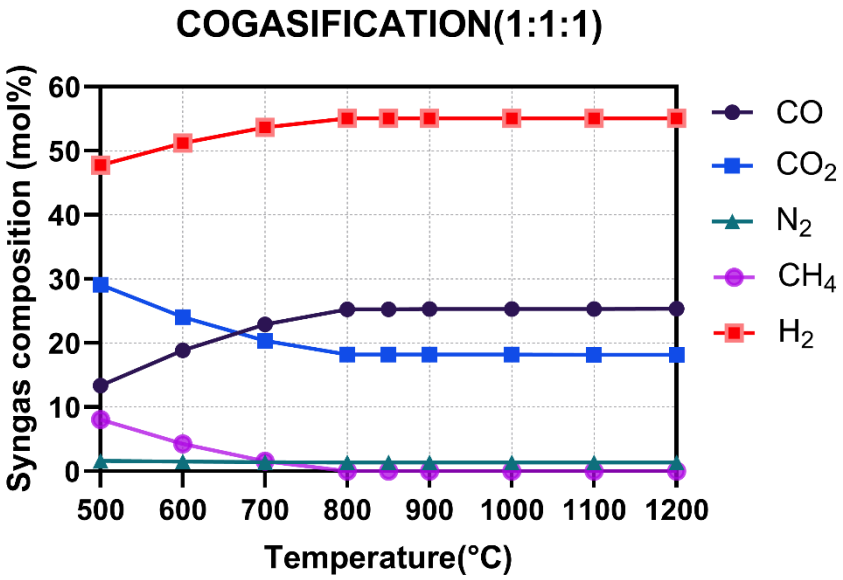

Fig. 5.7: The effect of temperature on syngas composition for blend (1:1:1).

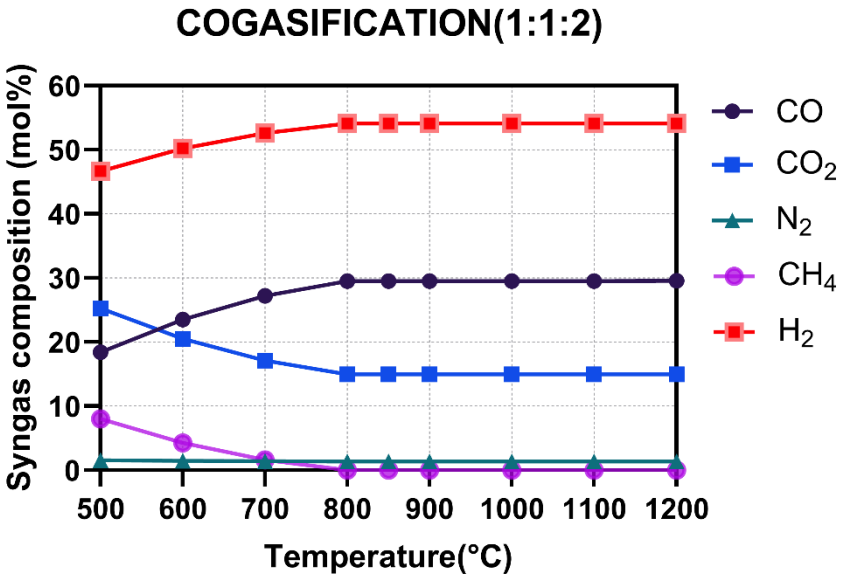

Fig. 5.8: The effect of temperature on syngas composition for blend (1:1:2).

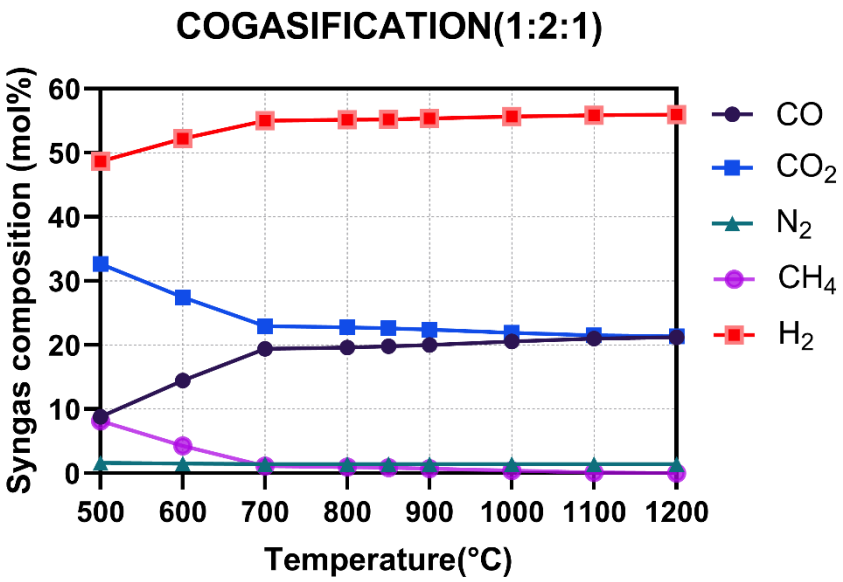

Fig. 5.9: The effect of temperature on syngas composition for blend (1:2:1).

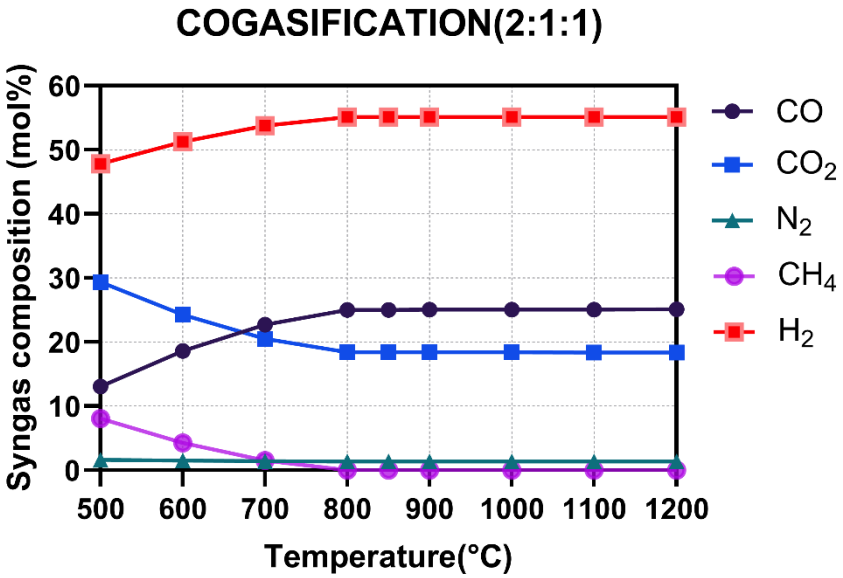

Fig. 5.10: The effect of temperature on syngas composition for blend (2:1:1).

5.3.2 Effect of pressure on syngas composition

The gasification pressure (P_g) effect on syngas composition is investigated in the pressure range between 1-20 bar as shown in Figures 5.11-5.17 at the conditions of steam to biomass ratio 0.2, gasifier temperature 850℃, air flow rate of 100 kg/hr, and biomass feed rate of 3000 kg/hr. An increase in pressure decreases the volume fraction of H_2 and CO and increases the amount of CO_2 and CH_4 due to the Le Chatelier principle. At higher pressure, methanation reactions are favored. Thus, the amount of H_2 and CO decreases. These show a

good alignment with other literature [117]. The volume fractions of H_2 decreased from 55.30%, 58.75%, 51.43%, 55.09%, 54.13%, 52.39%, and 51.17% to 51.88%, 57.69%, 47.06%, 51.59%, 49.80%, 52.39%, and 51.17%, respectively, for the corncob, coconut coir, coconut shell, blend (1:1:1), blend (1:1:2), blend (1:2:1), and blend (2:1:1) with the increase in pressure from 1 bar to 20 bar. CO content decreased from 24.26, 8.76, 41.38, 25.29, 29.52, 21.19, and 25.03% to 18.49, 6.97, 36.37, 19.50, 22.88, 14.79, and 18.44% respectively. However, CO_2 content increased with an increase in pressure. Thus, the optimal gasifier pressure is 1 bar for this co-gasification process.

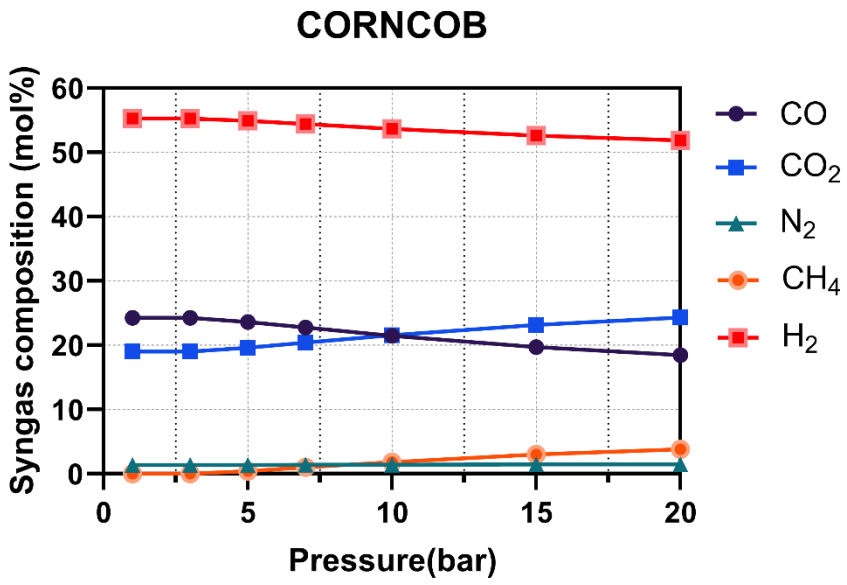

Fig. 5.11: The effect of pressure on syngas composition for corncob.

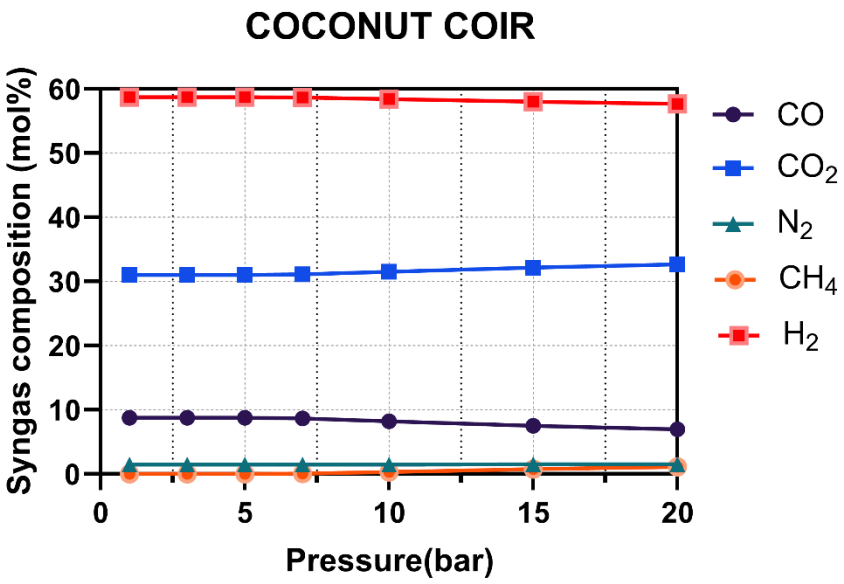

Fig. 5.12: The effect of pressure on syngas composition for coconut coir.

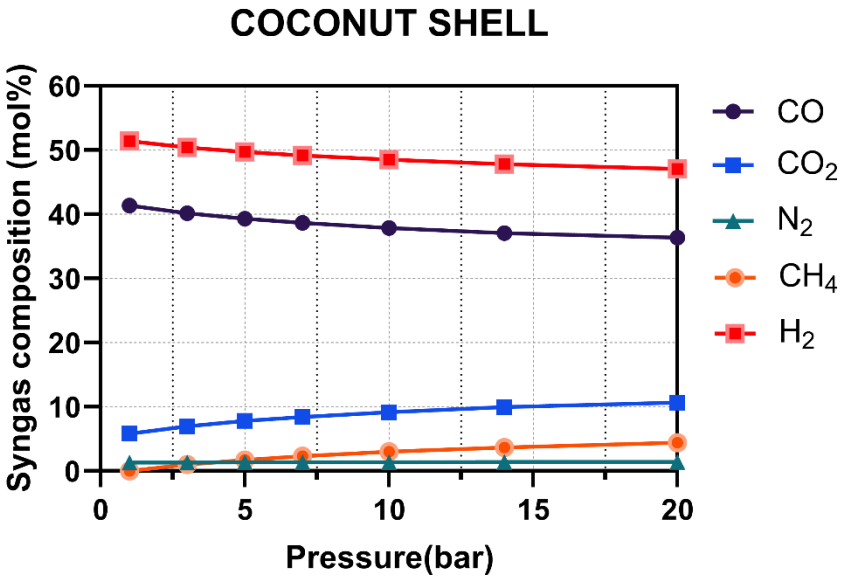

Fig. 5.13: The effect of pressure on syngas composition for coconut shell.

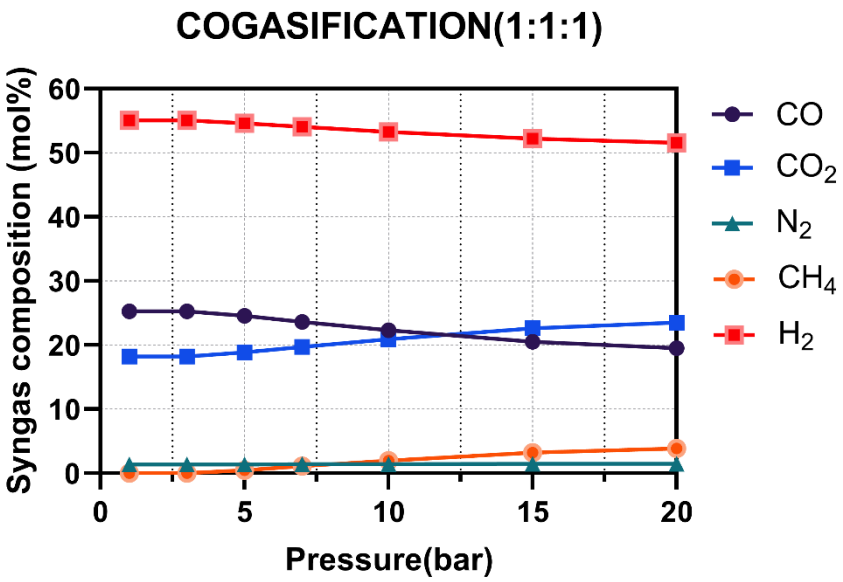

Fig. 5.14: The effect of pressure on syngas composition for blend (1:1:1).

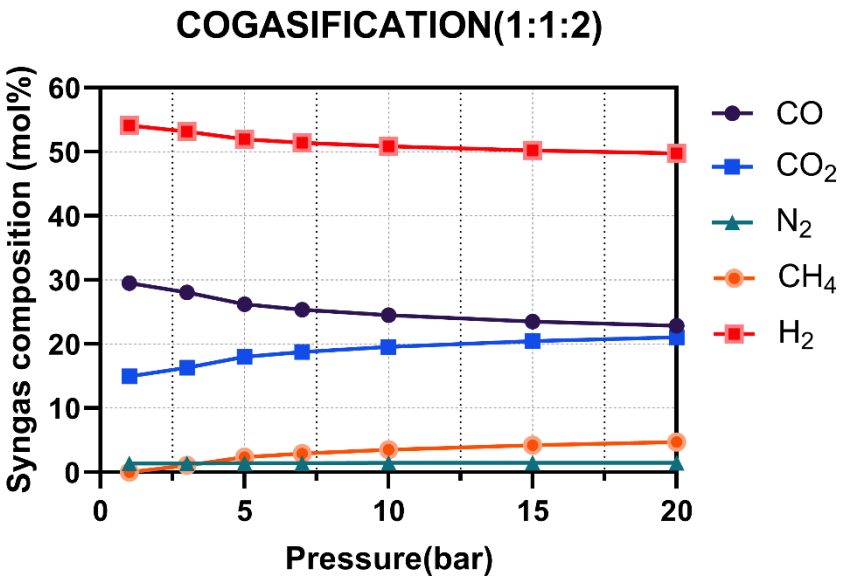

Fig. 5.15: The effect of pressure on syngas composition for blend (1:1:2).

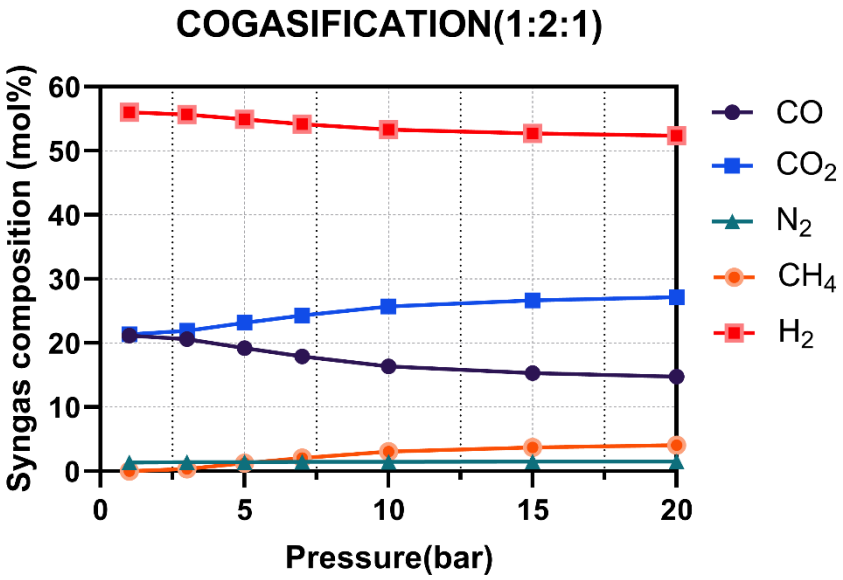

Fig. 5.16: The effect of pressure on syngas composition for blend (1:2:1).

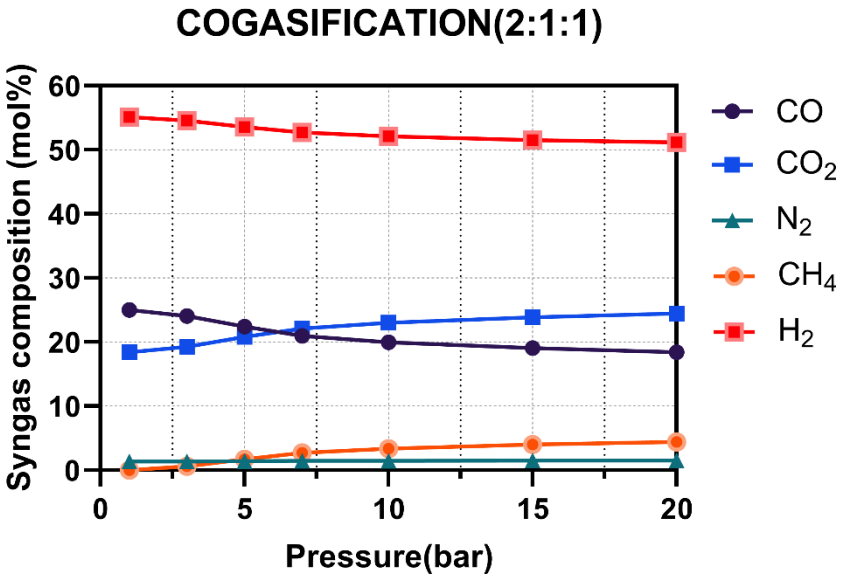

Fig. 5.17: The effect of pressure on syngas composition for blend (2:1:1).

5.3.3 Effect of SBR on syngas composition

The steam to biomass ratio (SBR) effect on syngas composition is investigated in the range between 0.2-1 as shown in Figure 5.18-5.24 at the conditions of gasifier temperature of 850℃, gasifier pressure of 1 bar, air flow rate of 100 kg/hr, and biomass feed rate of 3000 kg/hr. The Water-gas shift reaction is enhanced with the increase in SBR. Thus, An increase in SBR increases the volume fraction of H_2 and CO_2 and decreases the amount of CO. Cao et al. [116] also found the same effect in their study. The volume fractions of H_2 rise from 55.30%, 58.72%,

51.43%, 55.09%, 54.13%, 56.02%, and 55.14% to 63.90%, 62.03%, 64.92%, 64.01%, 64.35%, 63.61%, and 63.98% respectively, for the corncob, coconut coir, coconut shell, blend (1:1:1), blend (1:1:2), blend (1:2:1), and blend (2:1:1) with the increase in SBR from 0.2 to 1. However, the volume fractions of CO decreased sharply from 24.26, 8.76, 41.38, 25.29, 29.52, 21.19, and 25.03% to 0.36, 0.06, 2.13, 0.41, 0.66, 0.26, and 0.40% respectively. Thus, the total amount of H_2 and CO decreases with the increase in SBR, and from this analysis, the optimal SBR is 0.2.

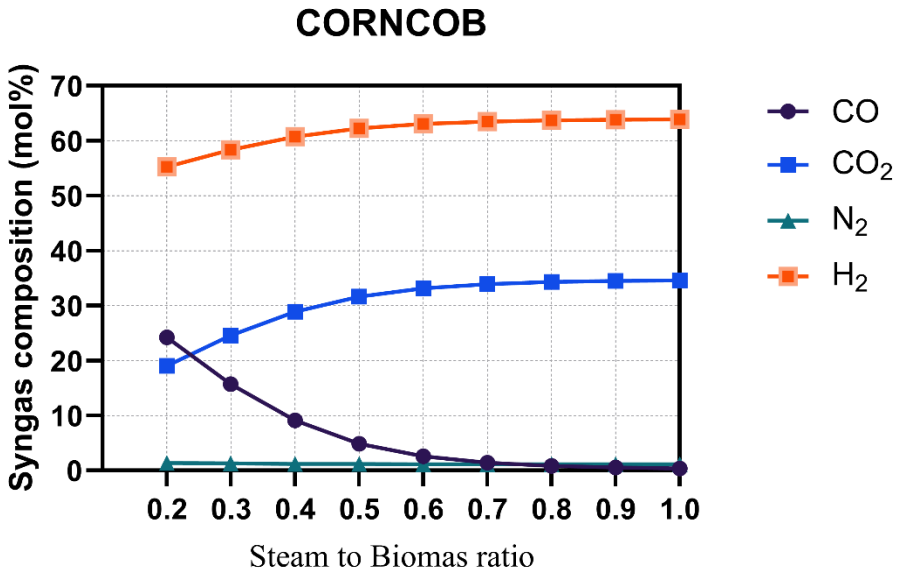

Fig. 5.18: The effect of SBR on syngas composition for corncob.

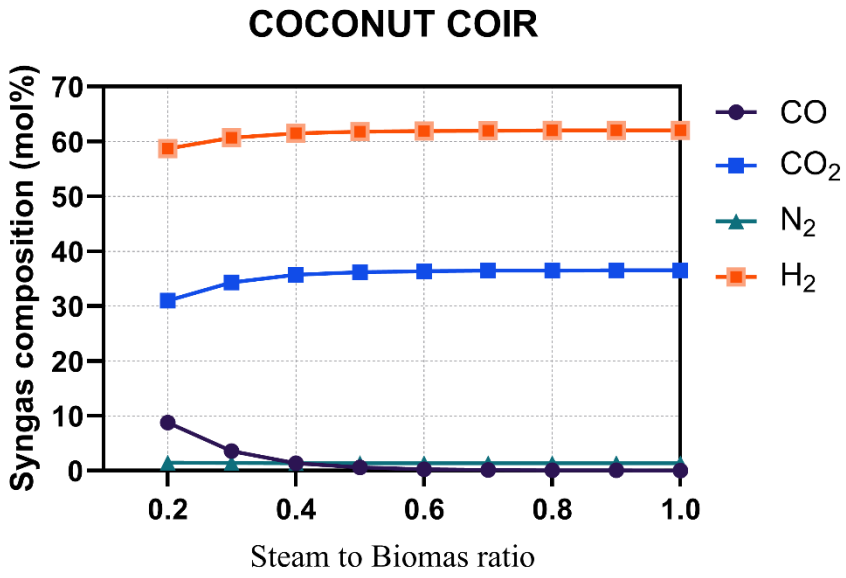

Fig. 5.19: The effect of SBR on syngas composition for coconut coir.

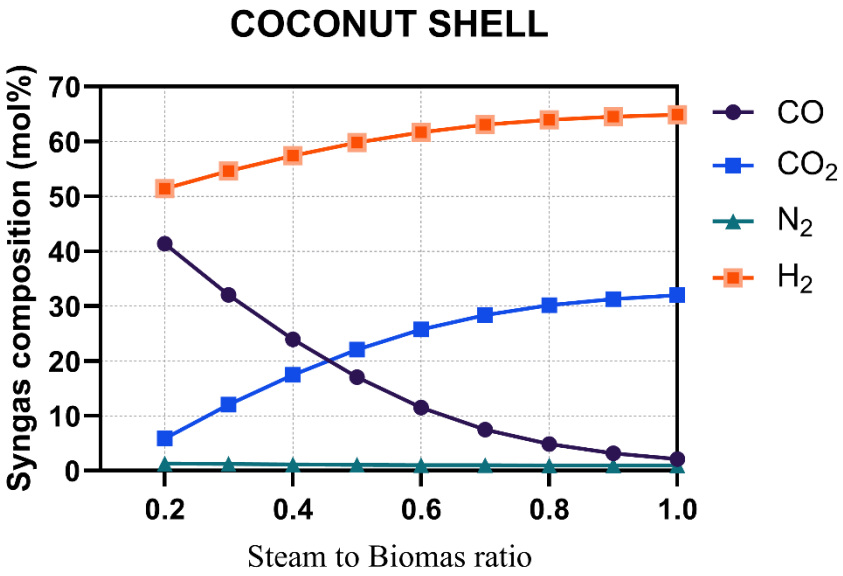

Fig. 5.20: The effect of SBR on syngas composition for coconut shell.

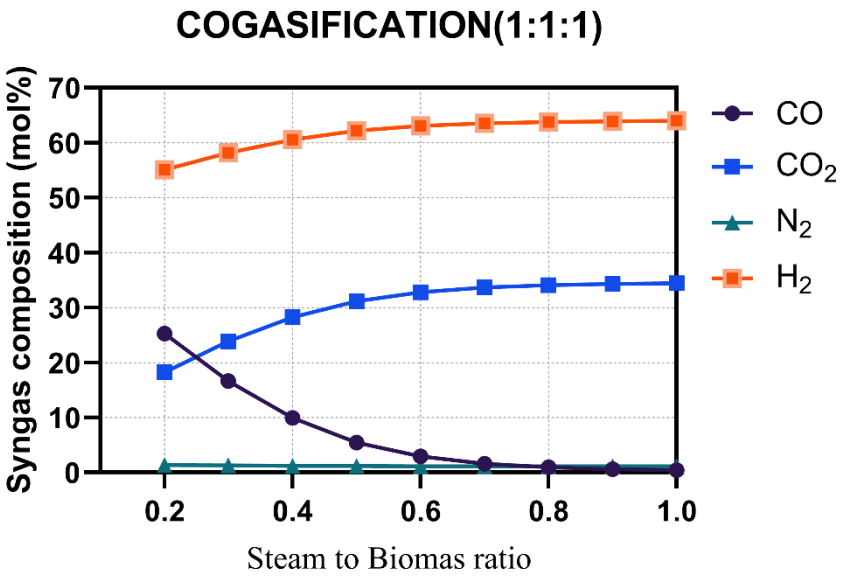

Fig. 5.21: The effect of SBR on syngas composition for blend (1:1:1).

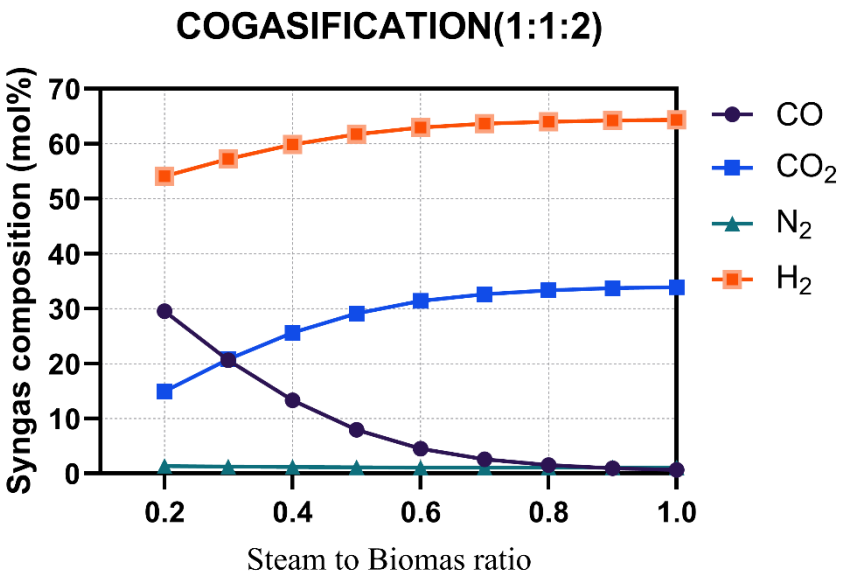

Fig. 5.22: The effect of SBR on syngas composition for blend (1:1:2).

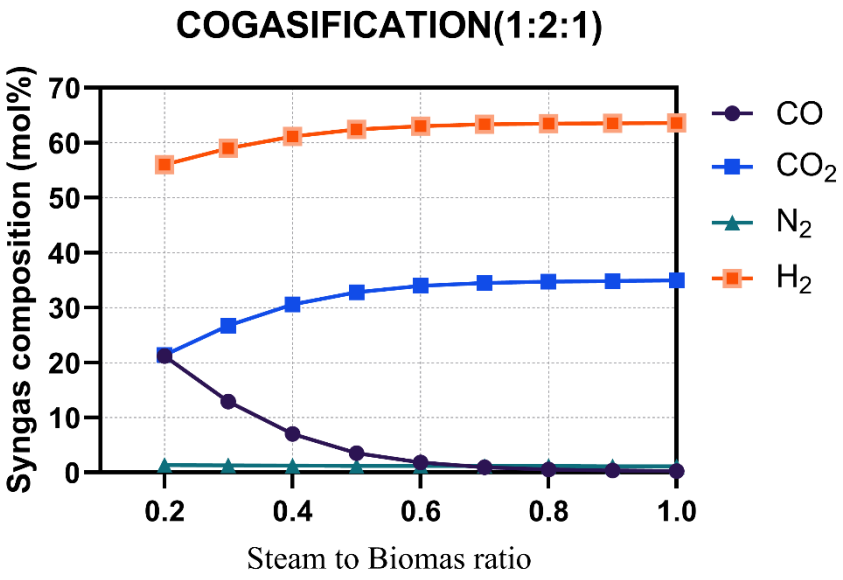

Fig. 5.23: The effect of SBR on syngas composition for blend (1:2:1).

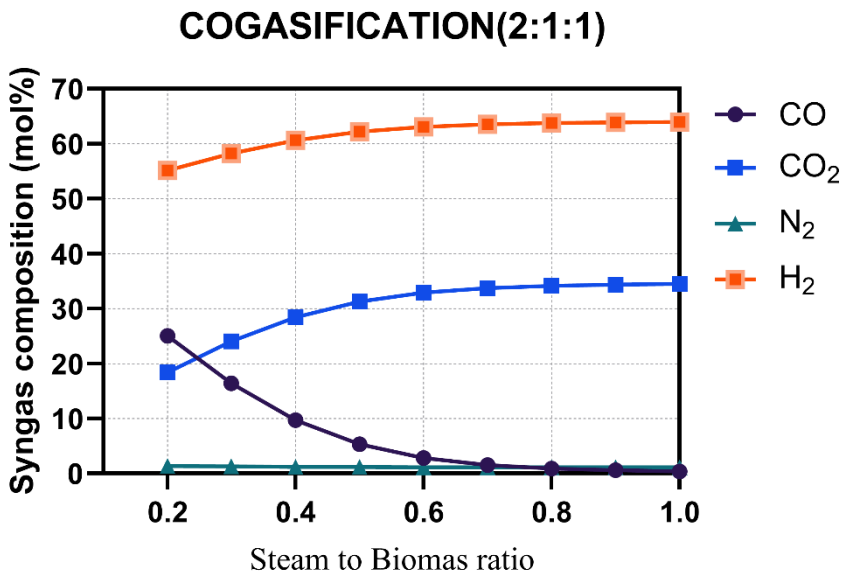

Fig. 5.24: The effect of SBR on syngas composition for blend (2:1:1).

5.3.4 Effect of ER on syngas composition

One of the most important variables in the gasification process is the equivalency ratio, which is the ratio of the real air-fuel ratio utilized in gasification to the stoichiometric air-fuel ratio for combustion. The air equivalence ratio can be calculated using equations (5.1) and (5.2).

$$ER = \frac{\text{Actual mass flow rate of air}}{\text{Stoichiometric mass flow rate of air}} \quad \ldots\ldots(5.1)$$

$$\text{Stoichiometric mass flow rate of air} = \frac{2.67C+8H-O}{0.23} \quad \ldots\ldots(5.2)$$

Here, C, H, and O are the weight percentages of carbon, hydrogen, and oxygen in the dry feedstock or feedstock mixture respectively.

ER is one of the key parameters in the gasification process which enhances the syngas quality and calorific value. Air gasification is cost-friendly; However, it produces a high amount of nitrogen in the producer gas thus decreasing both the overall energy efficiency and calorific value of the gasification process. The effect of ER in the range of 0.1 to 0.6 on syngas composition is illustrated in Figure 5.25-5.31 at the conditions of gasifier temperature of 850℃, gasifier pressure of 1 bar, SBR 0, and biomass feed rate of 3000 kg/hr. An increase in ER decreases the volume fraction of H_2 and CO and increases the amount of CO_2 up to an ER of 0.2-0.3 then decreases due to the enhanced oxidation of CO and H_2 with the increase of ER (oxygen content). The amount of N_2 and O_2 increases with ER as the amount of air increases. Barontini et al. [69] showed the same trend in their study.

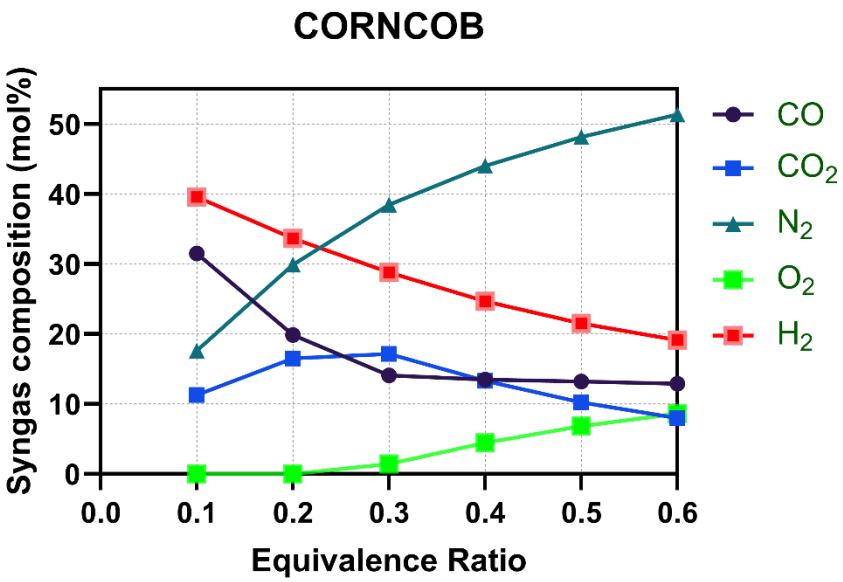

Fig. 5.25: The effect of ER on syngas composition for corncob.

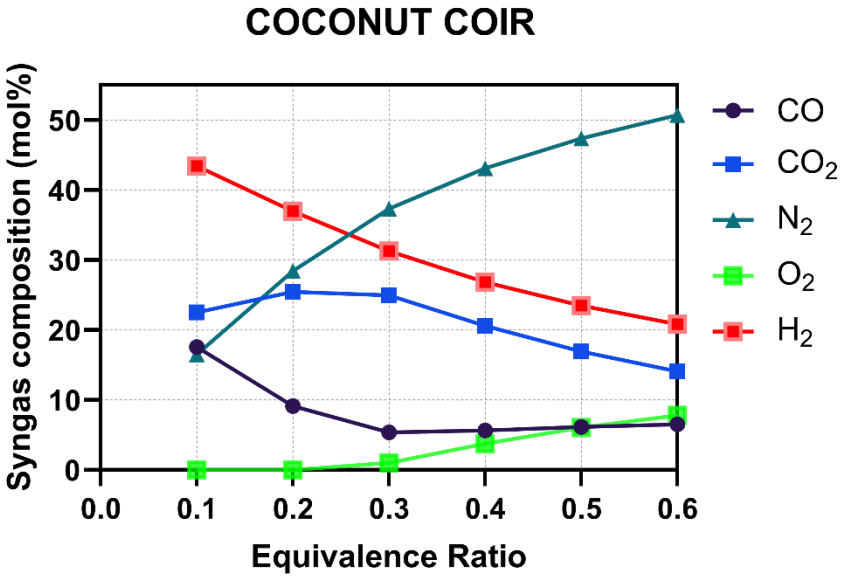

Fig. 5.26: The effect of ER on syngas composition for coconut coir.

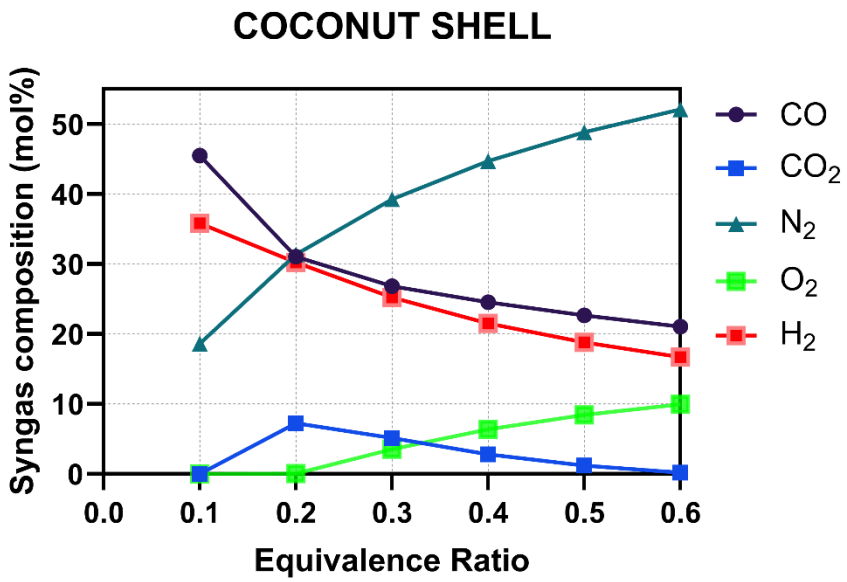

Fig. 5.27: The effect of ER on syngas composition for coconut shell.

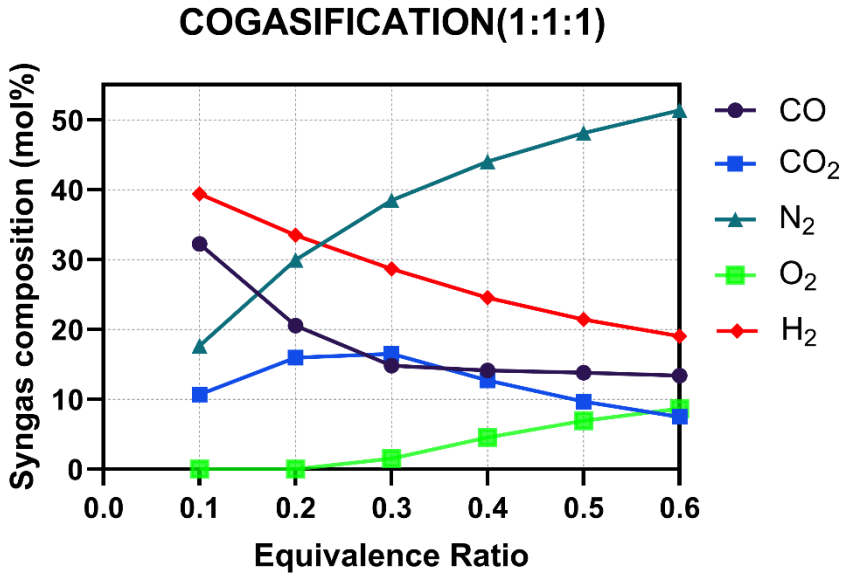

Fig. 5.28: The effect of ER on syngas composition for blend (1:1:1).

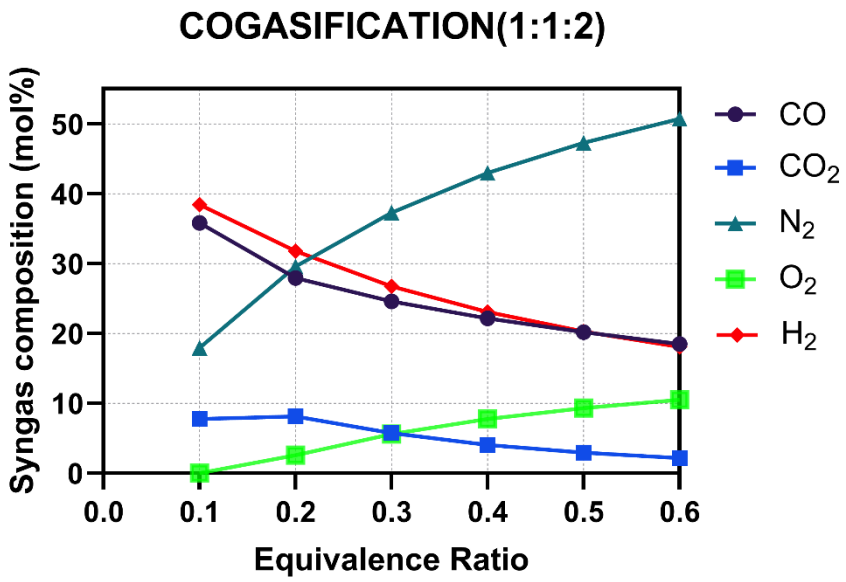

Fig. 5.29: The effect of ER on syngas composition for blend (1:1:2).

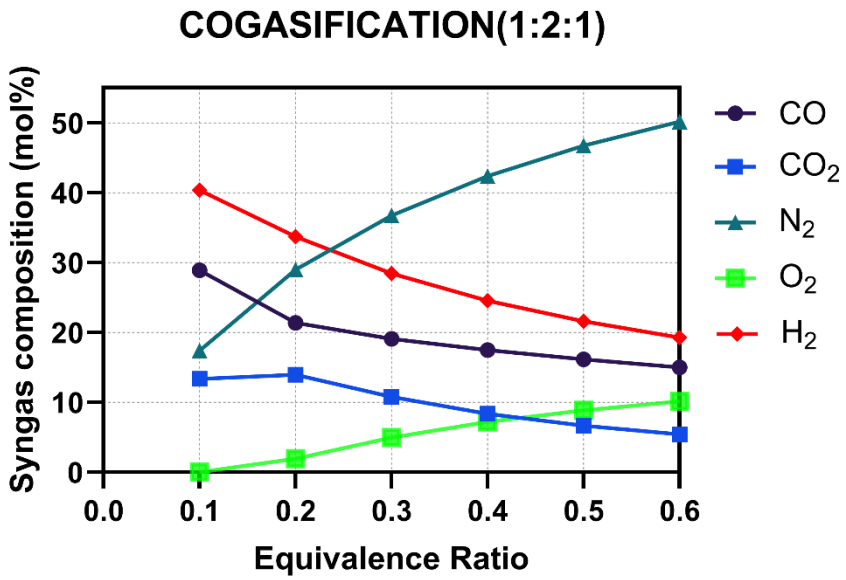

Fig. 5.30: The effect of ER on syngas composition for blend (1:2:1).

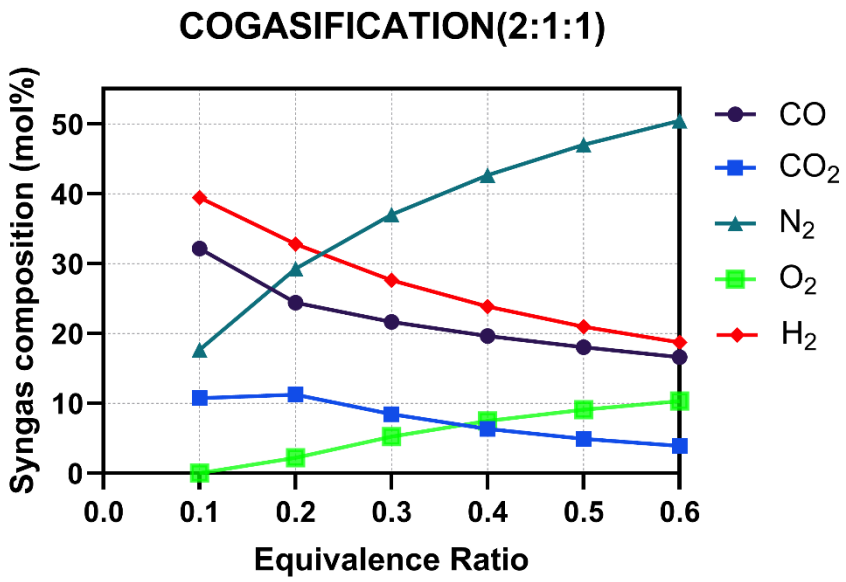

Fig. 5.31: The effect of ER on syngas composition for blend (2:1:1).

5.4 Lower heating value

5.4.1 Effect of temperature on LHV

A fuel's calorific value, also known as its heating value (HV), is the quantity of heat that is emitted when one unit of the fuel is completely burned. A fuel's heat of combustion is measured by its lower heating value (LHV), also known as its net heating value, and its higher heating value (HHV), also known as its gross heating value. Power output and combustion characteristics are highly dependent on a fuel's or fuel emulsion's HV. A CI engine performs better when the gasoline has a high HV [109]. The variation of the Lower heating Value (LHV) of syngas with the increase in gasifier temperature is shown in Figure 5.32. The LHV of syngas is the function of the mole fraction of H_2, CH_4, and CO. At the elevated temperature, CH_4 concentration decreases which has a higher heating value, and thus LHV decreases. The variation of H_2, CH_4, and CO occurs up to 800-850℃ and then variations are very low as shown in Fig. 5.4-5.10. The LHV decreased from 9.33, 8.48, 11.34, 9.74, 10.25, 9.30, and 9.72 to 9.03, 7.49, 10.77, 9.14, 9.57, 8.73, and 9.12 MJ/m^3, respectively, for the corncob, coconut coir, coconut shell, blend (1:1:1), blend (1:1:2), blend (1:2:1), and blend (2:1:1) with the increase in temperature from 500-1200℃. Fatin et al. [66] showed the same trend in their studies.

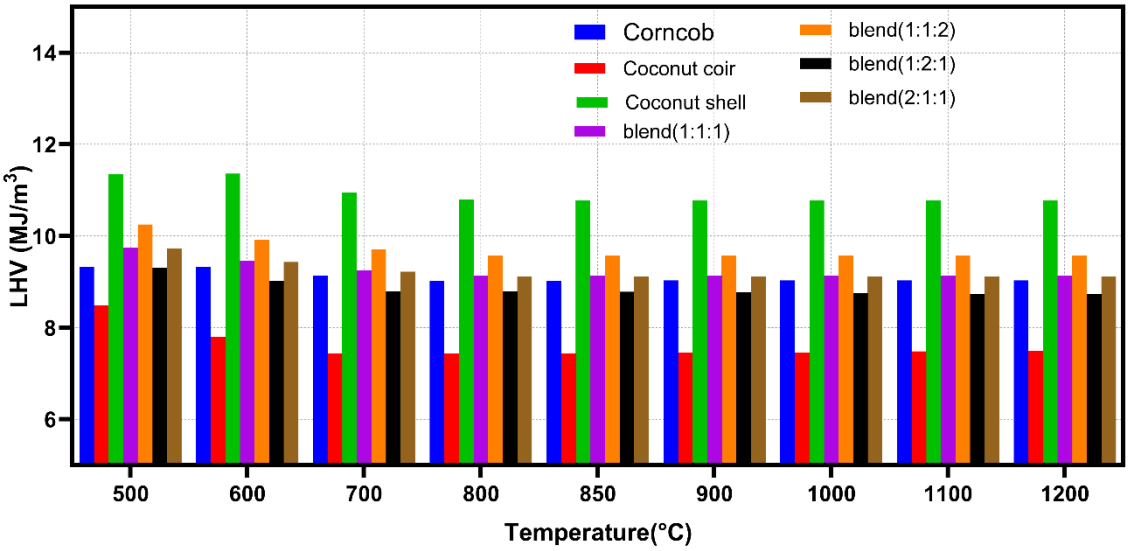

Fig. 5.32: The effect of temperature on LHV for corncob, coconut coir, coconut shell, blend (1:1:1), blend (1:1:2), blend (1:2:1), and blend (2:1:1)

5.4.2 Effect of pressure on LHV

The LHV of syngas increases with the increase in pressure due to the higher methane formation and the effect of pressure on the lower heating value (LHV) is illustrated in Figure 5.33. The LHV increased from 9.02, 7.44, 10.77, 9.13, 9.57, 8.72, and 9.11 to 9.29, 7.5, 11.25, 9.42, 9.96, 9, and 9.44 MJ/m^3, respectively, for the corncob, coconut coir, coconut shell, blend (1:1:1), blend (1:1:2), blend (1:2:1), and blend (2:1:1) with the increase in pressure from 1-20 bar.

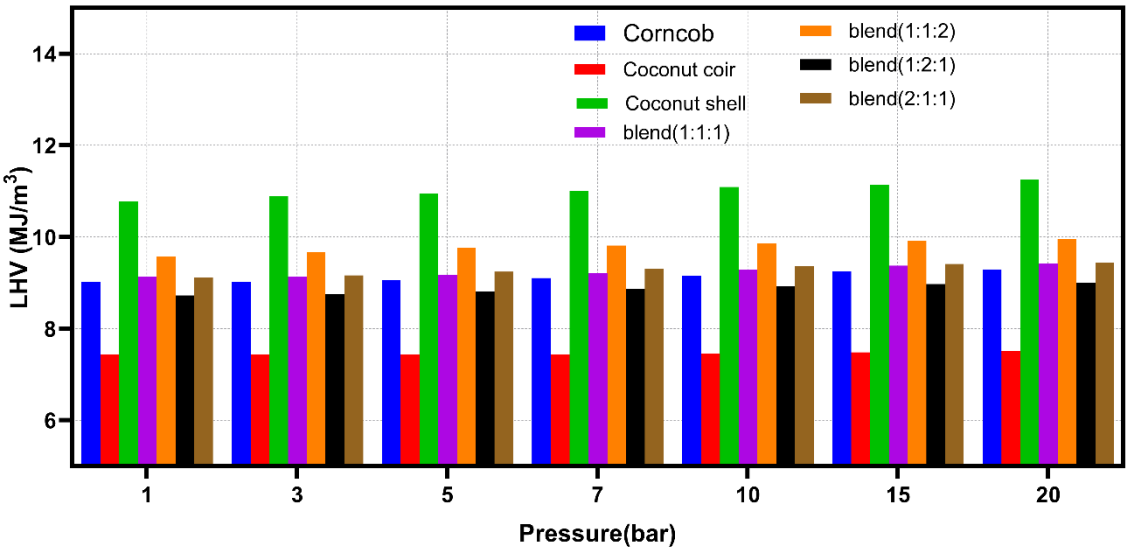

Fig. 5.33: The effect of pressure on LHV for corncob, coconut coir, coconut shell, blend (1:1:1), blend (1:1:2), blend (1:2:1), and blend (2:1:1)

5.4.3 Effect of SBR on LHV

Figure 5.34 shows the effect of SBR on the lower heating value (LHV) and demonstrates that the LHV of syngas decreases with the increase in SBR from 0.2 to 1 by thermal cracking of methane. The LHV decreased from 9.03, 7.45, 10.78, 9.14, 9.57, 8.72, and 9.11 to 6.94, 6.70, 7.27, 6.96, 7.03, 6.90, and 6.96 MJ/m^3 respectively. Cai. et al. [80] investigated co-steam gasification of straw and refuse-derived fuel (RDF) and showed a similar trend of LHV with SBR.

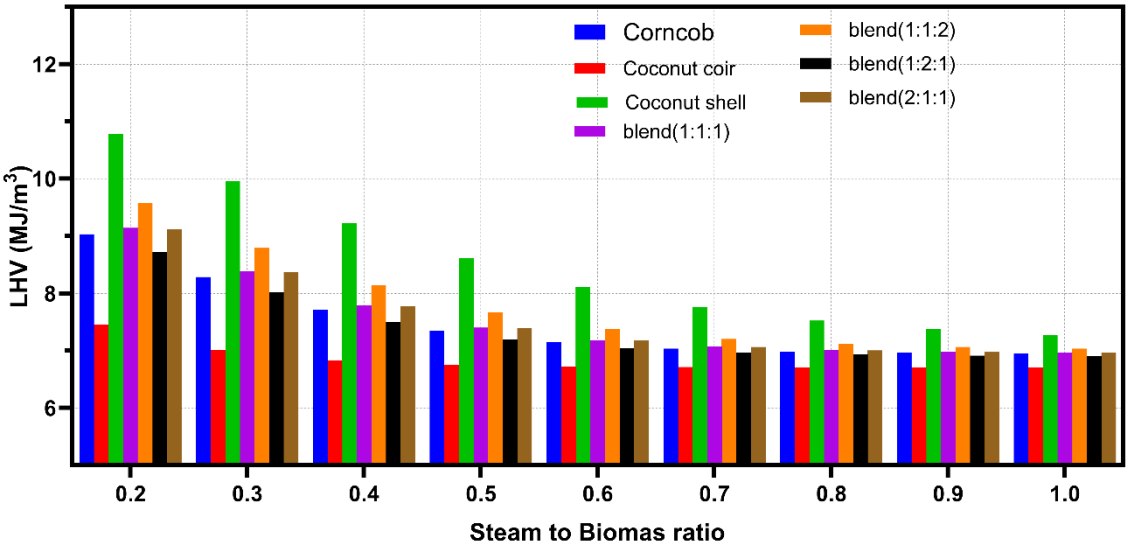

Fig. 5.34: The effect of SBR on LHV for corncob, coconut coir, coconut shell, blend (1:1:1), blend (1:1:2), blend (1:2:1), and blend (2:1:1)

5.4.4 Effect of ER on LHV

The amount of combustible gases (H_2, CO, and CO_2) decreases with the increase in ER, and thus the LHV of syngas decreases as illustrated in Figure 5.35. The amount of N_2 increases with an increase in ER also liable to reducing LHV of syngas. Biagini et al.[131] and Sing et al. [132] investigated the gasification of corn cobs and coconut shells separately in the downdraft gasifier and showed that the syngas LHV decreases with the increase of ER. The LHV of syngas decreased from 8.24, 6.90, 9.61, 8.32, 8.68, 8, and 8.32 to 3.69, 3.07, 4.46, 3.75, 4.29, 3.98, and 4.12 MJ/m^3 respectively, for the corncob, coconut coir, coconut shell, blend (1:1:1), blend (1:1:2), blend (1:2:1), and blend (2:1:1) with the increase in ER from 0.1 to 0.6.

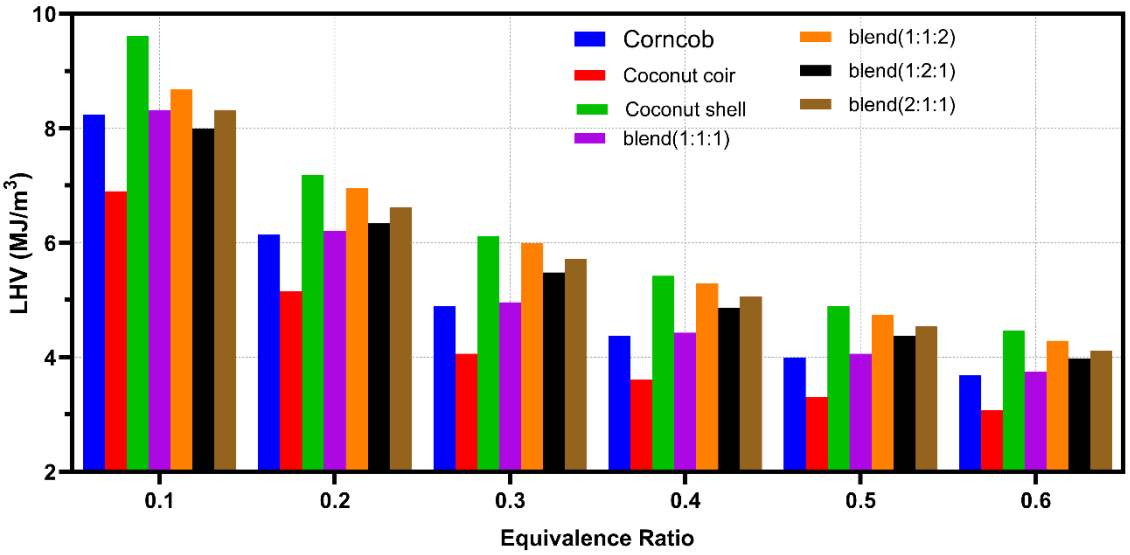

Fig. 5.35: The effect of ER on LHV for corncob, coconut coir, coconut shell, blend (1:1:1), blend (1:1:2), blend (1:2:1), and blend (2:1:1)

5.5 Cold gas efficiency

5.5.1 Effect of temperature on CGE

CGE is the ratio of chemical energy available in syngas to biomass energy. It indicates how effectively the chemical energy of biomass is converted into syngas chemical energy in the co-gasification process [133]. Equation 5.3 is used to determine the percentage of CGE and it varies with the type and composition of the feedstock, gasification temperature, pressure, agent, heat losses, and gasifier design. CGE increases with low MC (<10%), high VM, low ash content, steam or oxygen used as a gasifying agent due to its better conversion of C into syngas, and higher gasification temperature(800-1200℃). The blend (1:1:2) shows the highest CGE as the coconut shell has the lowest moisture (4.52%) and ash (1.26%) content and the highest VM (73.78%) followed by corncob and coconut coir.

$$CGE(\%) = \frac{LHV\left(\frac{MJ}{m^3}\right) of\ syngas\ \times Gas\ flow\ rate\ (Nm^3/hr)}{LHV\ (\frac{MJ}{kg})\ of\ Biomass\ \times Biomass\ flow\ rate(\frac{kg}{hr})} \times 100 \qquad (5.3)$$

The effect of temperature on CGE for the blend (1:1:1), (1:1:2), (1:2:1), and (2:1:1) is illustrated in Figure 5.36 and shows that CGE increases with the increase in temperature due to biomass conversion enhances and tar formation decreases at higher temperature. The CGE increases from 77.71, 83.42, 72.63, and 77.33% to 84.69, 90.30, 78.64, and 84.30% with the increase in temperature from 500-850℃ for the blend (1:1:1), (1:1:2), (1:2:1), and (2:1:1), respectively.

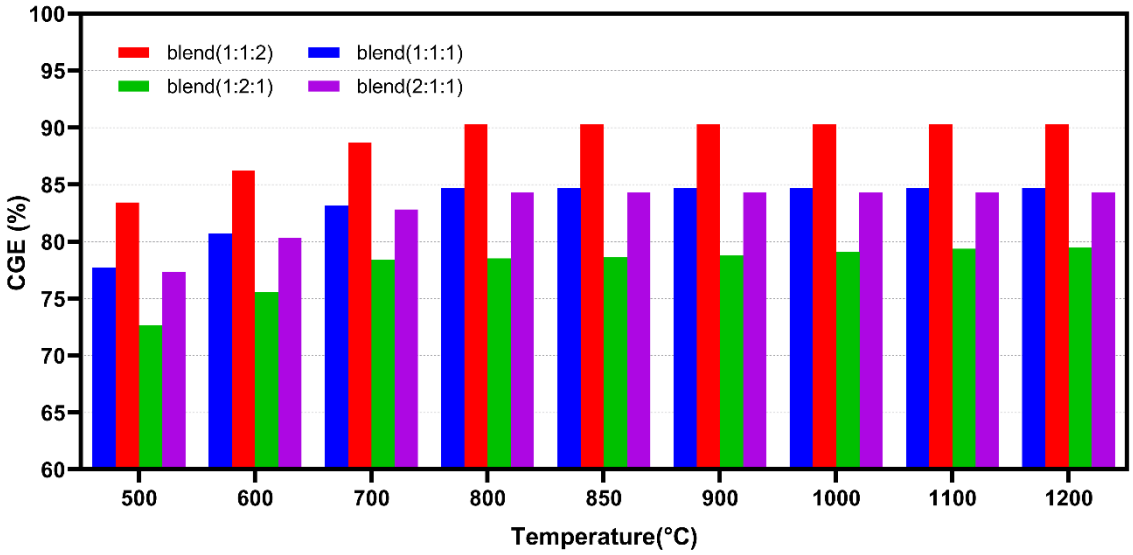

Fig. 5.36: The effect of temperature on CGE for blend (1:1:1), (1:1:2), (1:2:1), and (2:1:1)

5.5.2 Effect of pressure on CGE

Higher pressure enhances the gasification reaction kinetics, and syngas yield, and reduces heat losses. However, tar formation increases due to incomplete cracking of volatiles at elevated pressure. Thus, 1 bar pressure is optimal for CGE as shown in Figure 5.37.

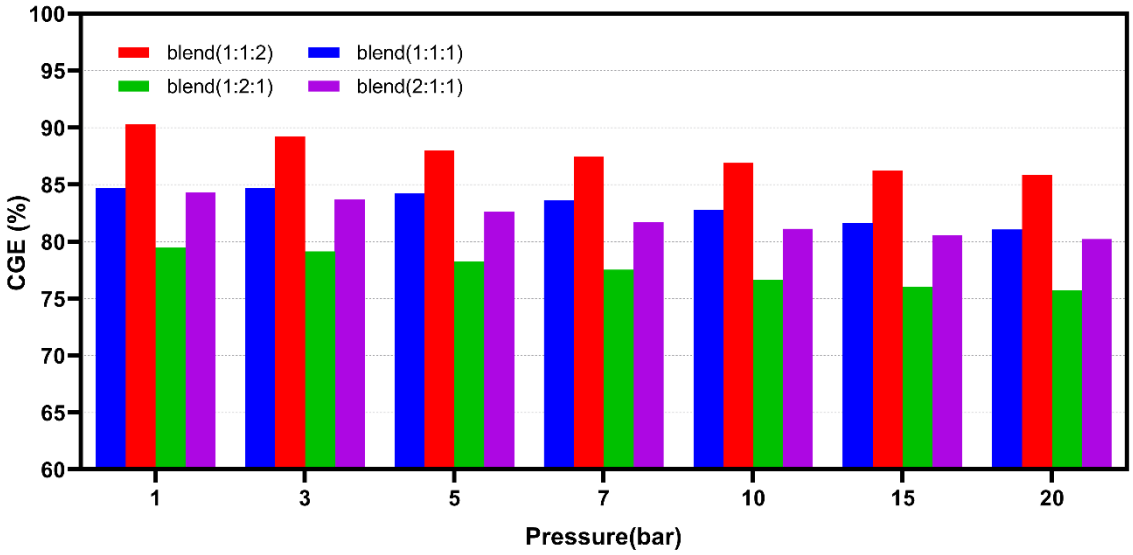

Fig. 5.37: The effect of pressure on CGE for blend (1:1:1), (1:1:2), (1:2:1), and (2:1:1)

5.5.3 Effect of SBR on CGE

A higher SBR increases the water-gas shift reaction leading to higher hydrogen production and improving syngas quality. Steam reacts with char, enhancing carbon utilization. However, excess steam absorbs heat, reducing the effective temperature for gasification and lowering the calorific value of syngas, reducing CGE. Figure 5.38 shows that the maximum CGE attained at SBR of 0.2.

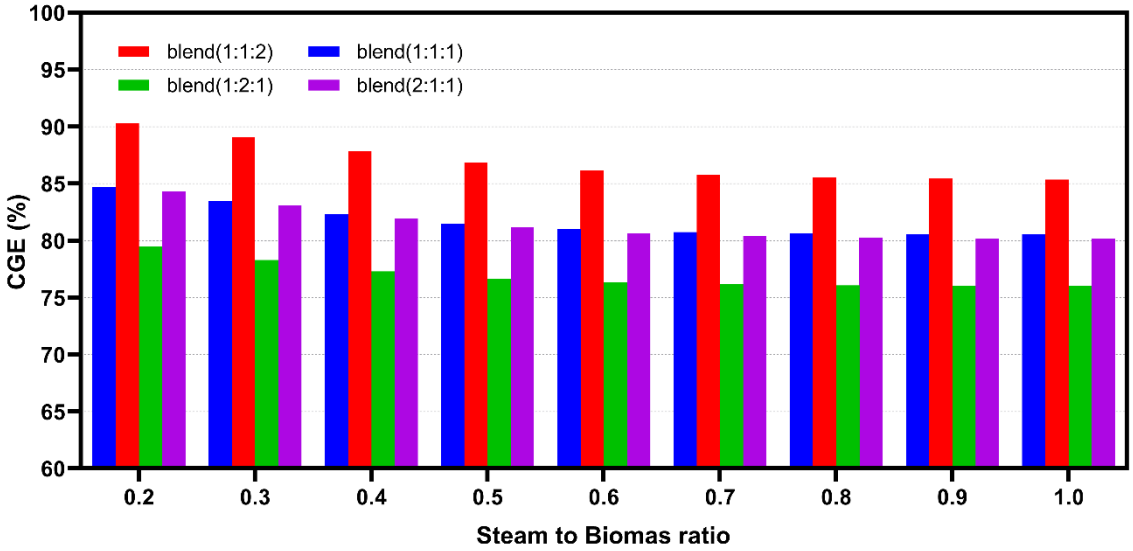

Fig. 5.38: The effect of SBR on CGE for blend (1:1:1), (1:1:2), (1:2:1), and (2:1:1)

5.5.4 Effect of ER on CGE

The effect of ER on CGE shows a decreasing and then increasing trend with the increase in ER as illustrated in Figure 5.39. Higher ER values can reduce tar formation by promoting partial oxidation. However, higher ER increases the production of CO_2 and water, diluting the syngas and reducing its LHV.

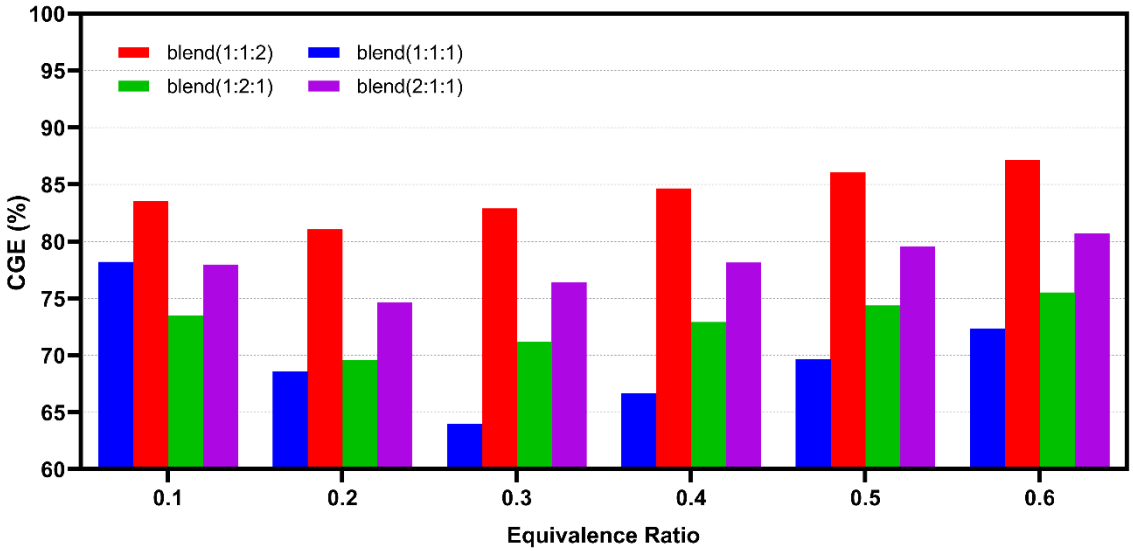

Fig. 5.39: The effect of SBR on CGE for blend (1:1:1), (1:1:2), (1:2:1), and (2:1:1)

5.6 H_2-rich syngas production using water gas shift reactor

Water gas shift reaction converts CO and steam into CO_2 and H_2. A two-step reactor is used and produces up to 62% H_2 for different blends at the operating conditions of 850℃, 1 bar and SBR of 1 shown in Figures 5.40-5.43. The mole fraction of CO, CO_2, and H_2 varies from 13.77, 13.30, and 36.24% to 4.83, 31.45, and 62.18%, respectively, using the water gas shift reactors in the blend (1:1:1). The maximum hydrogen production are 62.18, 62.42, 61.89, and 62.16% for the blend (1:1:1), (1:1:2), (1:2:1), and (2:1:1), respectively. The terms Gasifier, HTWGSR, LTWGSR, PSA-F, and Pure H_2 in the plots represent the outline stream of syngas after gasifier, high and low-temperature water gas shift reactor, after flash where steam removed, and after pressure swing adsorption, respectively.

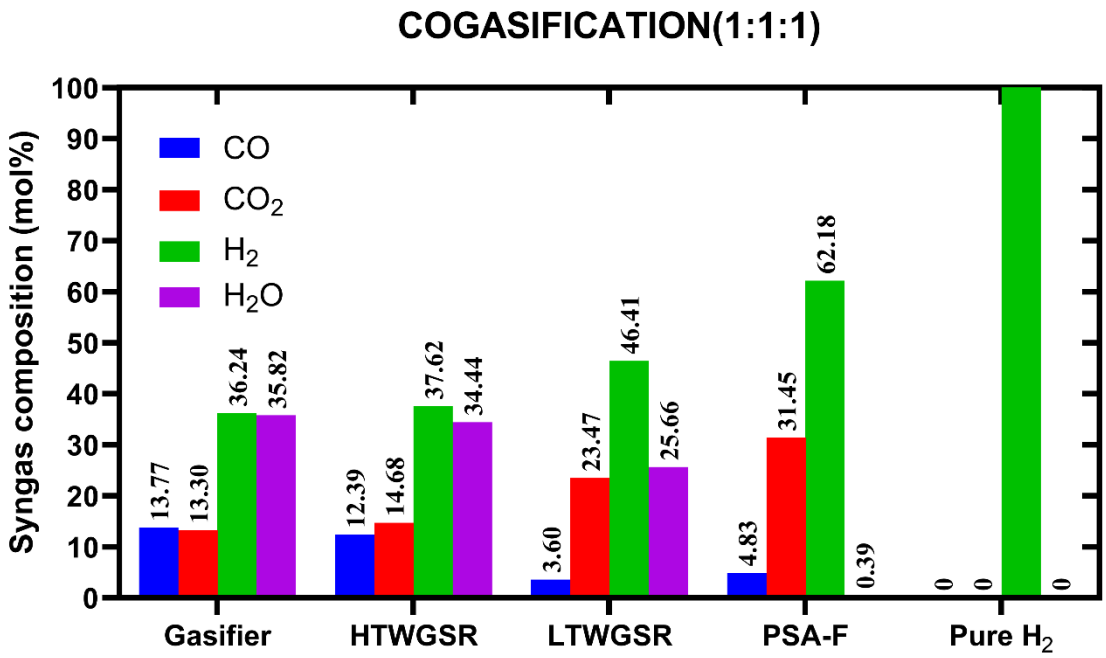

Fig. 5.40: The effect of WGSR to produce H_2-rich syngas for blend (1:1:1)

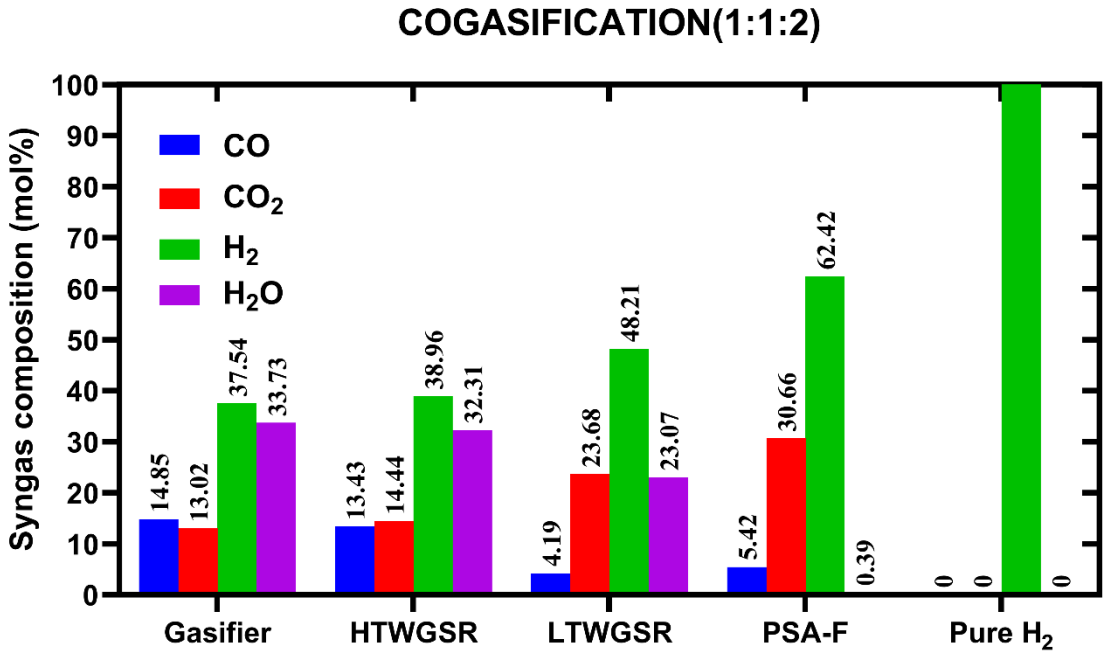

Fig. 5.41: The effect of WGSR to produce H_2-rich syngas for blend (1:1:2)

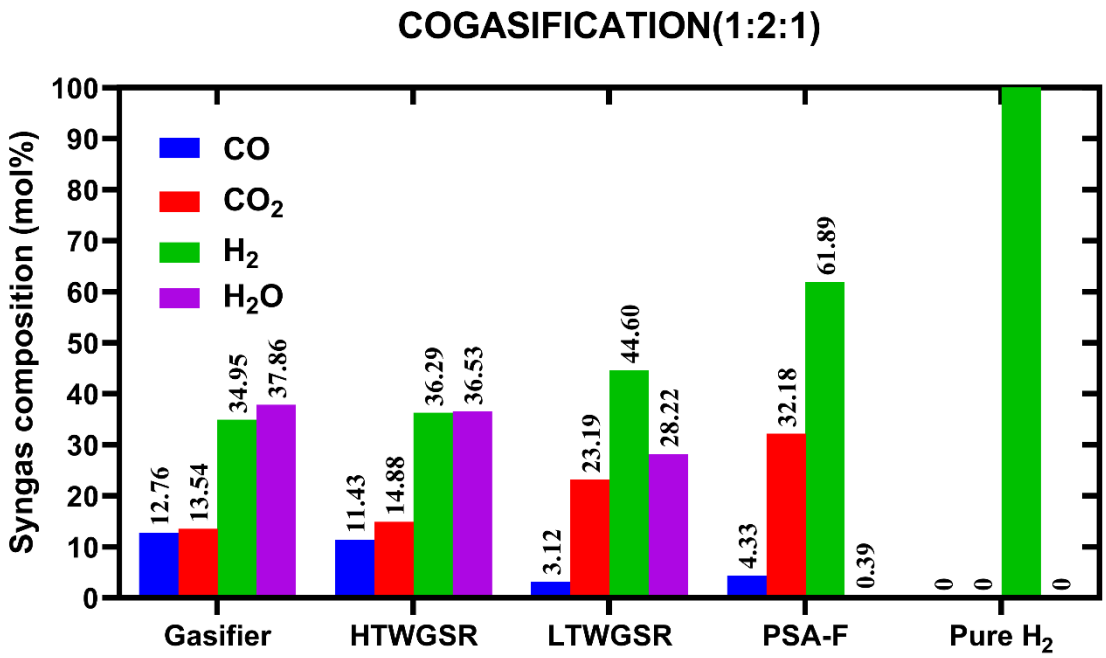

Fig. 5.42: The effect of WGSR to produce H_2-rich syngas for blend (1:2:1)

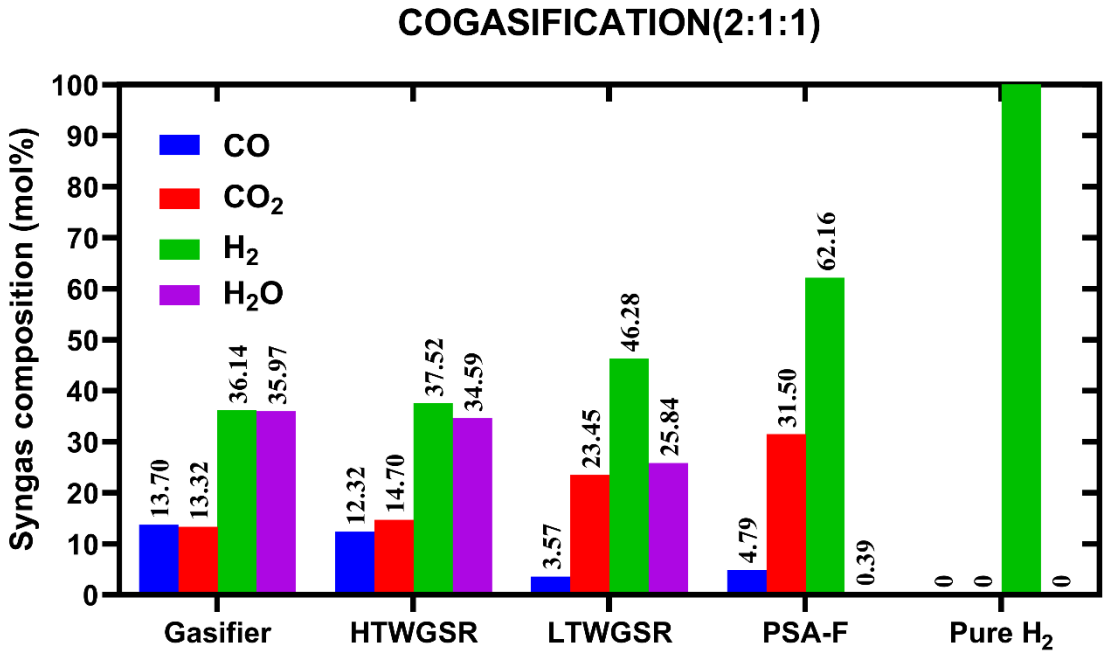

Fig. 5.43: The effect of WGSR to produce H_2-rich syngas for blend (2:1:1)

5.7 Machine learning model

5.7.1 Performance evaluation and optimization of operating condition

The scatter plots for the random forest and gradient boosting regression model illustrated in Figures 5.44 and 5.45 show the training and testing datasets and compare the actual and predicted values. The actual and predicted training datasets exhibit good alignment, clustering near the 45° lines. The R^2 values for the training date set are 0.99, 0.99, 0.99, 1, 1, and 0.99, respectively, for CO, CO_2, CH_4, H_2, LHV, and CGE in the random forest (RF) model and in the case of gradient boosting regression (GBR) model, the R^2 values (1,1,0.99,1,1, and 1) are closer to 1. The R^2 values for the testing date set are (0.88, 0.94, 0.97, 1, 0.96, 0.99) and (0.98, 0.98, 0.98, 1, 1, 0.83) for the random forest and gradient boosting regression models, respectively, show good agreement with previous literature [130]. The GBR model shows lower RMSE values for testing data sets than the RF model. Therefore, the GBR model is the fitted model for the prediction of CO, CO_2, CH_4, H_2, LHV, and CGE, and optimizing the co-gasification operating conditions. The model showed that maximum H_2 (54.13%), CO (29.52%), CGE (90.30%), and LHV (9.57 MJ/m^3), and minimum CO_2 (14.97%) produced at the operating conditions of 850℃, 1 bar pressure, SBR of 0.2, and blend ratio of (1:1:2).

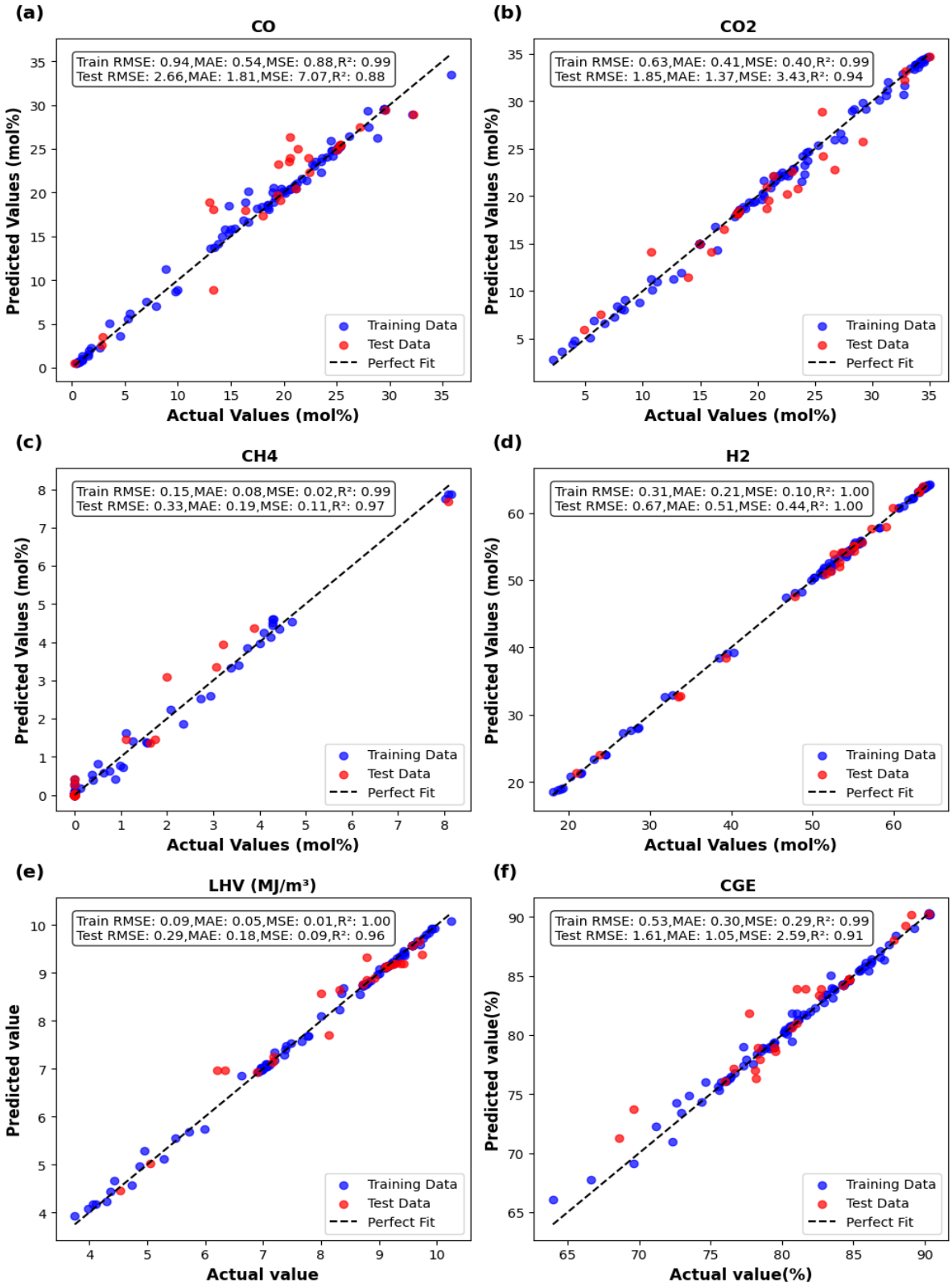

Fig. 5.44: The scatter plot using the random forest model represents the relationship between actual and predicted values for (a) CO, (b)CO_2, (c) CH_4, (d) H_2, (e) LHV, and (f) CGE

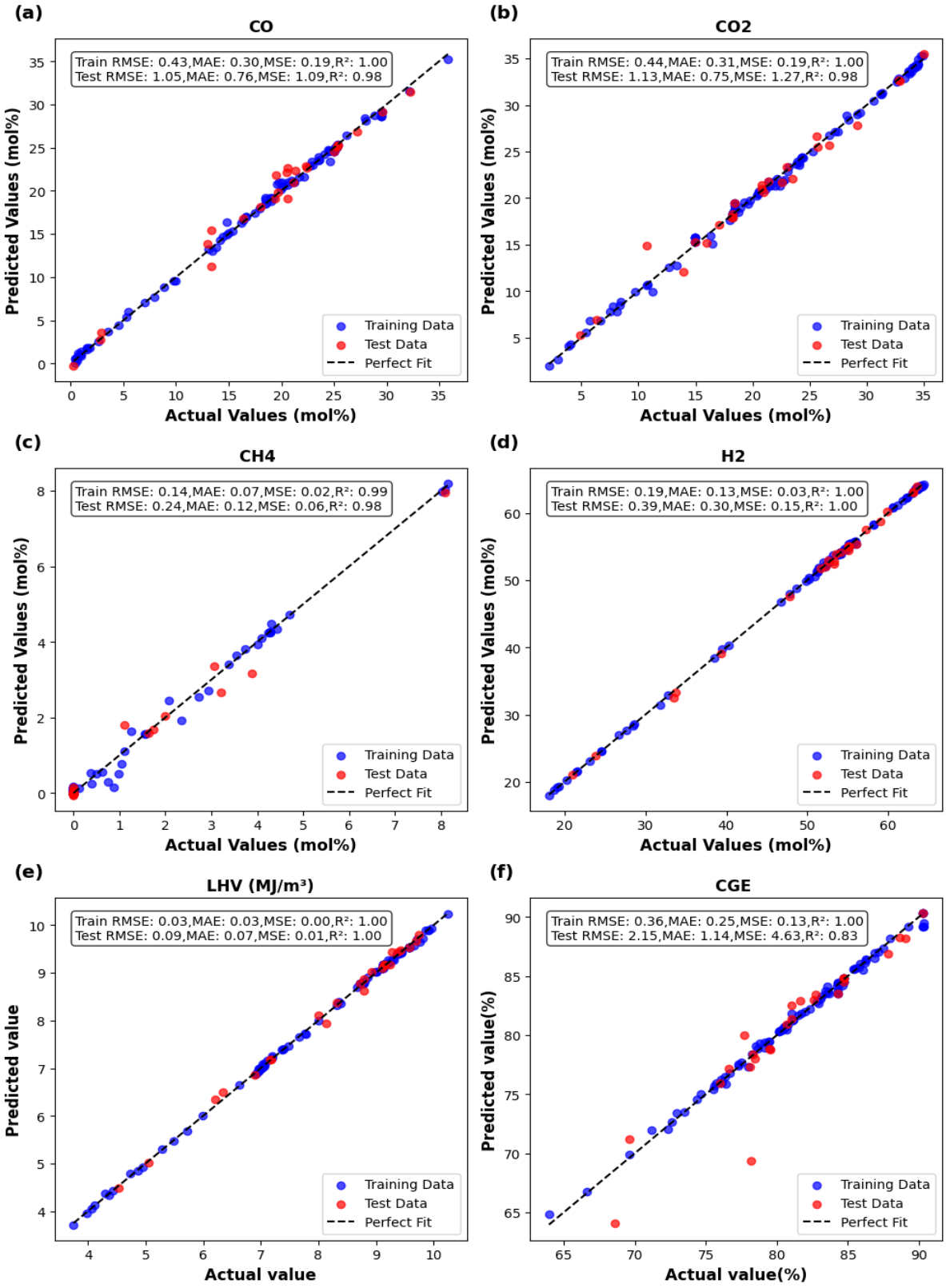

Fig. 5.45: The scatter plot using the gradient boosting regression model represents the relationship between actual and predicted values for (a) CO, (b)CO_2, (c) CH_4, (d) H_2, (e) LHV, and (f) CGE

5.7.2 Prediction

The trained GBR model is used to predict the output parameters such as CO, CO_2, H_2, and LHV by random input conditions. Table 5.1 shows the comparison between predicted and simulation value using the same input parameters. Predicted results are very close to the simulation's actual value.

Table 5.1: Comparison between the actual simulation and predicted result from ML model.

Input Parameters			**Predicted result from ML**				**Actual simulation result**			
T(℃)	**SBR**	**Blend**	**CO(%)**	**CO_2(%)**	**H_2(%)**	**LHV(MJ/m^3)**	**CO(%)**	**CO_2(%)**	**H_2(%)**	**LHV(MJ/m^3)**
880	0.25	1:2:1	18.87	22.73	57.89	8.58	18.83	22.20	57.60	8.34
950	0.2	1:2:1	20.42	22.03	55.54	8.75	21.22	21.35	56.01	8.72
980	0.35	1:1:2	21.56	20.09	58.50	9.10	20.36	21.73	58.61	8.45
1050	0.45	1:1:2	8.85	28.89	60.78	7.69	10.78	27.27	60.76	7.91
980	0.55	2:1:1	5.50	31.26	62.20	7.39	4.25	31.98	62.59	7.29

Chapter 6
Conclusion and Recommendations

Bangladesh's extensive agricultural operations, large animal population, and production of organic waste make it a country with enormous potential for using biomass energy. Biomass already plays a vital part in the nation's energy mix because a sizable portion of the rural population depends on conventional fuels like firewood and crop wastes. However, the energy extraction rate is very low by direct combustion. Gasification is one of the promising thermochemical conversion techniques to generate clean and green energy. This paper aims to investigate the effect of different parameters such as temperature, pressure, steam-to-biomass ratio, and equivalence ratio on the syngas composition, and lower heating value of the co-gasification of different biomass from agricultural residue generated in Bangladesh. The developed simulation model using ASPEN Plus considered corncob, coconut coir, and coconut shell as the input feedstock.

- An increase in temperature increases the volume fraction of H_2 and CO and decreases the amount of CO_2, and CH_4, and the increase in pressure decreases the volume fraction of H_2 and CO and increases the amount of CO_2 and CH_4.
- The results show that the increase in SBR increases the volume fraction of H_2 and CO_2 and decreases the amount of CO.
- An increase in ER decreases the volume fraction of H_2 and CO and increases the amount of CO_2 up to an ER of 0.2-0.3 then decreases.
- The CGE increases with higher temperatures. At elevated pressure and SBR, CGE decreases. However, CGE decreases with ER of 0.2-0.3 then increases.
- Syngas's LHV decreases with increased temperature, SBR, and ER. However, the gasification pressure increases LHV of syngas.
- Blend (1:1:1), (1:1:2), (1:2:1), and (2:1:1) has the H_2 (55.09, 54.13, 56.02, and 55.14%), CO (25.29, 29.52, 21.19, and 25.03%), CO_2 (18.23, 14.97, 21.38, and 18.43%), CGE (84.69, 90.30, 78.64, and 84.30%), and LHV of 9.14, 9.57, 8.72, and 9.11 MJ/m^3, respectively, at the gasification temperature 850 ℃, pressure 1 bar and SBR 0.2.
- Blend (1:1:2) exhibits the highest CO (29.52%), CGE (90.30%), and LHV (9.57 MJ/m^3) as its carbon content is maximum.
- H_2 yield increases with the increase in oxygen content in the raw biomass and thus blend (1:2:1) shows the highest 56.02%.

Two Machine learning models were developed in this study and the gradient boosting regression model shows better accuracy($R^2 \geq 0.99$ and RMSE ≤ 2.66) and is utilized for the prediction and optimization of the operating conditions.

- The model showed that maximum H_2 (54.13%), CO (29.52%), CGE (90.30%), and LHV (9.57 MJ/m^3), and minimum CO_2 (14.97%) were produced at the operating conditions of 850℃, 1 bar pressure, SBR of 0.2, and blend ratio of (1:1:2).

Further studies can be demonstrated by considering the effect of particle size distribution, reactor catalytic reaction, and the raw biomass's moisture content directly collected from the field. Current investigations can be done using an experimental setup. A techno-economic and environmental analysis can be demonstrated to show its industrial application. A graphical user interface can be incorporated using a machine learning model to predict the co-gasification output.

References

[1] Shahbaz M, Topcu BA, Sarıgül SS, Vo XV. The effect of financial development on renewable energy demand: The case of developing countries. Renew Energy 2021;178:1370–80.

[2] Smil V. Energy Transitions: Global and National Perspectives (Expanded and updated edition). vol. 30. 2nd ed. Praeger; 2017.

[3] Energy Institute - Statistical Review of World Energy (2024), Smil (2017). Our World Data 2024.

[4] Ellabban O, Abu-Rub H, Blaabjerg F. Renewable energy resources: Current status, future prospects and their enabling technology. Renew Sustain Energy Rev 2014;39:748–64.

[5] Fossil fuel energy consumption 1965-2023 | Statista n.d.

[6] Adib AR, Rahman MM, Hassan T, Ahmed M, Al Rifat A. Novel biofuel blends for diesel engines: Optimizing engine performance and emissions with C. cohnii microalgae biodiesel and algae-derived renewable diesel blends. Energy Convers Manag X 2024;23:100688.

[7] Martins F, Felgueiras C, Smitkova M, Caetano N. Analysis of fossil fuel energy consumption and environmental impacts in European countries. Energies 2019;12:964.

[8] Asokan MA, Vijayan R, Senthur Prabu S. A review on performance, emission and combustion characteristics of a diesel engine fuelled with various vegetable oil. Indian J Chem Technol 2018;25:225–34.

[9] Safarian S, Unnþórsson R, Richter C. A review of biomass gasification modelling. Renew Sustain Energy Rev 2019;110:378–91.

[10] Rahman MM, Hassan T, Rabbi MF, Shakil MF, Khan MA. Transesterification of vegetable oil with ethanol using different catalysts. AIP Conf. Proc., vol. 2324, AIP Publishing LLC; 2021, p. 50003.

[11] Suresh M, Jawahar CP, Richard A. A review on biodiesel production, combustion, performance, and emission characteristics of non-edible oils in variable compression ratio diesel engine using biodiesel and its blends. Renew Sustain Energy Rev 2018;92:38–49. https://doi.org/10.1016/j.rser.2018.04.048.

[12] Hassan T, Rahman MM, Rahman MA, Nabi MN. Opportunities and challenges for the application of biodiesel as automotive fuel in the 21st century. Biofuels, Bioprod Biorefining 2022;16:1353–87. https://doi.org/10.1002/bbb.2375.

[13] Rakopoulos CD, Antonopoulos KA, Rakopoulos DC, Hountalas DT, Giakoumis EG. Comparative performance and emissions study of a direct injection Diesel engine using blends of Diesel fuel with vegetable oils or bio-diesels of various origins. Energy Convers Manag 2006;47:3272–87. https://doi.org/10.1016/j.enconman.2006.01.006.

[14] Murillo S, Míguez JL, Porteiro J, Granada E, Morán JC. Performance and exhaust emissions in the use of biodiesel in outboard diesel engines. Fuel 2007;86:1765–71. https://doi.org/https://doi.org/10.1016/j.fuel.2006.11.031.

[15] Stringer FW, Clarke AE, Clarke JS. The spontaneous ignition of hydrocarbon fuels in a flowing system. Proc. Inst. Mech. Eng. Conf. Proc., vol. 184, SAGE Publications Sage UK: London, England; 1969, p. 212–25.

[16] Lertsathapornsuk V, Pairintra R, Aryusuk K, Krisnangkura K. Microwave assisted in continuous biodiesel production from waste frying palm oil and its performance in a 100 kW diesel generator. Fuel Process Technology 2008;89 1330–6. https://doi.org/https://doi.org/10.1016/j.fuproc.2008.05.024.

[17] Agarwal D, Agarwal AK. Performance and emissions characteristics of Jatropha oil (preheated and blends) in a direct injection compression ignition engine. Appl Therm Eng 2007;27:2314–23. https://doi.org/10.1016/j.applthermaleng.2007.01.009.

[18] Chauhan BS, Kumar N, Cho HM. A study on the performance and emission of a diesel engine fueled with Jatropha biodiesel oil and its blends. Energy 2012;37:616–22. https://doi.org/https://doi.org/10.1016/j.energy.2011.10.043.

[19] Qi DH, Chen H, Geng LM, Bian YZ. Experimental studies on the combustion characteristics and performance of a direct injection engine fueled with biodiesel/diesel blends. Energy Conversion and Management 2010;51:2985–92. https://doi.org/10.1016/j.enconman.2010.06.042.

[20] Hoque N, Mourshed M, Das BK. Performance and emission comparison of Karanja (pongamia pinnata), Pithraj (aphanamixis polystachya), Neem (azadira chtaindica) and Mahua (madhuca longofolia) seed oil as a potential feedstock for biodiesel production in Bangladesh. Int J Automot Mech Eng 2015;12.

[21] Wan Ghazali WNM, Mamat R, Masjuki HH, Najafi G. Effects of biodiesel from different feedstocks on engine performance and emissions : A review. Renew Sustain Energy Rev 2015;51:585–602. https://doi.org/10.1016/j.rser.2015.06.031.

[22] McKendry P. Energy production from biomass (part 1): overview of biomass. Bioresour Technol 2002;83:37–46.

[23] Grassi G, Gosse G, dos Santos G. Biomass for energy and industry. Elsevier Applied

Science London:; 1990.

[24] Lin Y, Tanaka S. Ethanol fermentation from biomass resources: current state and prospects. Appl Microbiol Biotechnol 2006;69:627–42.

[25] Kirubakaran V, Sivaramakrishnan V, Nalini R, Sekar T, Premalatha M, Subramanian P. A review on gasification of biomass. Renew Sustain Energy Rev 2009;13:179–86. https://doi.org/10.1016/j.rser.2007.07.001.

[26] Caputo AC, Palumbo M, Pelagagge PM, Scacchia F. Economics of biomass energy utilization in combustion and gasification plants: effects of logistic variables. Biomass and Bioenergy 2005;28:35–51.

[27] Faaij APC. Bio-energy in Europe: changing technology choices. Energy Policy 2006;34:322–42.

[28] Saghir M, Rehan M, Nizami A-S. Recent trends in gasification based waste-to-energy. Gasif Low-Grade Feed 2018;2018:97–113.

[29] Mishra S, Upadhyay RK. Review on biomass gasification: Gasifiers, gasifying mediums, and operational parameters. Mater Sci Energy Technol 2021;4:329–40. https://doi.org/10.1016/j.mset.2021.08.009.

[30] Baruah D, Baruah DC. Modeling of biomass gasification: A review. Renew Sustain Energy Rev 2014;39:806–15.

[31] Puig-Arnavat M, Bruno JC, Coronas A. Review and analysis of biomass gasification models. Renew Sustain Energy Rev 2010;14:2841–51.

[32] Inayat M, Sulaiman SA, Kurnia JC, Shahbaz M. Effect of various blended fuels on syngas quality and performance in catalytic co-gasification: A review. Renew Sustain Energy Rev 2019;105:252–67.

[33] Ram M, Mondal MK. Biomass gasification: A step toward cleaner fuel and chemicals. Biofuels and bioenergy, Elsevier; 2022, p. 253–76.

[34] Islam MW. A review of dolomite catalyst for biomass gasification tar removal. Fuel 2020;267:117095.

[35] Panwar SLNNL. Catalysts and their role in biomass gasification and tar abetment : a review. Springer Berlin Heidelberg; 2021. https://doi.org/10.1007/s13399-021-01981-1.

[36] Molino A, Chianese S, Musmarra D. Biomass gasification technology: The state of the art overview. Journal of Energy Chemical 2016;25:10–25. https://doi.org/10.1016/j.jechem.2015.11.005.

[37] Ahmed Y, Siddiqua Maya AA, Akhtar P, Alam MS, AlMohamadi H, Islam MN, et al. A novel interpretable machine learning and metaheuristic-based protocol to predict and

optimize ciprofloxacin antibiotic adsorption with nano-adsorbent. J Environ Manage 2024;370:122614. https://doi.org/10.1016/j.jenvman.2024.122614.

[38] Kundu K, Kumar A, Kodamana H, Pant KK. Obtaining high H2-rich syngas yield and carbon conversion efficiency from biomass gasification: From characterization to process optimization using machine learning with experimental validation. Fuel 2024;378:132931. https://doi.org/10.1016/j.fuel.2024.132931.

[39] Halder PK, Paul N, Beg MRA. Assessment of biomass energy resources and related technologies practice in Bangladesh 2014;39:444–60.

[40] Bangladesh Bureau of Statistics (BBS). Statistical yearbook Bangladesh 2022. 2023.

[41] Huda ASN, Mekhilef S, Ahsan A. Biomass energy in Bangladesh : Current status and prospects 2014;30:504–17.

[42] Kibria G, Paul UK, Hasan A, Mohtasim S, Das BK. Biomass and Bioenergy Current prospects and challenges for biomass energy conversion in Bangladesh : Attaining sustainable development goals. Biomass and Bioenergy 2024;183:107139. https://doi.org/10.1016/j.biombioe.2024.107139.

[43] Yearbook of Agricultural Statistics-2023 2023.

[44] Mondal MAH, Denich M. Assessment of renewable energy resources potential for electricity generation in Bangladesh. Renew Sustain Energy Rev 2010;14:2401–13. https://doi.org/10.1016/j.rser.2010.05.006.

[45] Rofiqul Islam M, Rabiul Islam M, Rafiqul Alam Beg M. Renewable energy resources and technologies practice in Bangladesh. Renew Sustain Energy Rev 2008;12:299–343. https://doi.org/10.1016/j.rser.2006.07.003.

[46] K Hossain A, Badr O. Prospects of renewable energy utilisation for electricity generation in Bangladesh. Renewable and Sustainable Energy Reviews 2007;11:1617–49. https://doi.org/10.1016/j.rser.2005.12.010.

[47] Rashed Al Mamun M, Mamun M, Kabir M, Alam M, Islam M. Utilization pattern of biomass for rural energy supply in Bangladesh. Int J Sustain Crop Prod 2009;4:62–71.

[48] Bhattacharya SC, Abdul Salam P, Runqing H, Somashekar HI, Racelis DA, Rathnasiri PG, et al. An assessment of the potential for non-plantation biomass resources in selected Asian countries for 2010. Biomass and Bioenergy 2005;29:153–66. https://doi.org/10.1016/j.biombioe.2005.03.004.

[49] Ferreira LRA, Otto RB, Silva FP, De Souza SNM, De Souza SS, Ando Junior OH. Review of the energy potential of the residual biomass for the distributed generation in Brazil. Renewable Sustainable Energy Reviews 2018;94:440–55.

https://doi.org/10.1016/j.rser.2018.06.034.

[50] Kartal F. Bioresource Technology Reports A comparative study for biomass gasification in bubbling bed gasifier using Aspen HYSYS 2021;13.

[51] Gallucci F, Palma A, Vincenti B, Carnevale M, Paris E, Ancona V, et al. Fluidized bed gasification of biomass from plant assisted bioremediation (PABR): Lab-scale assessment of the effect of different catalytic bed material on emissions. Fuel 2022;322:124214. https://doi.org/https://doi.org/10.1016/j.fuel.2022.124214.

[52] Safarian S, Unnthorsson R, Richter C. Hydrogen production via biomass gasification : simulation and performance analysis under different gasifying agents. Biofuels 2021;0:1–10. https://doi.org/10.1080/17597269.2021.1894781.

[53] Puig-gamero M, Pio DT, Tarelho LAC, Sanchez-silva L. Simulation of biomass gasification in bubbling fluidized bed reactor using aspen plus ® 2021;235. https://doi.org/10.1016/j.enconman.2021.113981.

[54] Alnouss A, Parthasarathy P, Shahbaz M, Al-ansari T, Mackey H, Mckay G. Techno-economic and sensitivity analysis of coconut coir pith-biomass gasification using ASPEN PLUS. Applied Energy 2020;261:114350. https://doi.org/10.1016/j.apenergy.2019.114350.

[55] Kumar P, Subbarao PM V, Kala LD, Vijay VK. Experimental assessment of producer gas generation using agricultural and forestry residues in a fixed bed downdraft gasifier. Chem Eng J Adv 2023;13:100431. https://doi.org/10.1016/j.ceja.2022.100431.

[56] Gomez RD, Palacio M, Arango JF, Avila AE, Mendoza JM. Evaluation of the energy generation potential by an experimental characterization of residual biomass blends from Córdoba , Colombia in a downdraft gasifier. Waste Management 2020. https://doi.org/10.1016/j.wasman.2020.10.014.

[57] Biagini E, Barontini F, Tognotti L. Bioresource Technology Gasification of agricultural residues in a demonstrative plant : Corn cobs 2014;173:110–6.

[58] Fatema J, Ahmed T, Islam M, Sakib N, Chowdhury AMS, Haque P. Gasification of kitchen wastes in an updraft fluidized bed gasifier and simulation of the process with Aspen Plus 2022;371.

[59] Inayat A, Shahbaz M, Khan Z, Inayat M, Mofijur M, Ahmed SF, et al. ScienceDirect Heat integration modeling of hydrogen production from date seeds via steam gasification 2021;6:0–13.

[60] Yeri E, Lang N, Njogu P, Malessa R, Weber C, Njoka F, et al. Numerical investigation of sugarcane bagasse gasification using Aspen Plus and response surface methodology

2022;254.

[61] Kakati U, Kumar A, Baghel P, Trada A, Mahapatra S, Upadhyay D, et al. Sustainable utilization of bamboo through air-steam gasi fi cation in downdraft gasi fi er : Experimental and simulation approach 2022;252.

[62] Sarker TR, Nanda S, Dalai AK. Parametric studies on hydrothermal gasification of biomass pellets using Box-Behnken experimental design to produce fuel gas and hydrochar 2023;388.

[63] Yousaf M, Jaffer H, Wasim M, Mehmood A. Journal of the Taiwan Institute of Chemical Engineers Maximizing hydrogen-rich syngas production from rubber wood biomass in an updraft fluidized bed gasifier : An advanced 3D simulation study. J Taiwan Inst Chem Eng 2024;156:105365. https://doi.org/10.1016/j.jtice.2024.105365.

[64] Striugas N, Zakarauskas K, Džiugys A, Navakas R, Paulauskas R. An evaluation of performance of automatically operated multi-fuel downdraft gasifier for energy production. Applied Thermal Engineering 2014;73:1151–9. https://doi.org/10.1016/j.applthermaleng.2014.09.007.

[65] AlNouss A, Mckay G, Al-Ansari T. Optimum Utilization of Biomass for the Production of Power and Fuels using Gasification. vol. 43. Elsevier Masson SAS; 2018. https://doi.org/10.1016/B978-0-444-64235-6.50258-8.

[66] Zafirah F, Ku C, Faizal M, Uddin M, Asma N, Abdul F, et al. ScienceDirect Co-gasification between coal / sawdust and coal / wood pellet : A parametric study using response surface methodology 2020;5.

[67] Jiang W, Tao J, Zhong X, Ye Y, Kang J, Tang Q, et al. Co-gasification of rural solid waste and biomass in rural areas : Simulation and plant-scale process. Environ Res 2023;235:116684. https://doi.org/10.1016/j.envres.2023.116684.

[68] Hameed Z, Khan Z, Khurram S, Inayat A, Amin N, Aslam M, et al. Co-gasification study of blends of municipal solid waste with sugarcane bagasse and rice husk using the Coats-Redfern method. Journal of Energy Institute 2024;113:101542. https://doi.org/10.1016/j.joei.2024.101542.

[69] Barontini F, Frigo S, Gabbrielli R, Sica P. Co-gasification of woody biomass with organic and waste matrices in a down-draft gasifier : An experimental and modeling approach 2021;245.

[70] Salisu J, Gao N, Quan C, Yanik J, Artioli N. Co-gasification of rice husk and plastic in the presence of CaO using a novel ANN model-incorporated Aspen plus simulation 2023;108.

[71] Li R, Yang Z, Duan Y. Energy , economic and environmental performance evaluation of co-gasification of coal and biomass negative-carbon emission system 2023;231.

[72] Shahabuddin M, Bhattacharya S. Enhancement of performance and emission characteristics by co- gasi fi cation of biomass and coal using an entrained fl ow gasi fi er 2021;95.

[73] Wojtacha-rychter K, Howaniec N. Investigation of co-gasification characteristics of coal with wood biomass and rubber seals in a fixed bed gasifier 2024;220. https://doi.org/10.1016/j.renene.2023.119725.

[74] Murugan PC, Sekhar SJ, Glivin G, Raveendran PS, Le THT, Mathimani T. Investigation on thermochemical co-gasification of rice husk and groundnut shell in open core gasifier for the generation of producer gas : An optimization by central composite design. Environ Res 2024;242:117741. https://doi.org/10.1016/j.envres.2023.117741.

[75] Valdés CF, Marrugo GP, Chejne F, Marin-Jaramillo A, Franco-Ocampo J, Norena-Marin L. Co-gasification and co-combustion of industrial solid waste mixtures and their implications on environmental emissions, as an alternative management. Waste Manag 2020;101:54–65. https://doi.org/https://doi.org/10.1016/j.wasman.2019.09.037.

[76] Chen Y-H, Lan Thao Ngo TN, Chiang K-Y. Enhanced hydrogen production in co-gasification of sewage sludge and industrial wastewater sludge by a pilot-scale fluidized bed gasifier. International Journal of Hydrogen Energy 2021;46:14083–95. https://doi.org/https://doi.org/10.1016/j.ijhydene.2020.10.081.

[77] Liu J, Wang D, Yu C, Jiang J, Guo M, Hantoko D, et al. A two-step process for energy-efficient conversion of food waste via supercritical water gasification: Process design, products analysis, and electricity evaluation. Sci Total Environ 2021;752:142331. https://doi.org/https://doi.org/10.1016/j.scitotenv.2020.142331.

[78] Zhang W, Gu Y, Fang H, Chen J, Chen H, Zhu Y, et al. International Journal of Hydrogen Energy Thermodynamic modeling and performance analysis on co-gasification of Chlorella vulgaris and petrochemical industrial sludge via Aspen plus combining with response surface methodology 2024;55:1037–49.

[79] Aentung T, Wu W, Patcharavorachot Y. Process design and muti-objective optimization of solid waste/biomass co-gasification considering tar formation. J Taiwan Inst Chem Eng 2024;164:105688. https://doi.org/10.1016/j.jtice.2024.105688.

[80] Cai J, Zhu L, Yang J, Guo M, Fang M, Yao S. Synergistic co-steam gasification of biomass and refuse-derived fuel: A path to enhanced gasification performance. Environ Technol Innov 2024;36:103745. https://doi.org/10.1016/j.eti.2024.103745.

[81] Sinisalu M, Järvik O, Mets B, Konist A. Co-gasification of biomass and oil shale under CO2 atmosphere: Comparative analysis of fixed-bed reactor, gas chromatography and thermogravimetric analysis coupled with mass spectroscopy (TGA-MS). Bioresour Technol 2024;393. https://doi.org/10.1016/j.biortech.2023.130086.

[82] Mafu LD, Neomagus HWJP, Everson RC, Okolo GN, Strydom CA, Bunt JR. The carbon dioxide gasification characteristics of biomass char samples and their effect on coal gasification reactivity during co-gasification. Bioresour Technol 2018;258:70–8. https://doi.org/10.1016/j.biortech.2017.12.053.

[83] Ajorloo M, Ghodrat M, Scott J, Strezov V. Experimental analysis of the effects of feedstock composition on the plastic and biomass Co-gasification process. Renew Energy 2024;231:120960. https://doi.org/10.1016/j.renene.2024.120960.

[84] Arenas E, Zapata Z, Jos A, Camargo-trillos DA. Biomass and Bioenergy CaCO 3 and air / steam effect on the gasification and biohydrogen performance of corn cob as received : Application in the Colombian Caribbean region 2021;153.

[85] Raj R, Tirkey JV, Jena P, Prajapati LK. Comparative analysis of Gasifier-CI engine performance and emissions characteristics using diesel with producer gas derived from coal– briquette-coconut shell-mahua feedstock and its blends. Energy 2024;293. https://doi.org/10.1016/j.energy.2024.130708.

[86] Liao Y, Deng F, Xiao B. Hydrogen-rich gas production from catalytic gasification of pine sawdust over Fe-Ce/olivine catalyst. International Journal of Energy Reservation 2019;43:7486–95. https://doi.org/10.1002/er.4781.

[87] Hajihashemi M, Mazhkoo S, Dadfar H, Livani E. Combined heat and power production in a pilot-scale biomass gasification system : Experimental study and kinetic simulation using ASPEN Plus. Energy 2023;276:127506. https://doi.org/10.1016/j.energy.2023.127506.

[88] Rahman M, Birk U, Ahrenfeldt J, Puig M. Design , construction and operation of a low-tar biomass (LTB) gasi fi er for power applications 2020;204.

[89] Wu R, Beutler J, Baxter LL. Biomass char gasification kinetic rates compared to data, including ash effects. Energy 2023;266:126392. https://doi.org/https://doi.org/10.1016/j.energy.2022.126392.

[90] Basu P. Chapter 3 - Biomass Characteristics. In: Basu Pyrolysis and Torrefaction (Second Edition) PBT-BG, editor., Boston: Academic Press; 2013, p. 47–86. https://doi.org/https://doi.org/10.1016/B978-0-12-396488-5.00003-4.

[91] Hailu A. Development and performance analysis of top lit updraft: natural draft gasifier

stoves with various feed stocks. Heliyon 2022;8:e10163. https://doi.org/10.1016/j.heliyon.2022.e10163.

[92] Tripodi A, Prada I, Tommasi M, Rossetti I. Gasification of mixed plastic-biomass pellets in an updraft fixed bed reactor: A simplified dynamic model. Biomass and Bioenergy 2024;190:107390. https://doi.org/10.1016/j.biombioe.2024.107390.

[93] Kuttin KW, Yu H, Yang M, Ding L, Chen X, Yu G, et al. Experimental and numerical modeling of carbonized biomass gasification: A critical review. Green Carbon 2024;2:176–96. https://doi.org/10.1016/j.greenca.2024.04.003.

[94] Kordi M, Masoud Seyyedi S. Biomass Gasification Systems and Different Types of Gasifiers, Effective Parameters on Gasification Process Efficiency: An Overview. vol. 4. 2021.

[95] Kirubakaran V, Sivaramakrishnan V, Nalini R, Sekar T, Premalatha M, Subramanian P. A review on gasification of biomass. Renew Sustain Energy Rev 2009;13:179–86. https://doi.org/https://doi.org/10.1016/j.rser.2007.07.001.

[96] Lapuerta M, Hernández JJ, Pazo A, López J. Gasification and co-gasification of biomass wastes: Effect of the biomass origin and the gasifier operating conditions. Fuel Process Technol 2008;89:828–37. https://doi.org/https://doi.org/10.1016/j.fuproc.2008.02.001.

[97] Martínez JD, Mahkamov K, Andrade R V., Silva Lora EE. Syngas production in downdraft biomass gasifiers and its application using internal combustion engines. Renew Energy 2012;38:1–9. https://doi.org/10.1016/j.renene.2011.07.035.

[98] Adil A, Brijesh, Rao L. Integrative approach to kinetic modeling and verification of a downdraft gasification model. Bioresour Technol Reports 2024;25:101701. https://doi.org/10.1016/j.biteb.2023.101701.

[99] Mahapatra S, Kumar S, Dasappa S. Gasification of wood particles in a co-current packed bed: Experiments and model analysis. Fuel Process Technol 2016;145:76–89. https://doi.org/https://doi.org/10.1016/j.fuproc.2016.01.032.

[100] Thomson R, Kwong P, Ahmad E, Nigam KDP. Clean syngas from small commercial biomass gasifiers; a review of gasifier development, recent advances and performance evaluation. International Journal of Hydrogen Energy 2020;45:21087–111. https://doi.org/10.1016/j.ijhydene.2020.05.160.

[101] Berger B. Experimental and numerical investigation of a two-stage downdraft biomass gasification process. Thesis UCL 2018:1–255.

[102] Midilli A, Kucuk H, Topal ME, Akbulut U, Dincer I. A comprehensive review on hydrogen production from coal gasification: Challenges and Opportunities. Int J

Hydrogen Energy 2021;46:25385–412. https://doi.org/10.1016/j.ijhydene.2021.05.088.

[103] Arena U. 17 - Fluidized bed gasification. In: Scala FBT-FBT for N-ZEC and G, editor. Woodhead Publ. Ser. Energy, Woodhead Publishing; 2013, p. 765–812. https://doi.org/https://doi.org/10.1533/9780857098801.3.765.

[104] Arena U, Di Gregorio F. Fluidized bed gasification of industrial solid recovered fuels. Waste Management 2016;50:86–92. https://doi.org/https://doi.org/10.1016/j.wasman.2016.02.011.

[105] Hofbauer H, Materazzi M. 7 - Waste gasification processes for SNG production. In: Materazzi M, Foscolo PUBT-SNG from W, editors., Academic Press; 2019, p. 105–60. https://doi.org/https://doi.org/10.1016/B978-0-12-815554-7.00007-6.

[106] Faraji M, Saidi M. Process simulation and optimization of groundnut shell biomass air gasification for hydrogen-enriched syngas production. Int J Hydrogen Energy 2022;47:13579–91. https://doi.org/https://doi.org/10.1016/j.ijhydene.2022.02.105.

[107] Faizan M, Song H. Critical review on catalytic biomass gasification: State-of-Art progress, technical challenges, and perspectives in future development. J Clean Prod 2023;408:137224. https://doi.org/10.1016/j.jclepro.2023.137224.

[108] Gao N, Śliz M, Quan C, Bieniek A, Magdziarz A. Biomass CO2 gasification with CaO looping for syngas production in a fixed-bed reactor. Renew Energy 2021;167:652–61. https://doi.org/10.1016/j.renene.2020.11.134.

[109] Giakoumis EG, Sarakatsanis CK. Estimation of biodiesel cetane number, density, kinematic viscosity and heating values from its fatty acid weight composition. Fuel 2018;222:574–85.

[110] Singh DK, Tirkey J V. Biomass and Bioenergy Process modelling and thermodynamic performance optimization of biomass air gasification fuelled with waste poultry litter pellet by integrating Aspen plus with RSM. Biomass and Bioenergy 2022;158:106370. https://doi.org/10.1016/j.biombioe.2022.106370.

[111] Rouanet A, Jeanmart H. Biomass and Bioenergy Improvement of syngas quality from two-stage downdraft wood gasification through steam and oxygen injection. Biomass and Bioenergy 2024;180:106998. https://doi.org/10.1016/j.biombioe.2023.106998.

[112] Zhou B, Chang J, Li J, Hong J. ScienceDirect Two-stage gasification process simulation and optimization of pulverized coal for hydrogen-rich production using Aspen plus 2023;9.

[113] Du C, Wu J, Ma D, Liu Y, Qiu P, Qiu R. ScienceDirect Gasification of corn cob using non-thermal arc plasma 2015;0.

[114] Mehrpooya M, Khalili M, Mehdi M, Sharifzadeh M. Model development and energy and exergy analysis of the biomass gasi fi cation process (Based on the various biomass sources) 2018;91:869–87.

[115] Paiva M, Vieira A, Gomes HT, Brito P. Simulation of a downdraft gasifier for production of syngas from different biomass feedstocks. ChemEngineering 2021;5. https://doi.org/10.3390/chemengineering5020020.

[116] Cao Y, Bai Y, Du J. H 2 -rich gas production from co-gasification of biomass / plastics blends : A modeling approach 2024;112.

[117] Alnouss A, Mckay G, Al-ansari T. Production of syngas via gasi fi cation using optimum blends of biomass. J Clean Prod 2020;242:118499. https://doi.org/10.1016/j.jclepro.2019.118499.

[118] Yin K, Wang Y, Wu Q, Zhang J, Zhou Y, Xu Z, et al. Thermodynamic analysis of a plasma co-gasification process for hydrogen production using sludge and food waste as mixed raw materials 2024;222.

[119] Arenas E, Henao J, Valencia G, Zapata-benabithe Z, Rafael G. Heliyon A new approach to obtain kinetic parameters of corn cob pyrolysis catalyzed with CaO and CaCO 3 2022;8.

[120] Zhang S, Wu M, Qian Z, Li Q, Zhang Y, Zhou H. CO rich syngas production from catalytic CO2 gasification-reforming of biomass components on Ni/CeO2. Fuel 2024;357:130087. https://doi.org/10.1016/j.fuel.2023.130087.

[121] Zhou F, Zhu L, Yang L, Hong Y, Xu J. Analysis of a novel power plant based on tars from biomass gasifier as fuel gas. Appl Therm Eng 2023;233:121148. https://doi.org/10.1016/j.applthermaleng.2023.121148.

[122] Niu M, Xie J, Liang S, Liu L. ScienceDirect Simulation of a new biomass integrated gasification combined cycle (BIGCC) power generation system using Aspen Plus : Performance analysis and energetic assessment. Int J Hydrogen Energy 2021;46:22356–67. https://doi.org/10.1016/j.ijhydene.2021.04.076.

[123] Yang D, Li S, He S. Zero/negative carbon emission coal and biomass staged co-gasification power generation system via biomass heating. Appl Energy 2024;357:122469. https://doi.org/10.1016/j.apenergy.2023.122469.

[124] Bao C, Wang Y, Feng D, Jiang Z, Zhang X. Macroscopic modeling of solid oxide fuel cell (SOFC) and model-based control of SOFC and gas turbine hybrid system. Prog Energy Combustion and Scientific 2018;66:83–140. https://doi.org/https://doi.org/10.1016/j.pecs.2017.12.002.

[125] Gebregergis A, Pillay P, Bhattacharyya D, Rengaswemy R. Solid Oxide Fuel Cell Modeling. IEEE Transactions on Industrial Electronics 2009;56:139–48. https://doi.org/10.1109/TIE.2008.2009516.

[126] Abouemara K, Shahbaz M, Boulfrad S, Mckay G, Al-ansari T. Energy Conversion and Management : X Design of an integrated system that combines the steam gasification of plastic waste and a solid oxide fuel cell for sustainable power generation 2024;21.

[127] Liu H, Tang Y, Ma X, Tang J, Deng J, Yue W. Calcium looping-enhanced biomass gasification for methanol production: Integrating methane dry reforming and carbon utilization. Sep Purif Technol 2025;354:129377. https://doi.org/10.1016/j.seppur.2024.129377.

[128] Kabli MR, Ali AM, Inayat M, Zahrani AA, Shahzad K, Shahbaz M, et al. H2-rich syngas production from air gasification of date palm waste: an experimental and modeling investigation. Biomass Convers Biorefinery 2022. https://doi.org/10.1007/s13399-022-02375-7.

[129] Shahbaz M, Alnouss A, Parthasarathy P, Abdelaal A, Mackey H, Mckay G, et al. Investigation of biomass components on the slow pyrolysis products yield using Aspen Plus for techno-economic analysis. Biomass Convers Biorefinery 2022. https://doi.org/10.1007/s13399-020-01040-1.

[130] Li J, Li L, Tong YW, Wang X. Understanding and optimizing the gasification of biomass waste with machine learning. Green Chem Eng 2023;4:123–33. https://doi.org/10.1016/j.gce.2022.05.006.

[131] Biagini E, Barontini F, Tognotti L. Gasification of agricultural residues in a demonstrative plant: Corn cobs. Bioresour Technol 2014;173:110–6. https://doi.org/https://doi.org/10.1016/j.biortech.2014.09.086.

[132] Jeya Singh VC, Sekhar SJ. Performance studies on a downdraft biomass gasifier with blends of coconut shell and rubber seed shell as feedstock. Appl Therm Eng 2016;97:22–7. https://doi.org/https://doi.org/10.1016/j.applthermaleng.2015.09.099.

[133] Thengane SK, Gupta A, Mahajani SM. Co-gasification of high ash biomass and high ash coal in downdraft gasifier. Bioresour Technol 2019;273:159–68. https://doi.org/https://doi.org/10.1016/j.biortech.2018.11.007.

Appendices

Appendix-A

Table A-1: Specifications of digital analytical balance.

Parameter	**Specification**
Model	SP 404D
Description	Top loader precision balance, 40/400 g, 230 V
Readability	0.005
Weighting units	g, oz, oz t, ct, dwt
Power	230 V, AC
Capacity	400 g
Calibration type	External

Table A-2: Specifications of bomb calorimeter.

Parameter	**Specification**
Temperature range	Room temperature – 99.9 °C
Display	3 Digit LED
Temperature accuracy	0.1 °C
Temperature resolution	0.1 °C
Temperature detector	RTD
Power supply	230 V ± 10%, 50 Hz AC
Standard accessories	Steel drum, bomb with sample holder, stirrer, temperature probe, Ni-Chrome wire, pellet press, cotton thread, safety valve for high pressure, oxygen pressure gauge, benzoic acid powder, tool kit, mains lead and instruction manual.

Appendix-B

Originality Report by Turnitin Plagiarism Software.

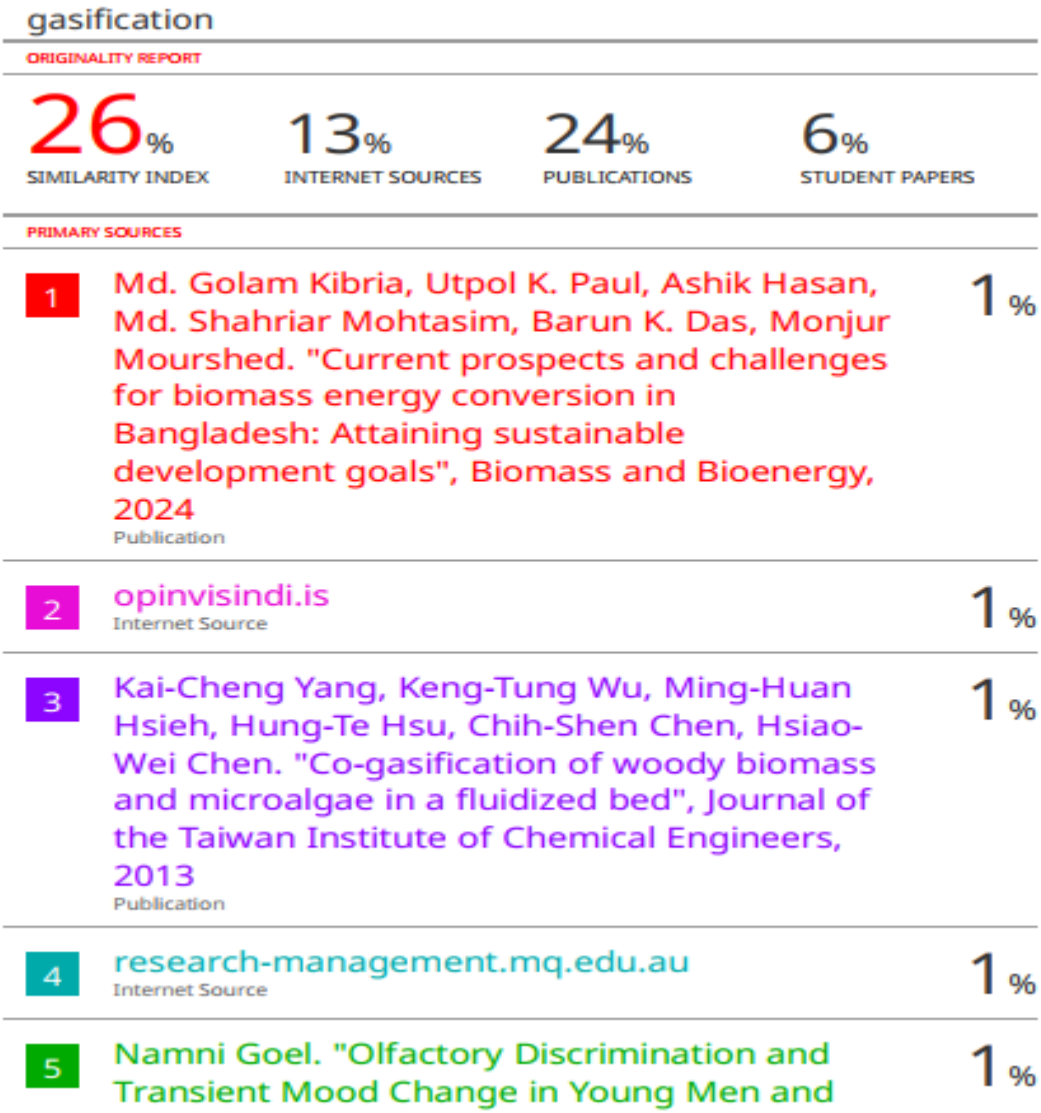

gasification

ORIGINALITY REPORT

26%	13%	24%	6%
SIMILARITY INDEX	INTERNET SOURCES	PUBLICATIONS	STUDENT PAPERS

PRIMARY SOURCES

1	Md. Golam Kibria, Utpol K. Paul, Ashik Hasan, Md. Shahriar Mohtasim, Barun K. Das, Monjur Mourshed. "Current prospects and challenges for biomass energy conversion in Bangladesh: Attaining sustainable development goals", Biomass and Bioenergy, 2024 Publication	1 %
2	opinvisindi.is Internet Source	1 %
3	Kai-Cheng Yang, Keng-Tung Wu, Ming-Huan Hsieh, Hung-Te Hsu, Chih-Shen Chen, Hsiao-Wei Chen. "Co-gasification of woody biomass and microalgae in a fluidized bed", Journal of the Taiwan Institute of Chemical Engineers, 2013 Publication	1 %
4	research-management.mq.edu.au Internet Source	1 %
5	Namni Goel. "Olfactory Discrimination and Transient Mood Change in Young Men and	1 %